

## **INFORMATION TO USERS**

**This material was produced from a microfilm copy of the original document. While the most advanced technological means to photograph and reproduce this document have been used, the quality is heavily dependent upon the quality of the original submitted.**

**The following explanation of techniques is provided to help you understand markings or patterns which may appear on this reproduction.**

- 1. The sign or "target" for pages apparently lacking from the document photographed is "Missing Page(s)". If it was possible to obtain the missing page(s) or section, they are spliced into the film along with adjacent pages. This may have necessitated cutting thru an image and duplicating adjacent pages to insure you complete continuity.**
- 2. When an image on the film is obliterated with a large round black mark, it is an indication that the photographer suspected that the copy may have moved during exposure and thus cause a blurred image. You will find a good image of the page in the adjacent frame.**
- 3. When a map, drawing or chart, etc., was part of the material being photographed the photographer followed a definite method in "sectioning" the material. It is customary to begin photoing at the upper left hand corner of a large sheet and to continue photoing from left to right in equal sections with a small overlap. If necessary, sectioning is continued again -- beginning below the first row and continuing on until complete.**
- 4. The majority of users indicate that the textual content is of greatest value, however, a somewhat higher quality reproduction could be made from "photographs" if essential to the understanding of the dissertation. Silver prints of "photographs" may be ordered at additional charge by writing the Order Department, giving the catalog number, title, author and specific pages you wish reproduced.**
- 5. PLEASE NOTE: Some pages may have indistinct print. Filmed as received.**

### **University Microfilms International**

**300 North Zeeb Road  
Ann Arbor, Michigan 48106 USA  
St. John's Road, Tyler's Green  
High Wycombe, Bucks, England HP10 8HR**

77-19,261

HINDUJA, Manohar Jhamandas, 1950-  
A NON-FICKIAN MODEL FOR DISPERSION IN PACKED  
BEDS.

Rice University, Ph.D., 1977  
Engineering, chemical

**Xerox University Microfilms**, Ann Arbor, Michigan 48106

RICE UNIVERSITY

A NON-FICKIAN MODEL FOR DISPERSION  
IN PACKED BEDS

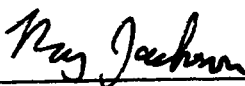
by

Manohar Jhamandas Hinduja

A THESIS SUBMITTED  
IN PARTIAL FULFILLMENT OF THE  
REQUIREMENTS FOR THE DEGREE OF

DOCTOR OF PHILOSOPHY

THESIS DIRECTOR'S SIGNATURE:



---

HOUSTON, TEXAS

APRIL, 1977

To my sister

Asha

who constantly reminds me

there is so much to know and understand

## ACKNOWLEDGEMENTS

I would like to convey my sincere appreciation to the following people:

My parents for providing me the basis for my life-style; my brothers and sisters, particularly Kumar, for their constant support and encouragement;

My advisor, Professor Roy Jackson, whose brilliant mind and penetrating sagacity has left a deep impression on me; if only I were able to learn more from him;

Professor Harry Deans for taking keen interest in my work and serving on my thesis committee;

Professor J.C. Wilhoit, Jr., for serving on my thesis committee;

Stig Wedel for his help in some of the computational aspects;

Pat Angel, whose quiet wisdom is as commendable as her artistic typewriting;

Members of the faculty and staff in the Chemical Engineering Department for lively discussions, both academic and otherwise;

Ruth Allston, for making me feel like reporting to work every day;

Gregory Johnson, Joe Gonsalves, and other fellow graduate students for being such good friends,

I would like to thank Rice University and Shell, Arco and Dow Companies for financial support,

## TABLE OF CONTENTS

	Page
1. INTRODUCTION . . . . .	1
1.1 Fluid Dynamics in a Packed Bed Reactor . . . . .	7
1.2 Heat Transfer in Packed Beds . . . . .	12
2. MATHEMATICAL FORMULATION OF THE NON-FICKIAN MODEL . . . . .	17
2.1 Material Balance Equations . . . . .	20
2.2 Energy Balance Equations . . . . .	28
3. DISPERSION IN ONE-DIMENSIONAL, ISOTHERMAL, NON-REACTIVE PACKED BEDS . . . . .	35
3.1 Moment Analysis . . . . .	35
3.2 Pulse Injection Simulation . . . . .	39
3.3 Stochastic Analysis of the Pulse Test Experiment . . . .	47
3.4 Frequency Response Analyses of Flow Through Packed Beds . . . . .	53
4. TRANSVERSE DISPERSION IN TWO-DIMENSIONAL, ISOTHERMAL NON-REACTIVE PACKED BEDS . . . . .	58
4.1 Moment Analysis . . . . .	58
4.2 Point Source, Steady State and No Reaction . . . . .	62
4.3 Evaluation of Parameters through Experimental Values of Peclet Number . . . . .	68
4.4 Momentum Transfer in Turbulent Flow in Packed Beds . .	70
5. ISOTHERMAL CHEMICAL REACTION IN PACKED BEDS . . . . .	74
5.1 First Order, Homogeneous Reaction in a One- Dimensional Bed at Steady State . . . . .	74
5.2 Second Order, Homogeneous Reaction in a One- Dimensional Bed at Steady State . . . . .	83

	Page
6. HEAT DISPERSION IN PACKED BEDS . . . . .	91
6.1 Moment Analysis . . . . .	91
6.2 Evaluation of Heat Transfer Parameters . . . . .	98
6.3 Transverse Heat Dispersion in Non-Reactive Packed Beds . . . . .	101
6.4 Steady State Heat Transfer Equations . . . . .	104
6.5 Numerical Simulation to Validate Use of Asymptotic Values . . . . .	107
7. DYNAMIC MODELING OF A GAS PHASE CATALYTIC PACKED BED REACTOR . . . . .	114
7.1 Introduction . . . . .	114
7.2 Dynamic Modeling Studies of Hansen and Jorgensen . . . .	116
7.3 Corresponding Non-Fickian Model . . . . .	119
7.4 Steady State Profiles . . . . .	125
7.5 Frequency Response Analysis . . . . .	128
NOMENCLATURE . . . . .	144
REFERENCES . . . . .	152

## 1. INTRODUCTION

The problem of modelling a packed bed reactor with porous catalyst pellets is ideally one of trying to ascertain pressure, temperature and concentration in two 3-dimensional space structures (time would constitute the seventh dimension in an unsteady state process). One of the 3-dimensional space structures, in which the balance equations are written for the moving fluid, would be a control volume, large if compared with the size of the catalyst pellet and small if compared with the size of the reactor. The pseudo-homogeneous models that have been developed in the last two decades have considered this size of the control volume. The other 3-dimensional space structure is one within the catalyst pellet with a control volume large if compared with the pores within the pellet and small if compared with the size of the pellet. An ideal model for a packed bed reactor would be one which effectively couples the fluxes within the catalyst pellet with those in the fluid moving in the interstices between the catalyst pellets in the bed. Unfortunately, it is quite a formidable task to develop such a model.

The simplest models treat the bed of catalyst pellets as though it were statistically homogeneous and the balance equations are written as if it were a one phase environ. The model most commonly used for simulation studies has been obtained by considering that heat and mass transfer in both axial and radial directions are the result of superposition of two processes, namely, a convective flow, and a diffusive flow following Fick's law of diffusion. Paris and Stevens 1970, N.R. Amundson 1970, Froment 1972, Ray 1972, Adler et al. 1973,



Hoffman 1974, have summarised the various approaches to the problem of modelling packed bed chemical reactors. The mathematical intractability of the Fickian model has been commented upon by several researchers. Particular attention has been drawn to the dispersion terms expressed by second order differentials (Wehner and Wilhelm 1956, Beek and Miller 1959) and considerable experimental as well as analytical work has been done in order to ascertain when one or more of the four second order differentials can be neglected in the heat and mass balance equations.

The intuitive justification for axial dispersion parallel to the flow as a form of Fickian diffusion has been increasingly suspect with recent investigations of the actual fluid dynamics in the packed bed. It would be reasonable to represent the dispersive effect as diffusion only if there is a significant amount of backmixing in packed bed reactors (Hiby 1963).

Deans and Lapidus 1960, assuming that backmixing is negligible, have recommended that, instead of trying to use diffusion to represent an essentially different dispersive effect, one should formulate a set of difference equations akin to the mixing cell theory (Aris and Amundson 1957). The geometrical arrangement for the mixing cells is based on a statistical model for a pattern of flow provided by the random walk theory (Bakhturov and Boreskov 1947, Baron 1952, Ranz 1952) by assuming that the fluid particle has equal probability of deviating on either side of the catalyst pellet when met head-on. The structure is effectively considered to be a sequence of continu-

ous stirred tank reactors in series. The temperature and concentration conditions of any given cell are dependent only on those of the previous row of cells. Both radial and axial dispersion as well as the mathematical complexity associated with axial and radial boundary conditions is automatically removed by the physical structure of the reactor.

Although this is a better representation of the behaviour of a packed bed, it may get expensive in computing time because it requires steps equal to a particle diameter. However, for long beds axial dispersion effects are not important and hence one could as well take axial steps equal to several particle diameters. The mixing cell model can be extended to incorporate all heat and mass transfer processes (including fluxes within the catalyst particle) except solid to solid heat conduction which is an important source of thermal feedback in the reactor. The two phase heat transfer model which distinguishes between solid and fluid phases has an advantage over the cell model in that all the transport coefficients can be easily related to experimental data.

A higher level of complexity is reached in the heterogeneous models which distinguish conditions in the fluid and on the catalyst surface or even inside the catalyst. This more detailed and more general representation of the packed bed reactor includes considerations of both heat and mass dispersion in the radial and axial directions in the external fluid, and the resistance to heat and mass transfer, both within the catalyst particles and across the film at the catalyst surface (Feick and Quon 1970, Amundson 1970, Beek 1972, Froment 1972, Ray 1972). Experimental studies on heterogeneous catalysis in packed beds have been reported (Maymo and Smith 1966,

Hawthorn et al. 1968, Richarz and Lattman 1968, Yamazaki et al. 1970, Karanth and Hughes 1974, Van Doesburg and De Jong 1974); however, they have been few and have not kept up with theoretical developments.

The rate of a heterogeneously catalysed reaction is determined by both the chemical reaction kinetics at the solid surface and by the rate of heat and mass transfer to this surface. When the reactor is operating at a steady state, the number of moles of a component destroyed at the catalyst surface by the chemical reaction is exactly equal to the number of moles of that component transported to the surface. Likewise, the heat generated by the reaction must be equal to the heat removed.

Two mechanisms of heat and mass transfer are involved when dealing with a catalyst pellet. The first mechanism is the hypothetical film of fluid surrounding the pellet. Both heat and mass transfer occur across this film because the bulk temperature and concentrations are different from those at the surface of the catalyst. Mass transfer across the film occurs by both convection and molecular diffusion. Heat transfer occurs by convection, conduction, and radiation.

The second heat and mass transfer mechanism involves the pores and solid material of the catalyst pellet. Both temperature and concentration gradients may exist through the porous catalyst particle. Mass transfer occurs by Knudsen diffusion, bulk diffusion, and surface migration. Heat transfer occurs by conduction in both solid and fluid phases. Effectiveness factors other than one are the result of temperature and concentration gradients within the porous catalyst pellet

and also across the film.

For any given system, it is difficult to evaluate the relative importance of film and pore effects unless detailed temperature and concentration profiles are measured within the porous catalyst pellets and the surrounding fluid. For instance, in a system where all the reactants which reach the catalyst surface are reacted on the outer surface before they have a chance to diffuse in the pores, then the surface film gradients would be of particular interest in the study of the kinetics of the reaction and the behaviour of the catalyst. In such a case, the particle diameter would have considerable influence on the reaction rate per unit external surface area (Fulton and Crossner 1965).

Measurements of temperature profiles in catalyst pellets have recently been reported. Irving and Butt 1967, in studying the hydrogenation of benzene and, Hughes and Koh 1970, in studying the hydrogenation of ethylene (both on 1.27 cm pellets) indicate that the external film offers the greatest resistance to heat transfer. Horak and Jiracek 1972, have shown that during catalytic exothermic reactions, significant temperature differences may be created between the external surface of the catalyst particle and the bulk of the reaction mixture. However, the experimental measurements of Kehoe and Butt 1972, of the response of the internal and external gradients to both startup and perturbations of the steady state in a catalyst particle ( $N_1$  on Kiesulguhr) for the benzene hydrogenation reaction indicate that both external and intraparticle temperature gradients must be

considered in some cases.

In the present work, the catalyst pellet is considered to have a constant temperature throughout its bulk and the heat transfer resistance is concentrated in the external film. At interparticle contact points (where there may be stationary fluid held up), heat transfer between adjacent particles takes place by pure conduction (see Fig. 1.a below). This particular heat transfer resistance has been concentrated in artificial "necks" connecting adjacent particles (see Fig. 2.a). Also it is apparent that the cross-sectional area of the particle through which conductive heat transfer takes place is smallest near the contact points. These artificial "necks" have no heat capacity and serve only as the heat transfer resistance due to conduction. The bulk of the catalyst pellet has all the heat capacity in it, but it has no resistance to heat transfer by conduction.

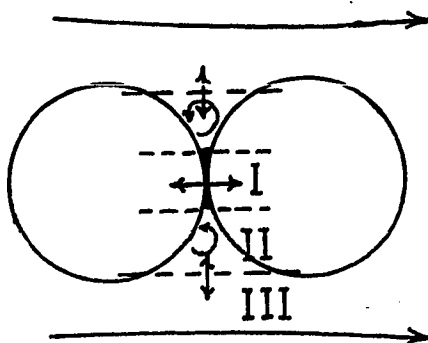


FIGURE 1.a. Schematic illustration of heat transfer between adjacent catalyst pellets. Region I: Heat transfer by pure

conduction. Region II: Heat transfer by the wake region.

Region III: Heat transfer by the moving fluid.

Hougen 1961, has discussed various aspects of the external heat and mass transfer resistances and has included figures for predicting when such resistances need to be considered. The experimental results of Maymo and Smith 1966, indicate that for a large  $\Delta H$  external temperature effects can be significant when the diffusion effect is negligible. Hutchings and Carberry 1966, also have predicted that negligible mass-transfer and finite heat-transfer resistances would exist for some reaction conditions. In the present work, wherever catalyst pellets are considered to be porous, the Knudsen limit is taken to be the operating regime and the external mass-transfer resistance is neglected.

### 1.1 Fluid Dynamics in a Packed Bed Reactor

The fluid phase containing the reactants moves through the interstices of the bed in a complicated manner because of the acceleration and deceleration in the passages between the particles. It is apparent that the situation at the upstream side of the catalyst particle where the fluid meets it head-on is quite different than on the downstream side half where there may be a fluid mechanical wake which involves a different transport mechanism and dispersion phenomenon. The present work recognises the significance of the wake in heat and mass transport in a packed bed. A mathematical model has been developed in which the dispersion in a packed bed reactor is considered to

be due to a wake entrainment and shedding phenomenon.

As flow impinges upon the surface of the catalyst pellet a boundary layer is formed and the cross-sectioned area available for flow is reduced compared to the fluid-free void cross-sectional area. Hence the actual velocity is no longer simply related to the superficial velocity and the total void fraction. Also at some critical bed voidage vortex flow is formed behind the particles in the wake region, thus further influencing the effective velocity. Kusik and Happel 1962, took a voidage of 0.2 to be very tightly packed and assumed that, at this low voidage, vortices would disappear and  $\epsilon_B$  would be zero, where  $\epsilon_B$  is the fraction of the total bed volume occupied by wakes. Debbas and Rumf 1966, have shown that the minimum possible porosity is 0.35 for a random packing of spheres. Thus, in most packed beds there would be vortices present, which would cut down the area available to fluid flow. Based on the above and other assumptions, Kusik and Happel derived the following equation for estimating  $\epsilon_B$  in the case of a packing of spheres:

$$\epsilon_B = 0.75 (1 - \epsilon_T) (\epsilon_T - 0.2)$$

where  $\epsilon_T$  is the fraction of the total bed volume not occupied by solids.

If the bed is densely packed the flow can be visualised as being composed of a series of "jets" and "wakes" in the interstitial space. The phenomena of axial and radial dispersion can be considered to be due to jet division, recombination, and the associated mixing in the

wakes. Deans and Lapidus 1960, have idealised this phenomenon in a model considering the flow as a number of stirred tanks in series. The above jet mixing process would lead one to believe that the turbulence intensity would be inversely proportional to the Peclet number for radial dispersion. Also the turbulence generated would interact with the boundary flow formed on the particles in much the same way as free-stream turbulence perturbs the laminar boundary flows and increases transport on a bluff body in a free stream.

In most industrial packed beds, however, the void fraction is 0.38 to 0.47, in which case the catalyst particles will be sufficiently far apart so that a vortex would be formed in the wake region of each particle. The boundary layer would in effect have been separated by the adverse pressure gradient. The vortex created would interact with the free stream in terms of an interchange flow which would essentially keep the wake volume constant. The vortex shedding would then interact with the flow in the next downstream particle and its boundary layer and vortex. As the voidage in the bed approaches unity, the turbulence level would decrease to that of the free stream turbulence of a single particle in an infinite medium. The turbulence measurements of Mickley et al. 1965, and the experimental local thermal transfer measurements of Galloway and Sage 1970, give credence to this mechanism. Galloway and Sage were probably the first to analyse transport phenomena in packed beds from a more realistic fluid dynamic point of view.

Kyle and Perrine 1971, from a photographic study of the flow through a matrix of cylinders which were used to simulate a packed



bed of spheres, showed that in turbulent flow there is a zone in the wake of each cylinder (which includes, but is greater in size than the standing vortex pairs), where the flow is definitely inhibited when compared to the rest of the region. As the turbulent intensity increases, this stagnant zone becomes smaller, until at high velocities, there is general turbulence throughout the cell. As the energy and frequency of the turbulent eddies increase so does the mixing efficiency: The liquid held back by the stagnant zones will bleed slowly into the main stream thus elongating the dispersion profile and producing the phenomenon called "tailing".

Gauvin and Katta 1973, have developed a theoretical approach on the basis of this discrete particle model, utilising, for the first time, the concept of stagnant void fraction to interpret the experimental data. The wake volume and a new shape factor  $k$ , defined on the basis of all possible orientations of the particle, were used to derive equations for estimating  $\epsilon_p$  for different shapes. A new friction factor based on  $\epsilon_p$  and  $k$  was defined and correlated with the shape factor satisfactorily. The momentum transfer was also correlated in terms of a different friction factor based on the channel model (Ergun's equation) and the sphericity of the particles. The channel model was shown to be applicable only at high sphericities ( $>0.6$ ) while the discrete particle model was proved to be valid at low as well as high sphericities. The concept of  $\epsilon_p$  also explained certain apparent anomalies in some studies on packed beds.

It has been assumed that  $\epsilon_p$  is independent of the Reynolds num-

ber although this may not be a valid assumption when large Reynolds number is considered. In the study made by Gauvin and Katta, Reynolds number was varied from 400 to 2800 and they obtained the following expression for spheres:

$$\epsilon_B = 2A(\epsilon_T - 0.2) (1 - \epsilon_T) \quad (1.1.a)$$

where A is a constant.

For spheres it was found that  $A = 0.8$ , so that for spheres:

$$\epsilon_B = 1.6(\epsilon_T - 0.2) (1 - \epsilon_T) \quad (1.1.b)$$

For non-spherical particles,

$$\epsilon_B = 2Ak_s (\epsilon_T - 0.2) (1 - \epsilon_T) \quad (1.1.c)$$

where,  $k_s$  = ratio of mean projected area of a particle (sphere, cylinder, ellipsoid) to that of a sphere of the same volume.

The non-Fickian model presented in this work takes into account all the above arguments. Since  $\epsilon_B$  is a constant, and material is transported back and forth between the stagnant volume and the flowing stream, there must be a volumetric exchange between the two "phases" which is equal in magnitude in both directions. Hence a new parameter,  $g$ , is defined as the interphase volumetric flow rate per unit volume of the bed. This parameter has been correlated with pressure drop in a packed bed for turbulent flow (form drag) and thus further insight into the momentum transfer in a packed bed has been obtained.

Also of interest is the probabilistic time delay approach of Buffham et al. 1970, Buffham and Gibilaro 1970, in describing flow

through packed beds. A semi-empirical model, considering the number of stops of a fluid element as a Poisson distribution and the delay of the fluid element at the stop as an exponential distribution, seems to fit the experimental data for a pulse test in trickle beds quite well. As stated earlier, the two "phases" with fluid interchange in the non-Fickian model are considered locally well mixed and hence correspond to the above conditions of the time-delay model with exponentially distributed delays. However, since the present work divides the interstitial space into two distinct phases, it is more directly akin to Giddings 1965, coupling theory of chromatography.

### 1.2. Heat Transfer in Packed Beds

The rates of most industrial reactions are strong functions of temperature, which thus affects conversion, selectivity and stability. Therefore, it is important to develop a mathematical model which identifies a temperature at all points in the reactor. Heat transfer in a packed bed occurs by several mechanisms which depend on the physical and thermal properties of the flowing fluid and the catalyst particles.

As indicated earlier, the simplest models consider the particles to be small enough compared to the size of the reactor so as to act as a continuum embedded in a field of concentration and temperature. The dispersion of heat is considered as Fickian diffusion and hence two parameters, namely, the axial effective thermal conductivity and the radial effective thermal conductivity, are defined. Considerable

experimental and theoretical work has been done in order to correlate these two very important parameters.

Yagii et al. 1960, proposed a model for axial effective thermal conductivity by separating the heat transfer mechanism into two parts, one independent of fluid flow and the other dependent on it. Thus,

$$\frac{k_e}{\lambda_f} = \frac{k_e^0}{\lambda_f} + 0.8 \text{ Re} \cdot \text{Pr}_f . \quad (1.2.a)$$

where,

$k_e$  = axial effective thermal conductivity in the packed bed.

$k_e^0$  = axial effective thermal conductivity in the packed bed with no flow.

$\lambda_f$  = thermal conductivity of the flowing fluid.

$\text{Re}$  = Reynolds number

$\text{Pr}_f$  = Prandtl number

More elaborate and accurate experimental setups have been devised recently to determine axial effective heat transfer (Votruba et al. 1972, Gunn and DeSouza 1974, Vortmeyer 1975, Hansen and Jorgensen 1976).

The transverse effective thermal conductivity is not well agreed upon, although there has been theoretical as well as experimental analysis (Singer and Wilhelm 1950, Argo and Smith 1950, Chu and Storrows 1952, de Wasch and Froment 1972). Argo and Smith consider all possible mechanisms for radial heat transfer, including heat

transfer through the solid phase and radiation, establishing the following relation:

$$(k_e)_r = \epsilon_T \left[ \lambda_f + \frac{G c_p d_p}{\epsilon_T (Pe)_{m,r}} + \frac{4 \epsilon_r \sigma d_p T^3}{2 - \epsilon_r} \right] + (1 - \epsilon_T) \frac{h' k_s d_p}{2k_s + h' d_p} \quad (1.2.b)$$

where,

$(k_e)_r$  = radial effective thermal conductivity in the packed bed.

$G$  = superficial mass velocity.

$c_p$  = heat capacity of the external fluid.

$d_p$  = particle diameter.

$(Pe)_{m,r}$  = radial effective mass Peclet number.

$\epsilon_r$  = emissivity of catalyst particles.

$\sigma$  = radiation constant

$T$  = temperature of the external fluid.

$h'$  = total heat transfer coefficient from particle surface to fluid or to other particles.

$k_s$  = molecular thermal conductivity of the solid particle, based on a unit area of solid.

In the heterogeneous or two phase models separate energy equations are written for the solid and the fluid phase. The equations typically written for one-dimensional, adiabatic packed bed with no chemical reaction are:

$$\alpha c_p \epsilon_T \frac{\partial T}{\partial t} + \alpha c_p \epsilon_T v \frac{\partial T}{\partial z} = ha(\hat{T} - T) \quad (1.2.c)$$

$$(1-\epsilon_T) \rho_s \hat{c}_p \frac{\partial \hat{T}}{\partial t} = \lambda_o \frac{\partial^2 \hat{T}}{\partial z^2} + ha(T-\hat{T}) \quad (1.2.d)$$

where,

$\alpha$  = density of the external fluid

$t$  = time

$v$  = interstitial velocity

$z$  = axial distance

$h$  = heat transfer coefficient from particle surface to fluid.

$a$  = particle surface area per unit bed volume, for spheres,  
 $6(1-\epsilon_T)/d_p$ ,  $L^{-1}$ .

$\hat{T}$  = temperature of the solid catalyst pellet.

$\rho_s$  = density of solid

$\hat{c}_p$  = heat capacity of the solid

$\lambda_o$  = axial effective thermal conductivity of the quiescent  
 bed, that is, a bed with no fluid flow.

Here heat transfer through adjacent sections of catalyst pellets is considered to be made up of three mechanisms. The first mechanism is heat transfer by pure heat conduction through the solids by direct contact and through the stationary fluid interstices. The second mechanism is heat exchange between the vortices and the solid by convection. But this effect is generally considered as part of heat transfer by conduction through the catalyst pellets, and is then responsible for increase of effective heat conductivity with increase in Reynolds number (Eigenberger 1972). Others seem to incorporate it by a heat transfer coefficient (Balakrishnan and Pei 1974,

Bhattacharya and Pei 1975). The third mechanism is the conventional fluid-to-particle convective heat transfer between the flowing fluid and the solid.

Littman and Sliva 1970, have experimentally evaluated the parameters involved in the two phase heat transfer model, particularly in the range of lower Reynolds numbers. Vortmeyer 1975, has effectively evaluated an axial dispersion Peclet number equivalent to the one phase (Fickian) model and has correlated it with extensive experimental data available in the literature.

There has been no significant work done in the literature for a two-dimensional two-phase model and therefore little or no information on transverse heat transfer coefficients is available.

The present work, in essence, has similar heat transfer parameters as in the two phase model described above. However, it has in perspective the actual fluid dynamics in the packed bed in relating the heat dispersion in the flowing stream; also, it proposes a two-dimensional heat transfer mechanism without any additional parameters.

## 2. MATHEMATICAL FORMULATION OF THE NON-FICKIAN MODEL

The system considered here is an assembly of particles packed together with a fluid flowing through the interstices. The fluid is, in general, a mixture of chemically discrete species which may take part in chemical reactions, either homogeneously or heterogeneously on or inside the catalytic surface of the particles (preliminary equations are written for non-porous catalyst particles, however). Keeping in mind the fact that most common packed bed reactors used in the industry are of cylindrical geometry, an "axial" symmetry is assumed so that the most general mathematical model can be considered to be two dimensional.

Other general qualifying assumptions are:

- 1) The fluid which flows among the packing is referred to as the "moving fluid" or "moving phase" to differentiate it from the "stagnant fluid" or "stagnant phase" in the lee side of the particle where there is wake formation.
- 2) The packing is taken to be non-porous.
- 3) The external fluid, that is, the moving as well as the stagnant phase, is assumed to be a pseudo-binary mixture of reactive components, one of them being the "tracer component" for which the material balance equations are written.
- 4) The moving fluid is in turbulent flow, at least insofar as axial and radial mixing is concerned.
- 5) Density and heat capacity of the external fluid as well as that of the solid is constant.



6) Molecular diffusion fluxes are negligible when compared with the corresponding turbulent fluxes.

7) The fraction of the total volume of the bed occupied by the wakes,  $\epsilon_B$ , is constant.

8) Material is transported back and forth between the moving phase and the stagnant phase and the volumetric exchange between the two phases is equal in magnitude in both directions.

9) Radiant heat transport and secondary fluxes of heat and material caused by thermodynamic coupling are negligible.

10) Driving forces for material transport and chemical reaction may be expressed in terms of molar concentrations rather than chemical potentials.

11) The resistance to heat transfer from the moving fluid to the solid catalyst pellet is lumped at the surface of the catalyst pellet.

12) Heat transfer by pure conduction occurs through the solids by direct contact and through the stationary fluid interstices. This heat transfer resistance by conduction is assumed to be concentrated in the artificial "necks" connecting adjacent pellets as shown in Fig. 2.a. (Also see Fig. 1.a).

13) The heat capacity of the solid is assumed to be concentrated in the bulk of the catalyst pellets.

14) The velocity of the flowing stream is constant, that is, plug-flow is assumed for this stream.

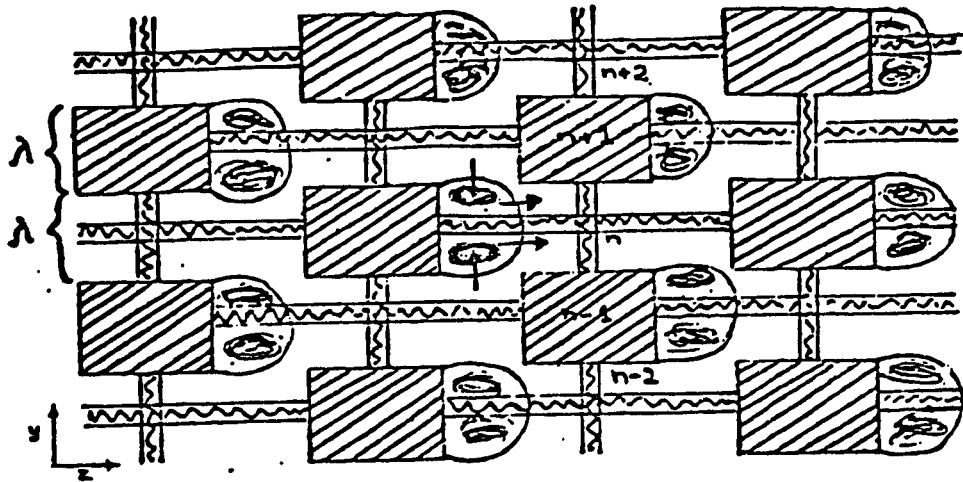


Fig. 2.a. Visual model for heat and mass transfer in packed beds with mixing mechanism I

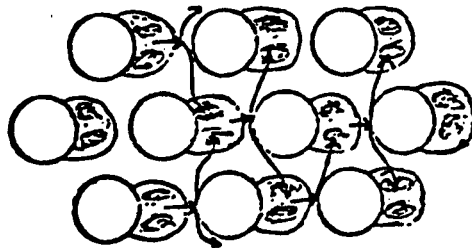


Fig. 2.b. Mixing Mechanism I

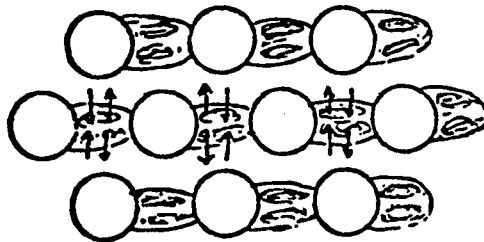


Fig. 2.c. Mixing Mechanism II

## 2.1 Material Balance Equations

Fig. 2.a shows the visual model which is used to simulate heat and mass transfer in packed beds. The shaded area behind each particle signifies the wake region and the arrows going to and from the wake regions represent the wake shedding mechanism which is used to explain axial and radial mixing in packed beds. The balance equations are written with the packed bed divided into discrete sections of length  $\lambda$  along the radial direction (y coordinate). Along the z direction, however, each phase is taken to be continuous. Balance equations are written for each phase across a cross-sectional area  $\delta A$  of the bed at an arbitrary point at distance z from the entrance of the bed and at section n along the radial direction.

At any instant it is assumed that the interphase volumetric flow rate between the moving phase and the stagnant phase per unit volume of the bed is  $g$ . This also maintains  $\epsilon_B$ , the fraction of the total bed volume occupied by wakes as a constant, independent of time and flow-rate.

Two mechanisms for wake shedding have been studied to simulate axial and radial mass dispersion as shown in Figs. 2.b and 2.c.

### 2.1.1 Mechanism I

This mechanism of mixing is illustrated in Fig. 2.b. It postulates that the particles in the bed are oriented such that the wake region (stagnant phase) of each particle is not in contact with the particle in front of it and thereby sheds its elemental volume of

fluid along the same radial section into the moving phase. At the same time, the wake region receives an equal amount of elemental volume of fluid from the moving fluid which is at the adjacent radial sections, one below and the other above the section being considered.

- i) Mass balance of component i in the moving phase at position n:

At any instant of time, in an elemental volume  $\delta A \cdot \delta z$ , of the bed, the convective net input of component i is  $(c_n(z) \cdot v_z \cdot \epsilon_A \cdot \delta A - c_n(z + \delta z) \cdot v_z \cdot \epsilon_A \cdot \delta A)$  moles;

where,  $c_n(z)$  = concentration of i in the moving phase at section n and axial distance z.

$v_z$  = actual average velocity of the moving phase  
(based on cross sectional area available to moving phase).

$\epsilon_A = \epsilon_T - \epsilon_B$  = fraction of total bed volume occupied by the moving phase.

The net input of component i due to the interphase volumetric flow is  $(g \bar{c}_n(z) \cdot \delta A \cdot \delta z - g \cdot c_n(z + \delta z) \cdot \delta A \cdot \delta z)$  moles per unit time;

where,  $\bar{c}_n(z)$  = concentration of i in the stagnant phase at section n and axial distance z.

The balance equation is written as

$$c_n(z) \cdot v_z \cdot \epsilon_A \cdot \delta A - c_n(z + \delta z) \cdot v_z \cdot \epsilon_A \cdot \delta A + g \cdot \bar{c}_n(z) \cdot \delta A \cdot \delta z - g \cdot c_n(z + \delta z) \cdot \delta A \cdot \delta z$$

$$+ R \cdot \epsilon_A \cdot \delta A \cdot \delta z = \frac{\partial c_n(z)}{\partial t} \cdot \epsilon_A \cdot \delta A \cdot \delta z \quad (2.1.1.a)$$

where,  $R$  = rate of production of  $i$  by chemical reaction, moles of  $i$ /volume-time, in the moving phase.

For a differential  $\delta z$ , equation 2.1.1.a can be written as

$$- \frac{\partial c_n}{\partial z} \cdot v_z \cdot \epsilon_A \cdot \delta A \cdot \delta z + g(\bar{c}_n - c_n) \delta A \cdot \delta z + R \cdot \epsilon_A \cdot \delta A \cdot \delta z = \frac{\partial c_n}{\partial t} \cdot \epsilon_A \cdot \delta A \cdot \delta z$$

Rearranging and dividing by  $\epsilon_A \cdot \delta A \cdot \delta z$

$$\frac{\partial c_n}{\partial t} + v_z \frac{\partial c_n}{\partial z} + \frac{g}{\epsilon_A} (c_n - \bar{c}_n) = R \quad (2.1.1.b)$$

ii) Mass balance of component  $i$  in the stagnant phase at position  $n$ :

There is no convective mass flux in the stagnant phase because of its "stagnant" nature. The moles of component  $i$  received by the stagnant phase in the elemental volume  $\delta A \cdot \delta z$  from the moving phase at the adjacent radial sections is  $(\frac{g}{2} \cdot c_{n+1}(z) \cdot \delta A \cdot \delta z + \frac{g}{2} \cdot c_{n-1}(z) \cdot \delta A \cdot \delta z)$ . The moles of component  $i$  shed into the moving phase at section  $n$  is  $g \cdot \bar{c}_n(z) \cdot \delta A \cdot \delta z$ . The balance equation is written as

$$\left[ \frac{g}{2} \cdot c_{n+1}(z) + \frac{g}{2} \cdot c_{n-1}(z) - g \cdot \bar{c}_n(z) \right] \delta A \cdot \delta z + \bar{R} \cdot \epsilon_B \cdot \delta A \cdot \delta z = \frac{\partial \bar{c}_n}{\partial t} \cdot \epsilon_B \cdot \delta A \cdot \delta z \quad (2.1.1.c)$$

where,  $\bar{R}$  = rate of production of  $i$  by chemical reaction, moles of  $i$ /volume-time, in the stagnant phase.

Dividing by  $\epsilon_B \cdot \delta A \cdot \delta z$  and rearranging, equation 2.1.1.c becomes

$$\frac{\partial \bar{c}_n}{\partial t} + \frac{g}{\epsilon_B} \left[ \bar{c}_n - \frac{1}{2} (c_{n+1} + c_{n-1}) \right] = \bar{R} \quad (2.1.1.d)$$

The discrete nature of equations 2.1.1.b and 2.1.1.d along the radial direction can be smoothed out by using Taylor series approximation over length  $\lambda$ . This would mean that radial mixing effects predicted by the smooth equations have meaning only over distances greater than  $\lambda$ .

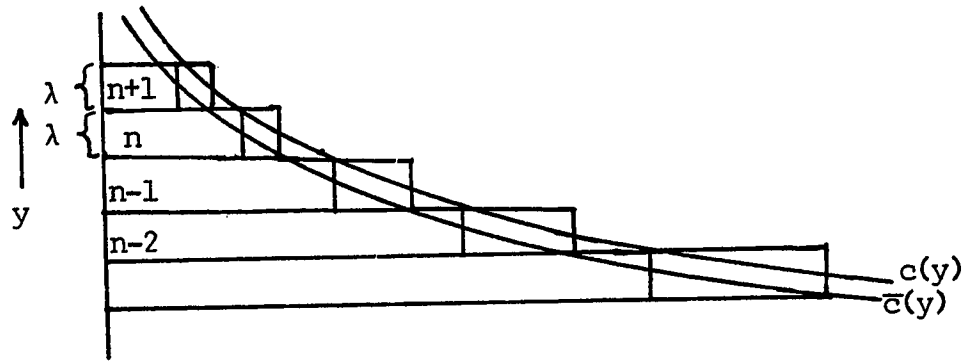


FIGURE 2.d

$$\text{Let } c_n = c(y)$$

$$\text{and } \bar{c}_n = \bar{c}(y)$$

Using the Taylor series up to second order terms and referring to Fig. 2.d,

$$c_{n+1} = c(y + \lambda) = c(y) + \lambda \cdot \left( \frac{\partial c}{\partial y} \right)_y + \frac{1}{2} \lambda^2 \cdot \left( \frac{\partial^2 c}{\partial y^2} \right)_y$$

$$c_{n-1} = c(y - \lambda) = c(y) - \lambda \cdot \left( \frac{\partial c}{\partial y} \right)_y + \frac{1}{2} \lambda^2 \cdot \left( \frac{\partial^2 c}{\partial y^2} \right)_y$$

Substituting in equations 2.1.1.b and 2.1.1.d, the following equations of continuity are obtained.

Moving phase:

$$\frac{\partial c}{\partial t} + v_z \frac{\partial c}{\partial z} + \frac{g}{\epsilon_A} (c - \bar{c}) = R \quad (2.1.1.e)$$

Stagnant phase:

$$\frac{\partial \bar{c}}{\partial t} + \frac{g}{\epsilon_B} (\bar{c} - c) - \frac{g\lambda^2}{2\epsilon_B} \frac{\partial^2 \bar{c}}{\partial y^2} = \bar{R} \quad (2.1.1.f)$$

Thus, two coupled partial differential equations represent the material balance in the packed bed. The second term in equation 2.1.1.e represents the mass flux due to convection, the third term is due to the volumetric exchange between the two phases and this generates the axial mixing in the packed bed. The last term on the left hand side of equation 2.1.1.f represents the radial mixing in the packed and is quite akin to the Fickian model representation of radial diffusion.

### 2.1.2 Mechanism II

Fig. 2.c shows this mechanism of mixing. The particles are assumed to be oriented such that the wake region (stagnant phase) of each particle extends over the particle in front of it and is in contact with it. Hence volumetric interchange cannot take place along the same radial section and therefore has to take place between adjacent radial sections. The external fluid can be represented as shown in Fig. 2.e.

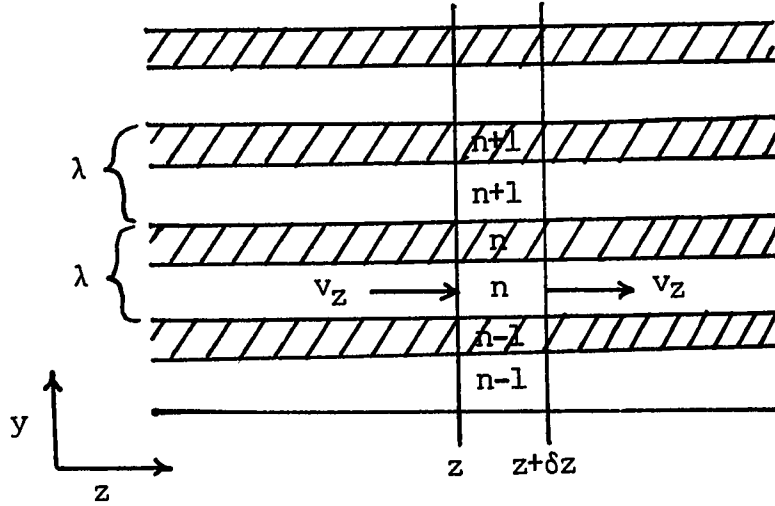


FIGURE 2.e

The shaded area represents the stagnant phase and the unshaded area is the moving phase.

- i) Mass balance of component  $i$  in the moving phase at position  $n$ :

In this mechanism, the net input due to interphase volumetric flow, of component  $i$  in the moving phase at position  $n$  is  $(\frac{g}{2} \cdot \bar{c}_n(z) \cdot \delta A \cdot \delta z + \frac{g}{2} \cdot \bar{c}_{n-1}(z) \cdot \delta A \cdot \delta z - g \cdot c_n(z) \cdot \delta A \cdot \delta z)$  moles per unit time, so the mass balance equation is written as

$$c_n(z) \cdot v_z \cdot \epsilon_A \cdot \delta A - c_n(z + \delta z) \cdot v_z \cdot \epsilon_A \cdot \delta A + \frac{g}{2} \bar{c}_n(z) \cdot \delta A \cdot \delta z + \frac{g}{2} \bar{c}_{n-1}(z) \cdot \delta A \cdot \delta z - g \cdot c_n(z) \cdot \delta A \cdot \delta z + R \cdot \epsilon_A \cdot \delta A \cdot \delta z = \frac{\partial c_n(z)}{\partial t} \cdot \epsilon_A \cdot \delta A \cdot \delta z \quad (2.1.2.a)$$

For a differential  $\delta z$ , equation 2.1.2.a can be written as

$$-\frac{\partial c_n}{\partial z} v_z \cdot \epsilon_A \cdot \delta A \cdot \delta z + \left( \frac{g}{2} \bar{c}_n + \frac{g}{2} \bar{c}_{n-1} - g \cdot c_n \right) \delta A \cdot \delta z + R \cdot \epsilon_A \cdot \delta A \cdot \delta z = \frac{\partial c_n}{\partial t} \epsilon_A \cdot \delta A \cdot \delta z$$



Rearranging and dividing by  $\epsilon_A \cdot \delta A \cdot \delta z$ ,

$$\frac{\partial c_n}{\partial t} + v_z \cdot \frac{\partial c_n}{\partial t} + \frac{g}{\epsilon_A} \left[ c_n - \frac{1}{2} (\bar{c}_n + \bar{c}_{n-1}) \right] = R \quad (2.1.2.b)$$

ii) Mass balance of component i in the stagnant phase at position n:

The stagnant phase receives equal volumes from the lower as well as the upper adjacent section of moving phase, each being equal to  $\frac{g}{2}$  per unit volume of bed per unit time. Correspondingly, the stagnant phase sheds equivalent amounts of fluid into the two adjacent sections of moving phase. The balance equation is written as

$$\begin{aligned} \frac{g}{2} c_{n+1}(z) \cdot \delta A \cdot \delta z + \frac{g}{2} c_n(z) \cdot \delta A \cdot \delta z - g \cdot \bar{c}_n(z) \cdot \delta A \cdot \delta z + \bar{R} \cdot \epsilon_B \cdot \delta A \cdot \delta z \\ = \frac{\partial \bar{c}_n}{\partial t} \cdot \epsilon_B \cdot \delta A \cdot \delta z \end{aligned} \quad (2.1.2.c)$$

Dividing by  $\epsilon_B \cdot \delta A \cdot \delta z$  and rearranging, equation 2.1.2.c becomes

$$\frac{\partial \bar{c}_n}{\partial t} + \frac{g}{\epsilon_B} \left[ \bar{c}_n - \frac{1}{2} (c_{n+1} + c_n) \right] = \bar{R} \quad (2.1.2.d)$$

As in Section 2.1.1, the discrete nature of equations 2.1.2.b and 2.1.2.d can be smoothed out by using a Taylor series approximation over length  $\lambda$ .

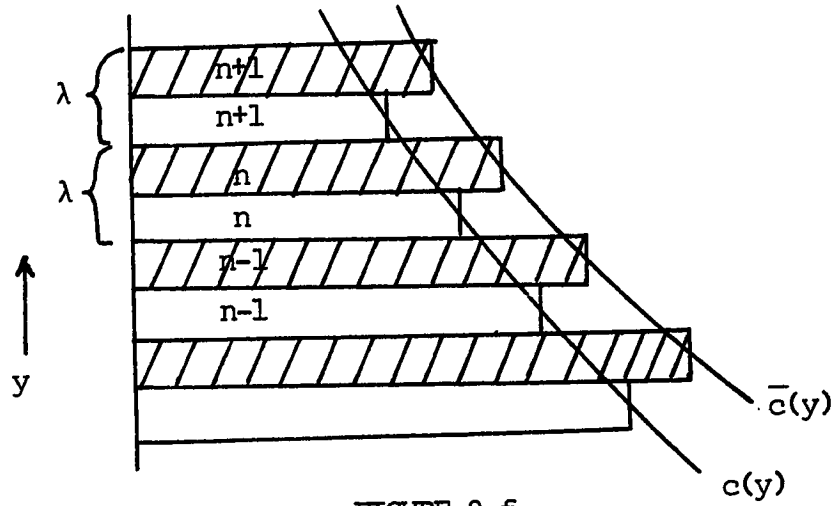


FIGURE 2.f

In order to smooth eqn. 2.1.2.b, the mass balance equation for the moving phase, let

$$c_n = c(y)$$

Using the Taylor series up to second order terms and referring to Fig. 2.f,

$$\begin{aligned}\bar{c}_n &= \bar{c}(y + \frac{\lambda}{2}) = \bar{c}(y) + \frac{\lambda}{2} \left( \frac{\partial \bar{c}}{\partial y} \right)_y + \frac{1}{2} \left( \frac{\lambda}{2} \right)^2 \left( \frac{\partial^2 \bar{c}}{\partial y^2} \right)_y \\ \bar{c}_{n+1} &= \bar{c}(y - \frac{\lambda}{2}) = \bar{c}(y) - \frac{\lambda}{2} \left( \frac{\partial \bar{c}}{\partial y} \right)_y + \frac{1}{2} \left( \frac{\lambda}{2} \right)^2 \left( \frac{\partial^2 \bar{c}}{\partial y^2} \right)_y\end{aligned}$$

Substituting in eqn. 2.1.2.b, the following equation of continuity in the moving phase is obtained:

$$\frac{\partial c}{\partial t} + v_z \frac{\partial c}{\partial z} + \frac{g}{\epsilon_A} (c - \bar{c}) - \frac{1}{2} \cdot \frac{g}{\epsilon_A} \left( \frac{\lambda}{2} \right)^2 \cdot \frac{\partial^2 \bar{c}}{\partial y^2} = R \quad (2.1.2.e)$$

In order to smooth eqn. 2.1.2.d, the mass balance equation for the stagnant phase, let

$$\bar{c}_n = \bar{c}(y)$$

Hence,

$$c_n = c(y - \frac{\lambda}{2}) = c(y) - \frac{\lambda}{2} \left( \frac{\partial c}{\partial y} \right)_y + \frac{1}{2} \left( \frac{\lambda}{2} \right)^2 \cdot \left( \frac{\partial^2 c}{\partial y^2} \right)_y$$

$$c_{n+1} = c(y + \frac{\lambda}{2}) = c(y) + \frac{\lambda}{2} \left( \frac{\partial c}{\partial y} \right)_y + \frac{1}{2} \left( \frac{\lambda}{2} \right)^2 \cdot \left( \frac{\partial^2 c}{\partial y^2} \right)_y$$

Substituting in eqn. 2.1.2.d, the following equation of continuity in the stagnant phase is obtained:

$$\frac{\partial \bar{c}}{\partial t} + \frac{g}{\epsilon_B} (\bar{c} - c) - \frac{1}{2} \frac{g}{\epsilon_B} \left( \frac{\lambda}{2} \right)^2 \cdot \frac{\partial^2 c}{\partial y^2} = \bar{R} \quad (2.1.2.f)$$

As in Section 2.1.1, two coupled partial differential equations represent the material balance in the packed bed. The axial mixing terms are the same as in Mechanism I. However, the radial mixing in this mechanism is generated by two second order differential terms, one in each equation.

## 2.2 Energy Balance Equations

There are three phases to contend with in order to represent heat transfer in packed beds, namely, the moving phase, the stagnant phase and the solid phase. Heat transfer occurs between all the three phases, and thus is responsible for the overall dispersion of heat in packed beds. The convective heat transfer between the stag-

nant phase and the solid is assumed to be negligible. Dispersion of heat is also generated by pure heat conduction in the solid phase and through the stationary fluid interstices. Fig. 2.a shows the artificial "necks" where this heat transfer resistance due to conduction is assumed to be concentrated.

The heat transfer equations are written for mixing Mechanism I; and, although it has been assumed catalyst particles are non-porous in the material balance equations, a heat source due to chemical reaction is included in the solid phase, for the sake of generality.

As in Section 2.1, the heat equations are written with the packed bed divided into discrete sections of length  $\lambda$  along the radial direction (y coordinate). However, each phase is taken to be continuous along the z direction. Balance equations are written for each phase across a cross-sectional area  $\delta A$  of the bed at an arbitrary point at distance z from the entrance of the bed and at section n along the radial direction.

i) Heat balance in the moving phase at position n:

The net heat input per unit time in an elemental volume  $\delta A \cdot \delta z$  of the bed, due to the convective flow of the moving phase is

$$\left( \alpha \cdot c_p \cdot T_n(z) \cdot v_z \cdot \epsilon_A \cdot \delta A - \alpha \cdot c_p \cdot T_n(z+\delta z) \cdot v_z \cdot \epsilon_A \cdot \delta A \right)$$

where,  $\alpha$  = density of the fluid

$c_p$  = heat capacity of the fluid.

$T_n(z)$  = temperature of the moving phase at section n and axial distance z.

The net heat input per unit time due to the interphase volumetric flow by Mechanism I is

$$\left[ \alpha \cdot c_p \cdot g \cdot \bar{T}_n(z) \cdot \delta A \cdot \delta z - \alpha \cdot c_p \cdot g \cdot T_n(z+\delta z) \cdot \delta A \cdot \delta z \right]$$

where,  $\bar{T}_n(z)$  = temperature of the stagnant phase at section n and axial distance z.

The net heat input per unit time due to the convective heat transfer between the moving fluid and the adjacent solid particles is

$$\left[ h \cdot \delta S \cdot \left[ \hat{T}_{n-1}(z) - T_n(z) \right] \cdot \delta A \cdot \delta z - h \cdot \delta S \cdot \left[ T_n(z) - \hat{T}_{n+1}(z) \right] \cdot \delta A \cdot \delta z \right]$$

where, h = heat transfer coefficient between the moving fluid and the catalyst surface.

$\delta S$  = surface area of the particle which is effective in convective heat transfer between moving fluid and solid per unit volume of the bed.

$\hat{T}_n(z)$  = temperature of the solid phase at section n and axial distance z.

The balance equation is

$$\begin{aligned} & \alpha \cdot c_p \cdot T_n(z) \cdot v_z \cdot \epsilon_A \cdot \delta A - \alpha \cdot c_p \cdot T_n(z+\delta z) \cdot v_z \cdot \epsilon_A \cdot \delta A \\ & + \alpha \cdot c_p \cdot g \cdot \bar{T}_n(z) \cdot \delta A \cdot \delta z - \alpha \cdot c_p \cdot g \cdot T_n(z+\delta z) \cdot \delta A \cdot \delta z \\ & + h \cdot \delta S \cdot \left[ \hat{T}_{n-1}(z) - T_n(z) \right] \cdot \delta A \cdot \delta z - h \cdot \delta S \cdot \left[ T_n(z) - \hat{T}_{n+1}(z) \right] \cdot \delta A \cdot \delta z \\ & + \epsilon_A \cdot R \cdot (-\Delta H) \cdot \delta A \cdot \delta z = \frac{\partial}{\partial t} (\alpha \cdot c_p \cdot T_n(z) \cdot \epsilon_A \cdot \delta A \cdot \delta z) \end{aligned} \quad (2.2.a)$$

where,  $\Delta H$  = heat of chemical reaction.

For a differential  $\delta z$ , equation 2.2.a can be written as

$$\begin{aligned} & - \frac{\partial T_n}{\partial z} \cdot \alpha \cdot c_p \cdot v_z \cdot \epsilon_A \cdot \delta A \cdot \delta z + \alpha \cdot c_p \cdot g \cdot \delta A \cdot \delta z (\bar{T}_n - T_n) \\ & - 2h \cdot \delta S \cdot \delta A \cdot \delta z \left[ T_n - \frac{1}{2} (\hat{T}_{n+1} + \hat{T}_{n-1}) \right] + \epsilon_A \cdot R(-\Delta H) \cdot \delta A \cdot \delta z \\ & = \alpha \cdot c_p \cdot \epsilon_A \cdot \delta A \cdot \delta z \cdot \frac{\partial T_n}{\partial t} \end{aligned}$$

Rearranging and dividing by  $\alpha \cdot c_p \cdot \epsilon_A \cdot \delta A \cdot \delta z$

$$\frac{\partial T_n}{\partial t} + v_z \frac{\partial T_n}{\partial z} + \frac{g}{\epsilon_A} (T_n - \bar{T}_n) + \frac{2h \cdot \delta S}{\alpha c_p \epsilon_A} \left[ T_n - \frac{1}{2} [\hat{T}_{n+1} + \hat{T}_{n-1}] \right] = \frac{R(-\Delta H)}{\alpha c_p} \quad (2.2.b)$$

The discrete nature of equation 2.2.b along the radial direction is smoothed out by using Taylor series approximation over length  $\lambda$ .

$$\hat{T}_{n+1} = \hat{T}(y+\lambda) = \hat{T}(y) + \lambda \cdot \left( \frac{\partial \hat{T}}{\partial y} \right)_y + \frac{1}{2} \cdot \lambda^2 \cdot \frac{\partial^2 \hat{T}}{\partial y^2}$$

$$\hat{T}_{n-1} = \hat{T}(y-\lambda) = \hat{T}(y) - \lambda \cdot \left( \frac{\partial \hat{T}}{\partial y} \right)_y + \frac{1}{2} \cdot \lambda^2 \cdot \frac{\partial^2 \hat{T}}{\partial y^2}$$

Substituting in equation 2.2.b,

$$\frac{\partial T}{\partial t} + v_z \frac{\partial T}{\partial z} + \frac{g}{\epsilon_A} (T - \bar{T}) + \frac{2h \cdot \delta S}{\alpha c_p \epsilon_A} (T - \hat{T}) - \frac{h \cdot \delta S \cdot \lambda^2}{\alpha c_p \epsilon_A} \frac{\partial^2 \hat{T}}{\partial y^2} = \frac{R(-\Delta H)}{\alpha c_p} \quad (2.2.c)$$

The third and fourth terms in equation 2.2.c generate the axial mixing of heat due to interaction of the moving phase with the stagnant phase and the solid phase, respectively. The last term on the left

hand side represents the radial heat dispersion, due to convective heat transfer with the solid.

ii) Heat balance in the stagnant phase at position n:

It is assumed that there is no convective heat transfer between the stagnant phase and the solid. There is interaction with the moving phase, however, due to the volumetric exchange by Mechanism I. The heat balance equation is

$$\left[ \frac{g}{2} T_{n+1}(z) + \frac{g}{2} T_{n-1}(z) - g \bar{T}_n(z+\delta z) \right] \alpha \cdot c_p \cdot \delta A \cdot \delta z + \epsilon_B \cdot \bar{R} \cdot (-\Delta H) \cdot \delta A \cdot \delta z$$

$$= \frac{\partial}{\partial t} (\alpha \cdot c_p \cdot \bar{T}_n(z) \cdot \epsilon_B \cdot \delta A \cdot \delta z) \quad (2.2.d)$$

Once again, using the Taylor series approximation,

$$T_{n+1} + T_{n-1} = 2T + \lambda^2 \frac{\partial^2 T}{\partial y^2} \quad (2.2.e)$$

Hence, the continuous form of equation (2.2.d) is

$$\frac{\partial \bar{T}}{\partial t} + \frac{g}{\epsilon_B} (\bar{T} - T) - \frac{g \lambda^2}{2 \epsilon_B} \cdot \frac{\partial^2 T}{\partial y^2} = \frac{\bar{R} (-\Delta H)}{\alpha c_p} \quad (2.2.f)$$

Equation 2.2.f is quite analogous to the corresponding mass transfer equation (2.1.1.f). The second term is the axial heat mixing term and the third term is due to radial heat mixing.

iii) Heat balance in the solid phase at position n:

In the heat balance for the solid phase there is convective heat transfer between it and the moving fluid and there is con-

duction in both the radial and the axial direction. Referring to Fig. 2.a, the heat balance equation is,

$$\begin{aligned}
 & h \cdot \delta S \cdot \delta A \cdot \delta z \left[ \bar{T}_{n-1}(z) - \hat{T}_n(z) \right] - h \cdot \delta S \cdot \delta A \cdot \delta z \left[ \bar{T}_n(z) - T_{n+1}(z) \right] \\
 & + k_s \frac{\left[ \bar{T}_{n-2}(z) - \hat{T}_n(z) \right]}{\lambda} \hat{S} \cdot \delta A \cdot \delta z - k_s \frac{\left[ \bar{T}_n(z) - \hat{T}_{n+2}(z) \right]}{\lambda} \hat{S} \cdot \delta A \cdot \delta z \\
 & - \left( q_z|_{z+\delta z} - q_z|_z \right)_n \hat{S} \cdot \delta A \cdot \delta z + \hat{R} \cdot \rho_B \cdot (-\Delta H) \cdot \delta A \cdot \delta z = \frac{\partial}{\partial t} \left( \rho_B \cdot \hat{C}_P \cdot \hat{T}_n(z) \cdot \delta A \cdot \delta z \right)
 \end{aligned}
 \tag{2.2.g}$$

where,  $k_s$  = thermal conductivity of the solid particles

$\hat{S}$  = cross-sectional area of the "necks" which is effective in conductive heat transfer between adjacent particles, per unit volume of the bed.

$(q_z)_n$  = conductive heat flux in the "necks" (solid phase) in the axial direction at section n.

$\hat{R}$  = rate of production of i by chemical reaction, moles of i/mass of catalyst-time, in the solid phase.

$\rho_B$  = bulk density of the catalyst in the bed.

$\hat{C}_P$  = heat capacity of the solid catalyst.

For a differential  $\delta z$ , eqn. 2.2.g is written as

$$\begin{aligned}
 & h \cdot \delta S \cdot \delta A \cdot \delta z (T_{n+1} + T_{n-1} - 2\hat{T}_n) + \frac{k_s \cdot \hat{S} \cdot \delta A \cdot \delta z}{\lambda} (\hat{T}_{n+2} + \hat{T}_{n-2} - 2\hat{T}_n) \\
 & - \lambda \frac{\partial (q_z)_n}{\partial z} \hat{S} \cdot \delta A \cdot \delta z + \hat{R} \cdot \rho_B \cdot (-\Delta H) \delta A \cdot \delta z = \frac{\partial}{\partial t} (\rho_B \cdot \hat{C}_P \cdot \hat{T}_n \cdot \delta A \cdot \delta z)
 \end{aligned}$$

Assuming Fourier's law applies,



$$(q_z)_n = -k_s \cdot \frac{\partial \hat{T}_n}{\partial z}$$

Substituting,

$$\begin{aligned} h \cdot \delta S \cdot \delta A \cdot \delta z (T_{n+1} + T_{n-1} - 2\hat{T}_n) + \frac{k_s \cdot \delta S \cdot \delta A \cdot \delta z}{\lambda} (\hat{T}_{n+2} + \hat{T}_{n-2} - 2\hat{T}_n) \\ + \lambda \cdot k_s \cdot \frac{\partial^2 \hat{T}_n}{\partial z^2} \delta S \cdot \delta A \cdot \delta z + \hat{R} \cdot \rho_B \cdot (-\Delta H) \cdot \delta A \cdot \delta z = \frac{\partial}{\partial t} (\rho_B \cdot \hat{C}_p \cdot \hat{T}_n \cdot \delta A \cdot \delta z) \end{aligned} \quad (2.2.h)$$

Using Taylor series,

$$\hat{T}_{n+2} + \hat{T}_{n-2} = 2\hat{T} + \lambda^2 \cdot \frac{\partial^2 \hat{T}}{\partial y^2} \quad (2.2.i)$$

Substituting the continuous forms of equations 2.2.d and 2.2.i and dividing by  $\rho_B \hat{C}_p \delta A \delta z$ ,

$$\begin{aligned} \frac{\partial T}{\partial t} + \frac{2h \cdot \delta S}{\rho_B \hat{C}_p} (\hat{T} - T) - \frac{k_s \cdot \delta S \cdot \lambda}{\rho_B \hat{C}_p} \frac{\partial^2 \hat{T}}{\partial z^2} - \frac{k_s \cdot \delta S \cdot \lambda}{\rho_B \hat{C}_p} \frac{\partial^2 T}{\partial y^2} - \frac{h \cdot \delta S \cdot \lambda^2}{\rho_B \hat{C}_p} \frac{\partial^2 T}{\partial y^2} \\ = \frac{\hat{R} \rho_B (-\Delta H)}{\rho_B \hat{C}_p} \end{aligned} \quad (2.2.j)$$

The second and last terms on the left hand side of eqn. 2.2.j represent the axial and radial heat mixing terms, respectively, due to convective heat transfer between the solid and the moving fluid. The third and fourth terms are the conduction terms in the axial and radial directions, respectively.

### 3. DISPERSION IN ONE-DIMENSIONAL, ISOTHERMAL, NON-REACTIVE PACKED BEDS

#### 3.1. Moment Analysis

In order to evaluate the axial dispersion in a packed bed, a moment analysis of the equations is done. Consider a unit pulse of a tracer injected at time  $t = 0$  on the plane  $z = 0$ . The solution is assumed independent of  $y$ , so equations for both mechanisms I and II are the same. With no chemical reaction, the equations are:

$$\frac{\partial c}{\partial t} + v_z \frac{\partial c}{\partial z} + \frac{g}{\epsilon_A} (c - \bar{c}) = 0 \quad (3.1.a)$$

$$\frac{\partial \bar{c}}{\partial t} + \frac{g}{\epsilon_B} (\bar{c} - c) = 0 \quad (3.1.b)$$

$$c(z, 0) = \delta(z) \quad ; \quad \bar{c}(z, 0) = \delta(z) \quad (3.1.c)$$

The  $n$ th moment of  $c(z, t)$ ,  $\mu_n(t)$ , is given by

$$\mu_n(t) = \int_{-\infty}^{\infty} z^n \cdot c(z, t) \cdot dz$$

$$n = 0, 1, 2, \dots, \infty$$

Also, defining the  $n$ th moment of  $\bar{c}(z, t)$ ,  $\bar{\mu}_n(t)$ , as

$$\bar{\mu}_n(t) = \int_{-\infty}^{\infty} z^n \cdot \bar{c}(z, t) \cdot dz$$

Therefore, the moment equations are written as

$$\frac{d\mu_n}{dt} - n v_z \mu_{n-1} + \frac{g}{\epsilon_A} (\mu_n - \bar{\mu}_n) = 0 \quad (3.1.d)$$

$$\frac{d\bar{\mu}_n}{dt} + \frac{g}{\epsilon_B} (\bar{\mu}_n - \mu_n) = 0 \quad (3.1.e)$$

$$\mu_0(o) = 1; \mu_1(o) = \mu_2(o) = \dots = 0 \quad (3.1.f)$$

$$\bar{\mu}_0(o) = 1 \quad ; \quad \bar{\mu}_1(o) = \bar{\mu}_2(o) = \dots = 0 \quad (3.1.g)$$

Solving the equations with the help of laplace transforms, the following are the expressions for the 0<sup>th</sup>, 1<sup>st</sup> and 2<sup>nd</sup> moments.

$$\mu_0 = 1$$

$$\bar{\mu}_0 = 1$$

$$\mu_1 = \left( \frac{\epsilon_A v_z}{\epsilon_T} \right) t + \frac{\epsilon_B v_z}{\epsilon_T} \frac{\epsilon_A \epsilon_B}{g \epsilon_T} (1 - e^{-t / \frac{\epsilon_A \epsilon_B}{g \epsilon_T}})$$

$$\bar{\mu}_1 = \left( \frac{\epsilon_A v_z}{\epsilon_T} \right) t - \frac{\epsilon_A v_z}{\epsilon_T} \cdot \frac{\epsilon_A \epsilon_B}{g \epsilon_T} \cdot (1 - e^{-t / \frac{\epsilon_A \epsilon_B}{g \epsilon_T}})$$

$$\begin{aligned} \mu_2 = 2v_z^2 \left\{ A^2 - A^2 e^{-t/A} - A t e^{-t/A} \right. \\ + 2 \frac{g}{\epsilon_B} [ A^2 t + A^2 t e^{-t/A} - 2A^3 (1 - e^{-t/A}) ] \\ \left. + \left( \frac{g}{\epsilon_B} \right)^2 \left[ \frac{A^2 t^2}{2} + 2A^4 (1 - e^{-t/A}) - 2A^3 t + A^2 - A^2 e^{-t/A} - A t e^{-t/A} \right] \right\} \end{aligned}$$

$$\text{where } A = \frac{\epsilon_A \epsilon_B}{g \epsilon_T}.$$

$$\begin{aligned} \bar{\mu}_2 = \frac{2g v_z^2}{\epsilon_B} \left\{ A^2 t + A^2 t e^{-t/A} - 2A^3 (1 - e^{-t/A}) \right. \\ \left. + \frac{g}{\epsilon_B} \left[ \frac{A^2 t^2}{2} + 3A^4 (1 - e^{-t/A}) - 2A^3 t - A^3 t e^{-t/A} \right] \right\} \end{aligned}$$

The average pulse velocity in the moving phase,

$$\bar{v} = \frac{d\bar{z}}{dt} = \frac{d(\frac{\mu_1}{\mu_0})}{dt} = \frac{\epsilon_A v_z}{\epsilon_T} + \frac{\epsilon_B v_z}{\epsilon_T} \cdot e^{-t/\frac{\epsilon_A \epsilon_B}{g \epsilon_T}} \quad (3.1.h)$$

and the asymptotic values of the velocity are:

$$\begin{aligned} t \rightarrow 0 & : \bar{v} = v_z \\ t \rightarrow \infty & : \bar{v} = \frac{\epsilon_A v_z}{\epsilon_T} \end{aligned}$$

Similarly, in the stagnant phase,

$$\bar{v} = \frac{d\bar{z}}{dt} = \frac{d(\frac{\bar{\mu}_1}{\bar{\mu}_0})}{dt} = \frac{\epsilon_A v_z}{\epsilon_T} - \frac{\epsilon_A v_z}{\epsilon_T} \cdot e^{-t/\frac{\epsilon_A \epsilon_B}{g \epsilon_T}} \quad (3.1.i)$$

and the asymptotic values of the velocity are:

$$\begin{aligned} t \rightarrow 0 & : \bar{v} = 0 \\ t \rightarrow \infty & : \bar{v} = \frac{\epsilon_A v_z}{\epsilon_T} \end{aligned}$$

The asymptotic velocity for large  $t$  is the same in both phases,

$$v = \bar{v} = \bar{\bar{v}} = \left( \frac{\epsilon_A v_z}{\epsilon_T} \right) \quad (3.1.j)$$

The deviation of the second moment about the mean,  $\omega$ , is given

by

$$\omega^2 = \left\{ \frac{\mu_2}{\mu_0} - (\bar{z})^2 \right\}$$

and the axial effective dispersion coefficient in the moving phase is defined as,

$$(De)_z = \frac{1}{2} \frac{d\omega^2}{dt}$$

The asymptotic values of the dispersivity are,

$$t \rightarrow 0 : (De)_z = 0 \quad (3.1.k)$$

$$t \rightarrow \infty : (De)_z = \left(\frac{\epsilon_A^V z}{\epsilon_T}\right)^2 \frac{\epsilon_B^2}{g\epsilon_T} . \quad (3.1.l)$$

Similarly, in the stagnant phase the deviation from the mean,  $\bar{\omega}$ , and the effective axial dispersion coefficient,  $(\bar{De})_z$ , are defined as

$$\bar{\omega}^2 = \left\{ \frac{\bar{\mu}_2}{\bar{\mu}_0} - (\bar{z})^2 \right\}$$

and

$$(\bar{De})_z = \frac{1}{2} \frac{d \bar{\omega}^2}{dt} .$$

The asymptotic values of the dispersivity are,

$$t \rightarrow 0 : (\bar{De})_z = 0 \quad (3.1.m)$$

$$t \rightarrow \infty : (\bar{De})_z = \left(\frac{\epsilon_A^V z}{\epsilon_T}\right)^2 \frac{\epsilon_B^2}{g\epsilon_T} . \quad (3.1.n)$$

The asymptotic axial dispersivity for large  $t$  is the same in both phases, namely,

$$D_z = (De)_z = (\bar{De})_z = \left(\frac{\epsilon_A^V z}{\epsilon_T}\right)^2 \frac{\epsilon_B^2}{g\epsilon_T} . \quad (3.1.o)$$

A moment analysis of the one-dimensional Fickian model,

$$\frac{\partial c_f}{\partial t} + v \frac{\partial c_f}{\partial z} = D \frac{\partial^2 c_f}{\partial z^2} \quad (3.1.p)$$

where  $c_f$  = concentration

$v$  = interstitial velocity

$D$  = axial effective diffusion coefficient.

gives a constant velocity,  $v$ , of the pulse and a constant effective diffusion coefficient,  $D$ . The plug flow model would have the same velocity, but, of course, there would be no diffusion.

### 3.2 Pulse Injection Simulation

A pulse injection only in the moving phase at the entrance to the bed gives an output which is identical to the residence time distribution. For this reason, it is quite an important test to perform.

In this section a general pulse test is simulated which, however, would not give the residence time distribution as the output. Consider a total of  $m$  moles of tracer injected as a pulse at the entrance of the bed. It is assumed the injected mass divides itself at the entrance of the bed into the two phases as the ratio of the relative volumes of the two phases. This means that the mass enters the two phases in equal concentrations. Thus,  $m_1 = \frac{\epsilon_A m}{\epsilon_T}$  moles go into the moving phase and  $m_2 = \frac{\epsilon_B m}{\epsilon_T}$  moles go into the stagnant phase.

The equations are:

$$\frac{\partial c}{\partial t} + v_z \frac{\partial c}{\partial z} + \frac{g}{\epsilon_A}(c - \bar{c}) = m \cdot \delta(t) \cdot \delta(z) \quad (3.2.a)$$

$$\frac{\partial \bar{c}}{\partial t} + \frac{g}{\epsilon_B}(\bar{c} - c) = m \cdot \delta(t) \cdot \delta(z) \quad (3.2.b)$$

Solving these equations by laplace transforms (Deans 1963), the following expressions for the concentration profiles are obtained:

$$c = \frac{m}{v_z} \cdot e^{\frac{-gz}{\epsilon_A v_z}} \cdot e^{\frac{-g}{\epsilon_B} \left(t - \frac{z}{v_z}\right)} \cdot \left\{ \sqrt{\frac{zg^2}{\epsilon_A \epsilon_B v_z \left(t - \frac{z}{v_z}\right)}} I_1 \left( 2 \sqrt{\frac{zg^2 \left(t - \frac{z}{v_z}\right)}{\epsilon_A \epsilon_B v_z}} \right) \right\}$$

$$+ \left. \delta\left(t - \frac{z}{v_z}\right) \right\} \\ + \frac{mg}{\epsilon_A v_z} \cdot e^{\frac{-gz}{\epsilon_A v_z}} \cdot e^{\frac{-g}{\epsilon_B} \left(t - \frac{z}{v_z}\right)} \cdot I_0 \left( 2 \sqrt{\frac{zg^2 \left(t - \frac{z}{v_z}\right)}{\epsilon_A \epsilon_B v_z}} \right) \quad (3.2.c)$$

$$\bar{c} = \frac{mg}{\epsilon_B v_z} \cdot e^{\frac{-gz}{\epsilon_A v_z}} \cdot e^{\frac{-g}{\epsilon_B} \left(t - \frac{z}{v_z}\right)} \cdot I_0 \left( 2 \sqrt{\frac{zg^2 \left(t - \frac{z}{v_z}\right)}{\epsilon_A \epsilon_B v_z}} \right) \\ + \frac{m}{v_z} \cdot e^{\frac{-gz}{\epsilon_A v_z}} \cdot e^{\frac{-g}{\epsilon_B} \left(t - \frac{z}{v_z}\right)} \cdot \sqrt{\frac{zg^2 \left(t - \frac{z}{v_z}\right)}{\epsilon_A \epsilon_B v_z}} \cdot I_1 \left( 2 \sqrt{\frac{zg^2 \left(t - \frac{z}{v_z}\right)}{\epsilon_A \epsilon_B v_z}} \right) \\ + m e^{\frac{-g}{\epsilon_B} t} \delta(z) \quad (3.2.d)$$

where  $I_0$  and  $I_1$  are the modified Bessel functions of zero and first order, respectively.

The first term in eqn. 3.2.c. is the contribution from the injection in the moving phase to the concentration in the moving phase. The delta function represents a spike which moves at velocity  $v_z$ ; it is the amount of tracer that never ever entered the stagnant phase. The second term in eqn. 3.2.c. is the contribution from the injection in the stagnant phase to the concentration in the moving phase. The first term in eqn. 3.2.d. is the contribution from the injection in the moving phase to the concentration in the stagnant phase. The second term in eqn. 3.2.d. is the contribution from the injection in the stagnant phase to the concentration in the stagnant phase. The third term represents the spike that remains at the injection point; it is the amount of tracer that never left the stagnant phase.

Writing the equations in dimensionless form and neglecting the wave front spike,

$$\left(\frac{c}{m} \frac{dp}{dz}\right) = \frac{X}{2\left(\frac{\epsilon_T}{\epsilon_A} \tau - z_0\right)} \cdot (\text{exp.}) \cdot I_1(X) + \left(\frac{\epsilon_B}{\epsilon_T}\right)^2 \cdot Pe_z \cdot (\text{exp.}) \cdot I_0(X) \quad (3.2.e)$$

$$\left(\frac{c}{m} \frac{dp}{dz}\right) = \frac{\epsilon_A \epsilon_B Pe_z}{\epsilon_T^2} \cdot (\text{exp.}) \cdot I_0(X) + \frac{X}{z z_0} \cdot (\text{exp.}) \cdot I_1(X) \quad (3.2.f)$$

where,  $d_p$  = particle diameter

$$\tau = \frac{\epsilon_A v_z t}{\epsilon_T d_p} ; \text{ dimensionless time}$$

$$z_0 = z/d_p ; \text{ dimensionless distance}$$

$$Pe_z = \frac{\frac{\epsilon_A v_z}{\epsilon_T} \cdot d_p}{D_z} = \frac{d_p g \epsilon_T^2}{\epsilon_A v_z \epsilon_B^2} ; \text{ asymptotic Peclet number}$$

$$X = \frac{2\epsilon_A \epsilon_B^2 Pe_z}{\epsilon_T^2} \cdot \sqrt{\frac{\epsilon_T}{z_0 \left(\frac{\epsilon_A}{\epsilon_T} \tau - z_0\right)}} ; \text{ dimensionless argument}$$

$$(\text{exp.}) = e^{-\left[\left(\frac{\epsilon_B}{\epsilon_T}\right)^2 Pe_z \cdot z_0 - \frac{\epsilon_A \epsilon_B Pe_z}{\epsilon_T^2} \left(\frac{\epsilon_T}{\epsilon_A} \tau - z_0\right)\right]}$$

The Fickian model gives the following solution for pulse injection:

$$\left(\frac{c_f d_p}{m}\right) = \sqrt{\frac{Pe_f}{4\pi\tau_f}} e^{-\frac{Pe_f(z_0 - \tau_f)^2}{4\tau_f}} \quad (3.2.g)$$

$$\text{where, } \tau_f = \frac{vt}{d_p} ; \text{ dimensionless time}$$

$$Pe_f = \frac{vd_p}{D} ; \text{ Peclet number}$$

For the Fickian model, the peak height is at  $z_0 = \tau_f$  ;



$$\left(\frac{c_f d_p}{m}\right)_{\max} = \sqrt{\frac{Pe_f}{4\pi\tau_f}} \quad (3.2.h)$$

On the other hand, in the case of the non-Fickian model, using the asymptotic expansion for the modified Bessel functions,

$$I_\mu(X) \approx \frac{e^X}{\sqrt{2\pi X}} + O\left(\frac{1}{X^{3/2}}\right) \quad (3.2.i)$$

the following simplifications from eqns. (3.2.e) and (3.2.f) are obtained,

$$\left(\frac{cd_p}{m}\right)_{\tau=z_0} = \frac{\epsilon_A}{\epsilon_T} \sqrt{\frac{Pe_z}{4\pi\tau}} + \frac{\epsilon_B}{\epsilon_T} \sqrt{\frac{Pe_z}{4\pi\tau}} = \sqrt{\frac{Pe_z}{4\pi\tau}} \quad (3.2.j)$$

$$\left(\frac{\bar{c} d_p}{m}\right)_{\tau=z_0} = \frac{\epsilon_A}{\epsilon_T} \sqrt{\frac{Pe_z}{4\pi\tau}} + \frac{\epsilon_B}{\epsilon_T} \sqrt{\frac{Pe_z}{4\pi\tau}} = \sqrt{\frac{Pe_z}{4\pi\tau}} \quad (3.2.k)$$

It is observed that the peak heights in both the Fickian and the non-Fickian model are identical when the pulse has progressed far enough downstream.

An interstitial average concentration is defined by

$$\left(\frac{\bar{c} d_p}{m}\right) = \frac{\epsilon_A}{\epsilon_T} \left(\frac{c d_p}{m}\right) + \frac{\epsilon_B}{\epsilon_T} \left(\frac{\bar{c} d_p}{m}\right) \quad (3.2.l)$$

where  $\left(\frac{c d_p}{m}\right)$  and  $\left(\frac{\bar{c} d_p}{m}\right)$  are obtained from equations 3.2.e and 3.2.f, respectively, where the Bessel functions need not be in the asymptotic form.

This interstitial average concentration is plotted in Figs. 3.2.a, 3.2.b, and 3.2.c, together with the corresponding Gaussian curve obtained by the Fickian model. As can be seen in Figs. 3.2.a, 3.2.b, and

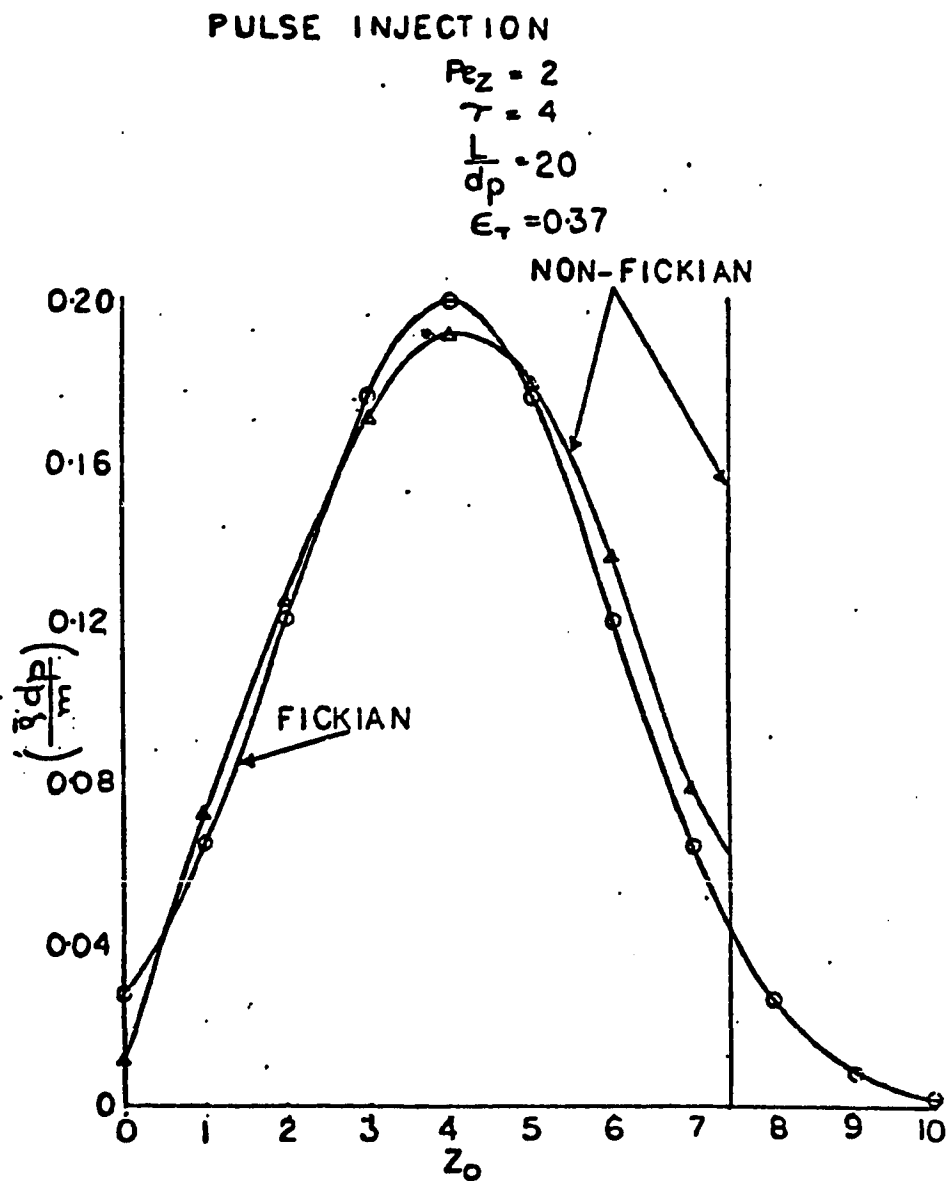


Fig. 3.2.a. Pulse test response for the Fickian and Non-Fickian models at  $\tau = 4$ .

## PULSE INJECTION

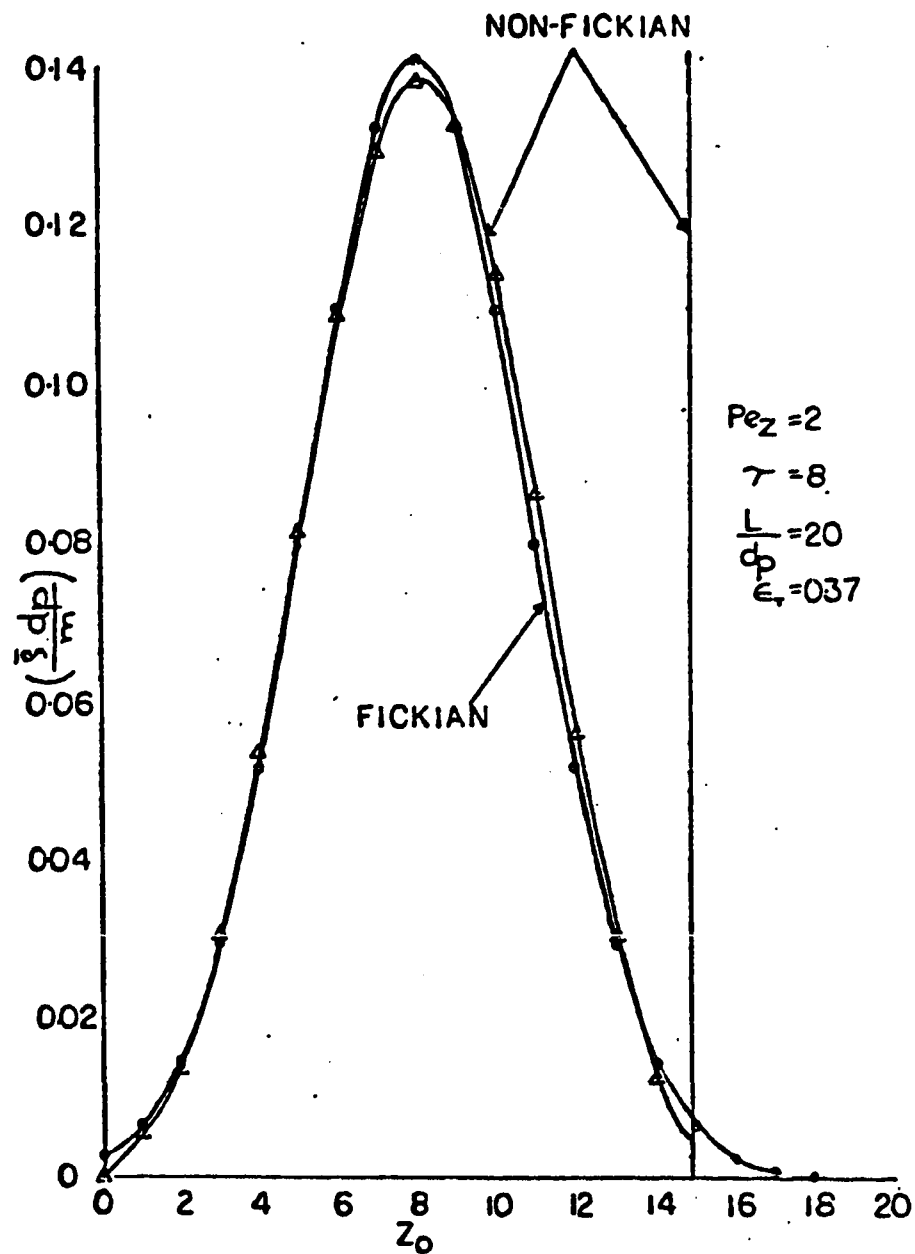


Fig. 3.2.b. Pulse test response for the Fickian and Non-Fickian models at  $T = 8$

## PULSE INJECTION

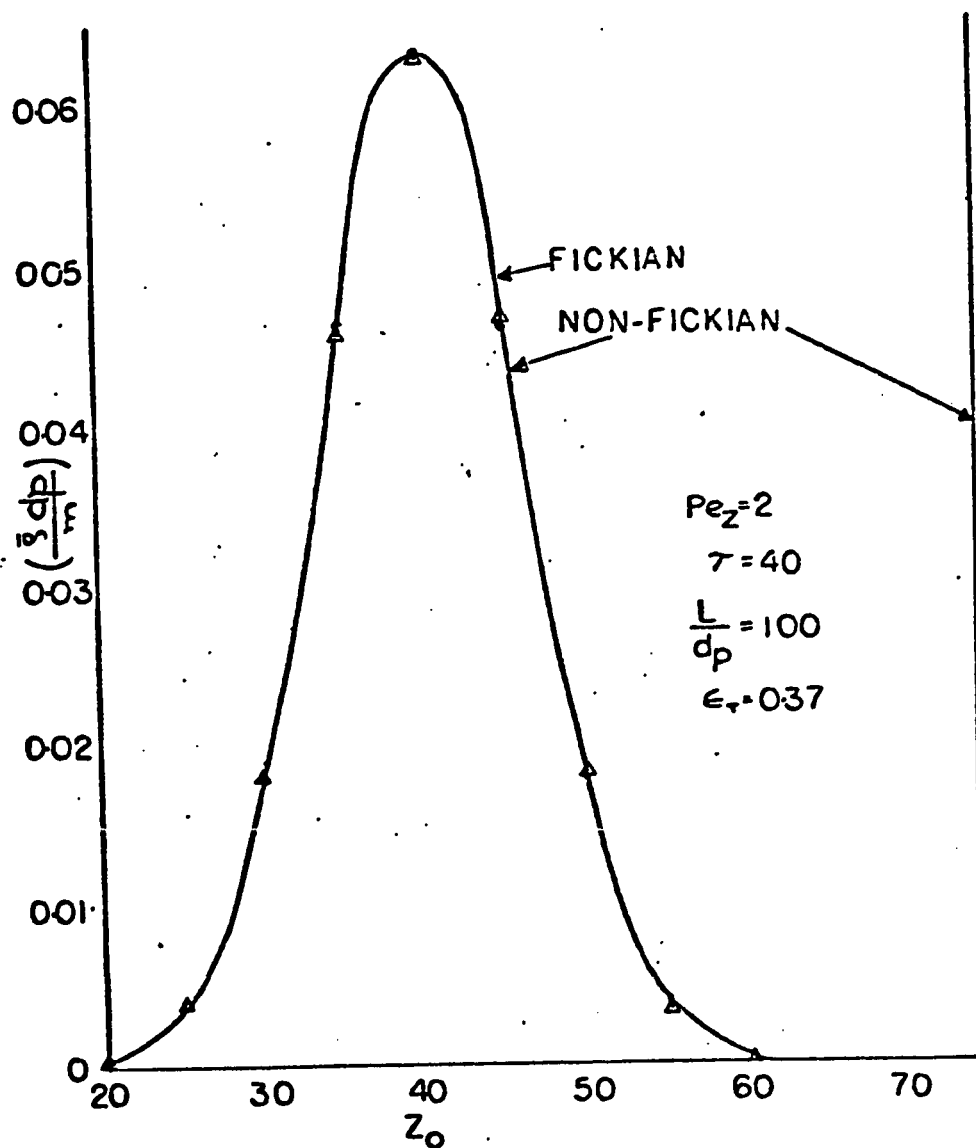


Fig. 3.2.c. Pulse test response for the Fickian and Non-Fickian models at  $\tau = 40$ .

3.2.c, the concentration profile obtained by the non-Fickian model approaches the Gaussian form of the Fickian model for large enough  $\tau$ .

The quasi-Gaussian form of the interstitial average concentration can be obtained from eqn. (3.2.1) by using the asymptotic expansion for the modified Bessel functions and the Taylor series.

$$\left(\frac{\bar{p} d}{m}\right)_{\text{large } \tau} = \left\{ \frac{\epsilon_A}{\epsilon_T} \left[ \frac{\epsilon_A}{\epsilon_T} c_1 + \frac{\epsilon_B}{\epsilon_T} c_2 \right] + \frac{\epsilon_B}{\epsilon_T} \left[ \frac{\epsilon_A}{\epsilon_T} c_3 + \frac{\epsilon_B}{\epsilon_T} c_4 \right] \right\} \cdot \sqrt{\frac{Pe}{4\pi\tau}} e^{-\frac{Pe(\tau-z_o)^2}{4\tau}} \quad (3.2.m)$$

where,

$$c_1 = 1 - \frac{(\tau-z_o)}{4\tau} \left(1 + 3\frac{\epsilon_A}{\epsilon_B}\right) - \frac{3}{32} \left(\frac{\tau-z_o}{\tau}\right)^2 \left[ 1 - 2\frac{\epsilon_A}{\epsilon_B} + 7\left(\frac{\epsilon_A}{\epsilon_B}\right)^2 \right]$$

$$c_2 = 1 + \frac{(\tau-z_o)}{4\tau} \left(1 - \frac{\epsilon_A}{\epsilon_B}\right) + \frac{1}{32} \left(\frac{\tau-z_o}{\tau}\right)^2 \left[ 5 - 2\frac{\epsilon_A}{\epsilon_B} + 4\left(\frac{\epsilon_A}{\epsilon_B}\right)^2 \right]$$

$$c_3 = 1 + \frac{(\tau-z_o)}{4\tau} \left(1 - \frac{\epsilon_A}{\epsilon_B}\right) + \frac{1}{32} \left(\frac{\tau-z_o}{\tau}\right)^2 \left[ 5 - 2\frac{\epsilon_A}{\epsilon_B} + 4\left(\frac{\epsilon_A}{\epsilon_B}\right)^2 \right]$$

$$c_4 = 1 + \frac{(\tau-z_o)}{4\tau} \left(3 + \frac{\epsilon_A}{\epsilon_B}\right) - \frac{1}{32} \left(\frac{\tau-z_o}{\tau}\right)^2 \left[ 35 + 2\frac{\epsilon_A}{\epsilon_B} + 3\left(\frac{\epsilon_A}{\epsilon_B}\right)^2 \right]$$

When  $\left| \frac{\tau-z_o}{\tau} \right| \ll 1$ , then

$$\left(\frac{\bar{p} d}{m}\right) = \sqrt{\frac{Pe}{4\pi\tau}} e^{-\frac{Pe(\tau-z_o)^2}{4\tau}} \quad (3.2.n)$$

and the non-Fickian curve becomes Gaussian (see eqns. 3.2.g and 3.2.n).

### 3.3 Stochastic Analysis of the Pulse Test Experiment

If a single tracer molecule is injected at the entrance of the bed, the time it would take to reach the exit would be random. A tracer pulse test is nothing but the simultaneous performance of such a test on a very large number of molecules so that the concentration profile can be regarded as a frequency diagram for a very large number of individual molecule experiments.

Because of the random nature of the process of migration of the molecules towards the exit, it is amenable to stochastic analysis. There is a certain probability of the event that a tracer molecule will arrive in the interval between  $z$  and  $z + \delta z$  after a time  $t$  after injection. If this probability is multiplied by the total number of such molecules, the number of molecules in the interval  $\delta z$  and hence the concentration profile is obtained.

Buffham et al. 1970, and Buffham and Gibilaro 1970, have developed a probabilistic time-delay description of flow in packed beds. The present work, however, divides the interstitial space into two distinct well-mixed phases and hence is akin to Giddings 1965, coupling theory of chromatography. In this section it is shown that applying Giddings' stochastic approach to the pulse test gives the same solution as that of the non-Fickian model (eqn. 3.2.c and 3.2.d).

Consider a distance  $z$  from the entrance of the bed. The tracer molecule has spent an average time  $t_m = \frac{z}{\bar{v}_z}$  in the moving phase. If the actual time  $t$  has elapsed, the time spent by the molecule in the

stagnant phase is  $t_s = t - t_m = (t - \frac{z}{v_z})$ .

The parameter  $g$  has been defined as the interphase volumetric flow per unit time per unit volume of the bed. Let  $g/\epsilon_A$  be the probability per unit time that a tracer molecule will go from the moving phase (m-phase) to the stagnant phase (s-phase); and  $g/\epsilon_B$  be the probability per unit time that a tracer molecule will go from the s-phase to the m-phase. These probabilities are independent of time or of the history of the molecule.

The event that a tracer molecule will go from the m-phase to the s-phase will occur in one interval as in any other; also the occurrence of an event has no effect on whether or not another occurs. Hence, the event can be considered to be a Poisson random variable and the expected value of this random variable is  $\frac{g}{\epsilon_A} t_m = \frac{g}{\epsilon_A} \frac{z}{v_z}$ , over a period of total time  $t$  that has elapsed. The probability that the event will occur  $n$  times in this period is

$$P(E=n) = \frac{\left(\frac{g}{\epsilon_A} \frac{z}{v_z}\right)^n}{n!} e^{-\frac{gz}{\epsilon_A v_z}} \quad (3.3.a)$$

### 3.3.1 Concentration in m-phase Due to Injection in m-phase

If the tracer molecule was injected in the m-phase, in order for it to end up in the m-phase at time  $t$ , it must have gone from the s-phase to the m-phase  $n$  times. The chance that the  $n$ th time that this happens is between  $t_s$  and  $t_s + dt_s$  is the chance that it has gone from the s- to the m-phase  $(n-1)$  times and the  $n$ th time it does that is between time  $t_s$  and  $t_s + dt_s$ . The probability differential is

$$dP_n = P_n \cdot dt_s$$

$$= \frac{\left(\frac{g}{\epsilon_B} t_s\right)^{n-1} e^{-\frac{g}{\epsilon_B} t_s}}{(n-1)!} \cdot \frac{g}{\epsilon_B} dt_s . \quad (3.3.1.a)$$

The expression  $dP_n$  is the conditional probability which gives the distribution in time spent in the s-phase provided it entered the s-phase from the m-phase exactly  $n$  times. To remove this restriction,  $dP_n$  is multiplied by the probability  $P(E=n)$  that it goes from the m- to the s-phase  $n$  times and then summed over all possible values of  $n$ .

$$dP = \sum_{n=1}^{\infty} P(E=n) \cdot dP_n \quad (3.3.1.b)$$

$$= \sum_{n=1}^{\infty} \frac{\left(\frac{g}{\epsilon_A} \frac{z}{v_z}\right)^n e^{-\frac{g}{\epsilon_A} \frac{z}{v_z}}}{n!} \cdot \frac{\left(\frac{g}{\epsilon_B} t_s\right)^{n-1} e^{-\frac{g}{\epsilon_B} t_s}}{(n-1)!} \cdot \frac{g}{\epsilon_B} \cdot dt_s$$

$$dP = e^{-E} \left(\frac{g}{\epsilon_A} \frac{g}{\epsilon_B} \frac{z}{v_z} \frac{1}{t_s}\right)^{1/2} \sum_{n'=0}^{\infty} \frac{(X/2)^{2n'+1}}{n'!(n'+1)!} dt_s \quad (3.3.1.c)$$

where  $E = \left(\frac{g}{\epsilon_A} \frac{z}{v_z} + \frac{g}{\epsilon_B} t_s\right)$

$$n' = n-1$$

$$X = \left(4 \frac{g}{\epsilon_A} \frac{g}{\epsilon_B} \frac{z}{v_z} t_s\right)^{1/2}$$

$$\text{Now, } I_{\mu}(z) = \sum_{m=0}^{\infty} \frac{\left(\frac{1}{2} z\right)^{2m+\mu}}{m! \Gamma(\mu+m+1)} \quad (\text{G.N. Watson, 1944}) \quad (3.3.1.d)$$

Therefore, the probability density function,  $P = dP/dt_s$

$$P = \frac{X}{2t_s} I_1(X) \cdot e^{-E} . \quad (3.3.1.e)$$



There is a finite chance, however, that the tracer molecule may never go to the s-phase, and it is equal to  $e^{\frac{-gz}{\epsilon_A v_z}}$ . Therefore, the following distribution function may be added to the P already obtained

$$P' = e^{\frac{-gz}{\epsilon_A v_z}} \delta(t_s) \quad (3.3.1.f)$$

The Dirac delta function,  $\delta(t_s)$ , indicates that the time  $t_s$  is precisely zero for that fraction of molecules not ever going into the stagnant phase.

$$P_{\text{total}} = P + P' \quad (3.3.1.g)$$

$\frac{m}{v_z} P_{\text{total}}$  gives the same expression obtained for the moles per unit length by the non-Fickian model (the first term in eqn. 3.2.c), when the pulse is injected in the moving phase.

### 3.3.2 Concentration in m-phase Due to Injection in s-phase.

If the pulse is injected in the s-phase and the tracer molecule enters the s-phase  $n$  additional times, then it should enter the m-phase  $(n+1)$  times in order to end up in the m-phase at time  $t$ ; and the  $(n+1)$ th time should be in the interval  $dt_s$ .

$$P'_n = \frac{\left(\frac{g}{\epsilon_B} t_s\right)^n}{n!} e^{\frac{-g}{\epsilon_B} t_s} \cdot \frac{g}{\epsilon_B} \quad (3.3.2.a)$$

where,  $P'_n$  is the probability that the tracer molecule has gone from the s- to the m-phase  $n$  times and the  $(n+1)$ st time it does that is between time  $t_s$  and  $t_s + dt_s$ .

In order to remove the restriction that the transfer occurs exactly  $n$  times,  $P'_n$  is multiplied by the probability  $P(E=n)$  that it

goes from the m- to the s-phase  $n$  times and then summed over all possible values of  $n$ .

$$\begin{aligned}
 P &= \sum_{n=0}^{\infty} P(E=n) \cdot P'_n \\
 &= \frac{g}{\epsilon_B} e^{-E} \sum_{n=0}^{\infty} \frac{\left(\frac{g}{\epsilon_B} t_s\right)^n \left(\frac{gz}{\epsilon_A v_z}\right)^n}{n!n!} \\
 &= \frac{g}{\epsilon_B} e^{-E} I_0(X) \quad . \quad (3.3.2.b)
 \end{aligned}$$

$\frac{m}{V_z} P \frac{\epsilon_B}{\epsilon_A}$  gives the moles per unit length. The fraction  $\frac{\epsilon_B}{\epsilon_A}$  converts the concentration based on stagnant phase volume to the moving phase volume, which is what the second term in eqn. 3.2.c represents.

### 3.3.3 Concentration in s-phase Due to Injection in m-phase

If the tracer molecule enters the s-phase from the m-phase  $n$  times and the  $n$ th time it does that is between time  $t_m$  and  $t_m + dt_m$  then the probability distribution is

$$\frac{g}{\epsilon_A} P(E=n-1) = \frac{g}{\epsilon_A} \cdot \frac{\left(\frac{g}{\epsilon_A} \frac{z}{v_z}\right)^{n-1} e^{-\frac{gz}{\epsilon_A v_z}}}{(n-1)!} \quad (3.3.3.a)$$

The tracer molecule, however, would have gone from the s-phase to the m-phase  $(n-1)$  times, the probability distribution function of which is

$$P'_{n-1} = \frac{\left(\frac{g}{\epsilon_B} t_s\right)^{n-1} e^{-\frac{g}{\epsilon_B} t_s}}{(n-1)!} \quad (3.3.3.b)$$

Once again, the overall probability distribution function,  $P$ , re-

moving the restriction that the transfer occurs  $n$  times, is obtained as follows:

$$\begin{aligned}
 P &= \sum_{n=1}^{\infty} P(E=n-1) \frac{g}{\epsilon_A} P'_{n-1} \\
 &= \frac{g}{\epsilon_A} e^{-E} \sum_{n=1}^{\infty} \frac{\left(\frac{g}{\epsilon_A} \frac{g}{\epsilon_B} \frac{z}{v_z} t_s\right)^{n-1}}{(n-1)! (n-1)!} \\
 &= \frac{g}{\epsilon_A} e^{-E} \sum_{n'=0}^{\infty} \frac{\left(\frac{g}{\epsilon_A} \frac{g}{\epsilon_B} \frac{z}{v_z} t_s\right)^{n'}}{n'! n'!} \\
 &= \frac{g}{\epsilon_A} e^{-E} I_0(X) \quad . \quad (3.3.3.c)
 \end{aligned}$$

$\frac{m}{v_z} \cdot P \cdot \frac{\epsilon_A}{\epsilon_B}$  gives the expression for concentration in the stagnant phase which is identical to the first term in eqn. 3.2.d.

### 3.3.4 Concentration in s-phase Due to Injection in s-phase

If the tracer molecule goes from the s-phase to the m-phase  $n$  times, the probability density function is

$$P'_n = \frac{\left(\frac{g}{\epsilon_B} t_s\right)^n e^{-\frac{g}{\epsilon_B} t_s}}{n!} \quad (3.3.4.a)$$

In order for it to end up in the s-phase at time  $t$ , it should have returned from the m-phase  $n$  times and the  $n$ th time should be between time  $t_m$  and  $t_m + dt_m$  the probability distribution function for which is

$$P(E=n-1) \cdot \frac{g}{\epsilon_A} = \frac{\left(\frac{g}{\epsilon_A} \frac{z}{v_z}\right)^{n-1} e^{-\frac{g}{\epsilon_A} \frac{z}{v_z}}}{(n-1)!} \cdot \frac{g}{\epsilon_A} \quad (3.3.4.b)$$

The overall probability distribution function,  $P$ , removing the restriction that the transfer occurs  $n$  times, is

$$\begin{aligned}
 P &= \sum_{n=1}^{\infty} P_n''' P(E=n-1) \frac{g}{\epsilon_A} \\
 &= \frac{g}{\epsilon_A} e^{-E} \sum_{n=1}^{\infty} \frac{\left(\frac{g}{\epsilon_B} t_s\right)^n \left(\frac{g}{\epsilon_A} \frac{z}{v_z}\right)^{n-1}}{n! (n-1)!} \\
 &= \frac{v_z}{z} \cdot e^{-E} \sum_{n=1}^{\infty} \frac{(X/2)^{2n}}{n! (n-1)!} \\
 &= \frac{v_z}{z} e^{-E} \sum_{n'=0}^{\infty} \frac{(X/2)^{2n'+2}}{(n'+1)! n'!} \\
 &= \frac{v_z}{z} \frac{X}{2} I_1(X) \quad . \quad (3.3.4.c)
 \end{aligned}$$

Also, considering the chance that the tracer molecule never goes to the  $m$ -phase in time  $t$ , the total probability distribution is

$$P_{\text{total}} = \frac{v_z}{z} \frac{X}{2} I_1(X) + e^{\frac{-g}{\epsilon_B} t} \delta\left(\frac{z}{v_z}\right) \quad . \quad (3.3.4.d)$$

$\frac{m}{v_z} \cdot P_{\text{total}}$  gives the expression for concentration in the stagnant phase which is identical to the second and third terms in eqn. 3.2.d.

### 3.4 Frequency Response Analyses of Flow Through Packed Beds

Let  $C$  be considered the deviation of a sinusoidal signal (tracer concentration) from its average value. For purposes of calculations, it is customary to regard the signal as a complex harmonic function

with a circular frequency  $\omega$ . The value of the signal at any place in the system is given by:

$$C = Y e^{i\omega t} \quad (3.4.a)$$

$Y$  is a complex magnitude which can be represented by a radius vector in the complex plane, having a certain length (modulus) and phase angle (argument) with respect to the positive real axis.

Kramers and Alberda 1953, have compared the response function for  $n$  perfect mixers in series and the Fickian model.

The harmonic response function of one perfect mixer is

$$\frac{Y_e}{Y_i} = \frac{1}{1 + i\omega\bar{\tau}} \quad (3.4.b)$$

where,  $Y_e$  = complex magnitude of harmonic signal at the exit

$Y_i$  = complex magnitude of harmonic signal at the entrance

$\bar{\tau}$  = average residence time: volume of the mixer divided by constant volumetric flow rate.

Applying the result to  $n$  perfect mixers in series having equal times of residence  $\bar{\tau}/n$ , the response function is

$$\frac{Y_e}{Y_i} = \left(1 + \frac{i\omega\bar{\tau}}{n}\right)^{-n} \quad (3.4.c)$$

For large values of  $n$ , this can be approximated by:

$$\ln \frac{Y_e}{Y_i} = -i\omega\bar{\tau} - \frac{\omega^2\bar{\tau}^2}{2n} + i\frac{\omega^3\bar{\tau}^3}{3n^2} + \dots \quad (3.4.d)$$

The Fickian model with the usual boundary conditions

$$z = 0 \quad ; \quad vc_i = vc - D \frac{\partial c}{\partial z} \quad (3.4.e)$$

$$z = L \quad : \quad \frac{\partial c}{\partial z} = 0 \quad (3.4.f)$$

has the following frequency response solution

$$\frac{Y_e}{Y_i} = \frac{4p}{(1+p)^2 \exp \left[ \frac{-vL}{2D} (1-p) \right] - (1-p)^2 \exp \left[ \frac{-vL}{2D} (1+p) \right]} \quad (3.4.g)$$

where

$$p = \sqrt{1 + \frac{4 i \omega D}{v^2}}$$

Note that for unsteady state processes the exit boundary condition of the Fickian model (eqn. 3.4.f) is not physically justifiable. Even so, it is widely used in simulations. The non-Fickian model, however, does not need an exit boundary condition because of its initial value nature and hence completely circumvents the problem of exactly determining the exit boundary condition.

For small values of  $\frac{2D}{vL} = \frac{2}{P_{e_{m,z}}} \cdot \frac{d_p}{L}$  (that is, for long beds), eqn. 3.4.g can be approximated by

$$\frac{Y_e}{Y_i} = \left(1 - \frac{\omega^2 DL}{v^3}\right) e^{\frac{-i\omega D}{v}} \quad ; \quad \frac{\omega D}{v^2} < 1 \quad (3.4.h)$$

which can be written as

$$\ln \frac{Y_e}{Y_i} = -i \frac{\omega L}{v} - \frac{\omega^2 DL}{v^3} + \dots \quad (3.4.i)$$

The Fickian model yields the same frequency response diagram as a number of  $n$  perfect mixers in series with the same total residence

time  $\bar{\tau}$ , if

$$\frac{1}{n} = \frac{2}{P_{e_{m,z}}} \cdot \frac{d_p}{L} \quad \text{(mixing cell is of length equal to one particle diameter)} \quad (3.4.j)$$

and  $\frac{\omega \bar{\tau}}{n} < 1$  (that is, for low enough frequencies) (3.4.k)

In the non-Fickian model, assuming  $C = Y_e^{i\omega t}$  and  $\bar{C} = \bar{Y}_e^{i\omega t}$  and substituting in equation 3.1.b gives

$$\bar{Y} = \frac{\frac{g}{\epsilon_B} Y}{\left( \frac{g}{\epsilon_B} + i\omega \right)} \quad (3.4.l)$$

Substituting for  $C$  and  $\bar{C}$  in eqn. 3.1.a with the initial condition  $Y = Y_i$  at  $z = 0$ , the following solution is obtained

$$\ln \frac{Y_e}{Y_i} = -i \frac{\omega L}{v_z} \frac{\frac{g^2 \epsilon_T}{\epsilon_A \epsilon_B} \left[ \frac{1}{2} + \omega^2 \right]}{\left[ \left( \frac{g}{\epsilon_B} \right)^2 + \omega^2 \right]} - \frac{\omega^2 L}{\epsilon_A v_z} \frac{g}{\left[ \left( \frac{g}{\epsilon_B} \right)^2 + \omega^2 \right]} \quad (3.4.m)$$

Relating  $g$  with the axial asymptotic dispersivity  $D_z$  (eqn. 3.1.o), the following solutions are obtained for the moving and stagnant phase:

$$\ln \frac{Y_e}{Y_i} = -i \frac{\omega L}{v_z} \frac{\left[ \left( \frac{\epsilon_A v_z}{\epsilon_T} \right)^4 \frac{\epsilon_B^2}{\epsilon_A \epsilon_T D_z^2} + \omega^2 \right]}{\left[ \left( \frac{\epsilon_A v_z}{\epsilon_T} \right)^4 \frac{\epsilon_B^2}{\epsilon_T^2 D_z^2} + \omega^2 \right]}$$

$$- \frac{\omega^2 L}{(\epsilon_{A^V Z})^2 D_Z} \frac{(\frac{\epsilon_{A^V Z}}{\epsilon_T})^2 \frac{\epsilon_B^2}{\epsilon_T}}{[(\frac{\epsilon_{A^V Z}}{\epsilon_T})^4 \frac{\epsilon_B^2}{\epsilon_T^2 D_Z^2} + \omega^2]} \quad (3.4.n)$$

$$\ln \frac{\bar{Y}_e}{Y_i} = \ln \frac{Y_e}{Y_i} - \ln \left[ 1 + \frac{i\omega}{(\frac{\epsilon_{A^V Z}}{\epsilon_T})^2 \frac{\epsilon_B}{\epsilon_T D_Z}} \right] \quad (3.4.o)$$

If  $(\frac{\epsilon_{A^V Z}}{\epsilon_T})^2 \frac{\epsilon_B}{\epsilon_T D_Z} \gg \omega$ , then eqns. 3.4.n and 3.4.o reduce to eqn.

3.4.p. This condition implies that the probability per unit time that a tracer molecule will go from the s-phase to the m-phase is much larger than the circular frequency  $\omega$  of the tracer concentration.

$$\ln \frac{Y_e}{Y_i} \approx \ln \frac{\bar{Y}_e}{Y_i} \approx -i \frac{\omega L}{(\frac{\epsilon_{A^V Z}}{\epsilon_T})} - \frac{\omega^2 L D_Z}{(\frac{\epsilon_{A^V Z}}{\epsilon_T})^3} \quad (3.4.p)$$

Hence the non-Fickian model yields the same frequency response as the Fickian model for small values of  $\frac{2D}{VL}$  (that is, for long beds), and hence also the mixing cell model response under equivalent conditions (eqns. 3.4.j and 3.4.k).



#### 4. TRANSVERSE DISPERSION IN TWO-DIMENSIONAL, ISOTHERMAL NON-REACTIVE PACKED BEDS

##### 4.1 Moment Analysis

In order to evaluate the transverse dispersion in a packed bed, a moment analysis of the equations is done for both kinds of wake shedding and entrainment phenomena described in Chapter 2, namely, Mechanism I and Mechanism II.

##### 4.1.1 Mechanism I

Consider an infinite pulse at  $t = 0$  on the plane  $y = 0$ . The solution is assumed independent of  $z$ , so the equations become:

$$\frac{\partial c}{\partial t} + \frac{g}{\epsilon_A} (c - \bar{c}) = 0 \quad (4.1.1.a)$$

$$\frac{\partial \bar{c}}{\partial t} + \frac{g}{\epsilon_B} (\bar{c} - c) - \frac{g\lambda}{2\epsilon_B} \frac{\partial^2 c}{\partial y^2} = 0 \quad (4.1.1.b)$$

and the boundary conditions are

$$c(y, 0) = \delta(y) \quad ; \quad \bar{c}(y, 0) = \delta(y) \quad (4.1.1.c)$$

The  $n$ th moments of  $c(y, t)$  and  $\bar{c}(y, t)$  are defined as:

$$\mu_n(t) = \int_{-\infty}^{\infty} y^n \cdot c(y, t) \cdot dy \quad ; \quad \bar{\mu}_n(t) = \int_{-\infty}^{\infty} y^n \cdot \bar{c}(y, t) \cdot dy \quad (4.1.1.d)$$

The moment equations are:

$$\frac{d\mu_n}{dt} + \frac{g}{\epsilon_A} (\mu_n - \bar{\mu}_n) = 0 \quad (4.1.1.e)$$

$$\frac{d\bar{\mu}_n}{dt} + \frac{g}{\epsilon_B} (\bar{\mu}_n - \mu_n) - \frac{g\lambda^2}{2\epsilon_B} n(n-1) \mu_{n-2} = 0 \quad (4.1.1.f)$$

$$\mu_0(0) = 1 \quad ; \quad \mu_1(0) = \mu_2(0) = \dots = 0 \quad (4.1.1.g)$$

$$\bar{\mu}_0(0) = 1 \quad ; \quad \bar{\mu}_1(0) = \bar{\mu}_2(0) = \dots = 0 \quad (4.1.1.h)$$

Solving these equations with the help of laplace transforms, the following are the expressions for zeroth, first and second moments:

$$\mu_0 = 1 \quad (4.1.1.i)$$

$$\bar{\mu}_0 = 1 \quad (4.1.1.j)$$

$$\mu_1 = 1 \quad (4.1.1.k)$$

$$\bar{\mu}_1 = 1 \quad (4.1.1.l)$$

$$\mu_2 = 2 \left[ \frac{g\lambda^2}{2\epsilon_t} t + \frac{\epsilon_A \epsilon_B g \lambda^2}{2\epsilon_t^2} \left( 1 - e^{-\frac{g\epsilon_t t}{\epsilon_A \epsilon_B}} \right) \right] \quad (4.1.1.m)$$

$$\begin{aligned} \bar{\mu}_2 = \frac{g^3 \lambda^2}{\epsilon_A \epsilon_B^2} & \left\{ \frac{A \epsilon_B}{g} t - A \left[ \frac{\epsilon_B}{g} \right]^2 \left[ 1 - e^{-\frac{g}{\epsilon_B} t} \right] - \frac{A^2}{\left[ \frac{1}{A} - \frac{g}{\epsilon_B} \right]} \left( e^{-t/A} - e^{-\frac{g}{\epsilon_B} t} \right) \right. \\ & \left. - \frac{A^2 \epsilon_B}{g} \left[ 1 - e^{-\frac{g}{\epsilon_B} t} \right] \right\} - \lambda^2 \left[ 1 - e^{-\frac{g}{\epsilon_B} t} \right] \quad (4.1.1.n) \end{aligned}$$

where,  $A = \frac{\epsilon_A \epsilon_B}{g \epsilon_t}$

The asymptotic values of the dispersivity in the radial direction are obtained from the second moments as in Section 3.1.

$$t \rightarrow 0 : (De)_y = 0 \quad (4.1.1.o)$$

$$t \rightarrow \infty : (De)_y = \frac{g\lambda^2}{2\epsilon_T} \quad (4.1.1.p)$$

Similarly, for the stagnant phase,

$$t \rightarrow 0 : (\bar{De})_y = \frac{g\lambda^2}{2\epsilon_B} \quad (4.1.1.q)$$

$$t \rightarrow \infty : (\bar{De})_y = \frac{g\lambda^2}{2\epsilon_T} \quad (4.1.1.r)$$

The asymptotic transverse dispersivity for large  $t$  is the same in both phases,

$$D_y = (De)_y = (\bar{De})_y = \frac{g\lambda^2}{2\epsilon_T} \quad (4.1.1.s)$$

#### 4.1.2 Mechanism II

Consider an infinite pulse at  $t = 0$  on the plane  $y = 0$ . The solution is independent of  $z$ , so the equations become

$$\frac{\partial \bar{c}}{\partial t} + \frac{g}{\epsilon_A} (c - \bar{c}) - \frac{1}{2} \frac{g}{\epsilon_A} \left(\frac{\lambda}{2}\right)^2 \frac{\partial^2 \bar{c}}{\partial y^2} = 0 \quad (4.1.2.a)$$

$$\frac{\partial \bar{c}}{\partial t} + \frac{g}{\epsilon_B} (\bar{c} - c) - \frac{1}{2} \frac{g}{\epsilon_B} \left(\frac{\lambda}{2}\right)^2 \frac{\partial^2 c}{\partial y^2} = 0 \quad (4.1.2.b)$$

and the boundary conditions are

$$c(y,0) = \delta(y) \quad ; \quad \bar{c}(y,0) = \delta(y) \quad (4.1.2.c)$$

The moment equations are

$$\frac{d\mu_n}{dt} + \frac{g}{\epsilon_A} (\mu_n - \bar{\mu}_n) - \frac{1}{2} \frac{g}{\epsilon_A} \left(\frac{\lambda}{2}\right)^2 n(n-1) \bar{\mu}_{n-2} = 0 \quad (4.1.2.d)$$

$$\frac{d\bar{\mu}_n}{dt} + \frac{g}{\epsilon_B} (\bar{\mu}_n - \mu_n) - \frac{1}{2} \frac{g}{\epsilon_B} \left(\frac{\lambda}{2}\right)^2 n(n-1) \mu_{n-2} = 0 \quad (4.1.2.e)$$

$$\mu_0(o) = 1 \quad ; \quad \mu_1(o) = \mu_2(o) = \dots = 0 \quad (4.1.2.f)$$

$$\bar{\mu}_0(o) = 1 \quad ; \quad \bar{\mu}_1(o) = \bar{\mu}_2(o) = \dots = 0 \quad (4.1.2.g)$$

Solving the equations with laplace transforms, the moments are:

$$\mu_0 = 1 \quad (4.1.2.h)$$

$$\bar{\mu}_0 = 1 \quad (4.1.2.i)$$

$$\mu_1 = 1 \quad (4.1.2.j)$$

$$\bar{\mu}_1 = 1 \quad (4.1.2.k)$$

$$\begin{aligned} \mu_2 = & 2 \cdot \frac{g}{\epsilon_T} \left(\frac{\lambda}{2}\right)^2 \cdot t - 2 \cdot \frac{g}{\epsilon_T} \left(\frac{\lambda}{2}\right)^2 \cdot \frac{\epsilon_A \epsilon_B}{g \epsilon_T} \left[ 1 - e^{\frac{-g \epsilon_T t}{\epsilon_A \epsilon_B}} \right] \\ & + \frac{\epsilon_A}{\epsilon_B} \left(\frac{\lambda}{2}\right)^2 \left[ 1 - e^{\frac{-g \epsilon_T t}{\epsilon_A \epsilon_B}} \right] \end{aligned} \quad (4.1.2.l)$$

$$\begin{aligned} \bar{\mu}_2 = & 2 \cdot \frac{g^3}{\epsilon_A \epsilon_B^2} \cdot \left(\frac{\lambda}{2}\right)^2 \cdot \left\{ \frac{A \epsilon_B}{g} t + A \left(\frac{\epsilon_B}{g}\right)^2 e^{\frac{-g}{\epsilon_B} t} - A \left(\frac{\epsilon_B}{g}\right)^2 \right. \\ & \left. - \frac{A^2}{\left(\frac{1}{A} - \frac{g}{\epsilon_B}\right)} \left( e^{-t/A} - e^{\frac{-g}{\epsilon_B} t} \right) - \frac{A^2 \epsilon_B}{g} \left( 1 - e^{\frac{-g}{\epsilon_B} t} \right) \right\} \\ & + \frac{\left[ \left( \frac{g}{\epsilon_B} - \frac{1}{A} \right) - \frac{g}{\epsilon_B} e^{-t/A} + \frac{1}{A} e^{\frac{-g}{\epsilon_B} t} \right]}{\left( \frac{g}{\epsilon_B} - \frac{1}{A} \right) \cdot \frac{g}{\epsilon_B} \cdot \frac{1}{A}} + \left(\frac{\lambda}{2}\right)^2 \left[ 1 - e^{\frac{-g}{\epsilon_B} t} \right] \end{aligned} \quad (4.1.2.m)$$

The asymptotic values of the transverse dispersivity obtained are:

$$t \rightarrow 0 : (De)_y = \frac{1}{2} \frac{g}{\epsilon_A} \left(\frac{\lambda}{2}\right)^2 \quad (4.1.2.n)$$

$$t \rightarrow \infty : (\overline{De})_y = \frac{g}{\epsilon_T} \left(\frac{\lambda}{2}\right)^2 \quad (4.1.2.o)$$

Similarly, for the stagnant phase,

$$t \rightarrow 0 : (\overline{De})_y = \frac{1}{2} \frac{g}{\epsilon_B} \left(\frac{\lambda}{2}\right)^2 \quad (4.1.2.p)$$

$$t \rightarrow \infty : (\overline{De})_y = \frac{g}{\epsilon_T} \left(\frac{\lambda}{2}\right)^2 \quad (4.1.2.q)$$

The asymptotic transverse dispersivity is the same in both phases,

$$D'_y = (De)_y = (\overline{De})_y = \frac{g}{\epsilon_T} \left(\frac{\lambda}{2}\right)^2 \quad (4.1.2.r)$$

#### 4.2 Point Source, Steady State and No Reaction

Bernard and Wilhelm 1950, conducted experiments with a point source of tracer at steady state and with no chemical reaction, and fitted their experimental data with the solution to the Fickian equation neglecting the axial diffusion term. H.A. Wilson 1904, has solved the complete equation including the axial diffusion term. Wilson's solution, however, approaches the solution to the equation neglecting the axial diffusion term, for a distance far enough downstream, which is a condition encountered in the experimental concentration profiles of Bernard and Wilhelm.

### 4.2.1 Mechanism I

For steady state, no chemical reaction, the equations are:

$$v_z \frac{\partial c}{\partial z} + \frac{g}{\epsilon_A} (c - \bar{c}) = 0 \quad (4.2.1.a)$$

$$\frac{g}{\epsilon_B} (\bar{c} - c) - \frac{g\lambda^2}{2\epsilon_B} \frac{\partial^2 c}{\partial y^2} = 0 \quad (4.2.1.b)$$

which can be rewritten as

$$\left( \frac{\epsilon_A v_z}{\epsilon_T} \right) \frac{\partial c}{\partial z} - D_y \cdot \frac{\partial^2 c}{\partial y^2} = 0 \quad (4.2.1.c)$$

$$\bar{c} = c + \frac{\epsilon_T D_y}{2g} \cdot \frac{\partial^2 c}{\partial y^2} \quad (4.2.1.d)$$

Eqn. 4.2.1.c is nothing but the Fickian equation with the axial diffusion term neglected.

#### 4.2.1.1 Cylindrical Bed With Axial Symmetry

For a cylindrical bed with axial symmetry equations equivalent to eqns. 4.2.1.c and 4.2.1.d are:

$$\left( \frac{\epsilon_A v_z}{\epsilon_T} \right) \frac{\partial c}{\partial z} - D_y \cdot \left( \frac{\partial^2 c}{\partial r^2} + \frac{1}{r} \frac{\partial c}{\partial r} \right) = 0 \quad (4.2.1.1.a)$$

$$\bar{c} = c + \frac{\epsilon_T D_y}{2g} \left( \frac{\partial^2 c}{\partial r^2} + \frac{1}{r} \frac{\partial c}{\partial r} \right) \quad (4.2.1.1.b)$$

In some experiments of Bernard and Wilhelm, radial diffusion was limited to the central core of the tube; whereas, in others, diffusion proceeded until the tube wall boundary became important in stop-

ping radial diffusive flux. In the former case, the Wilson's solution to the Fickian model has been used to simulate experiments. When the wall boundary becomes important, a solution with a no-flux boundary condition at the wall has been derived by Bernard and Wilhelm which was used to simulate experiments. In this section an example case with no wall effect is being considered. The boundary conditions for the point source condition are:

$$2\pi \int_0^{\infty} \left( \frac{\epsilon_A v_z}{\epsilon_T} \right) \cdot c \cdot r \cdot dr = Q, \quad z > 0 \quad (4.2.1.1.c)$$

where,  $Q$  is the rate of injection of tracer (moles/time)

$$c(r, 0) = 0, \quad r > 0 \quad (4.2.1.1.d)$$

and assuming the concentration is decreasing exponentially in the radial direction,

$$c(\infty, z) = 0 \quad (4.2.1.1.e)$$

The analytic solution to eqns. 4.2.1.1.a and 4.2.1.1.b with the above boundary conditions is

$$c = \frac{Q}{4\pi \cdot D_y \cdot z} e^{\frac{-r^2 \left( \frac{\epsilon_A v_z}{\epsilon_T} \right)}{4 D_y z}} \quad (4.2.1.1.f)$$

and

$$\bar{c} = \left[ 1 - \frac{\epsilon_A v_z}{2gz} \left\{ 1 - \frac{r^2 \left( \frac{\epsilon_A v_z}{\epsilon_T} \right)}{4 D_y z} \right\} \right] \cdot c \quad (4.2.1.1.g)$$

Assuming the exponent is small ( $z$  large enough) so that the second order terms can be neglected, then

$$\left[ 1 - \frac{r^2 \left( \frac{\epsilon_A v_z}{\epsilon_T} \right)}{4 D_y z} \right] \approx e^{-\frac{r^2 \left( \frac{\epsilon_A v_z}{\epsilon_T} \right)}{2 D_y z}}$$

and eqn. 4.2.1.1.g reduces to

$$\bar{c} = c - \frac{Q \epsilon_A v_z}{8\pi g D_y z^2} e^{-\frac{r^2 \left( \frac{\epsilon_A v_z}{\epsilon_T} \right)}{2 D_y z}} \quad (4.2.1.1.h)$$

or

$$\bar{c} = c - \frac{2 \pi D_y}{Q \cdot g} c^2$$

For large  $z$ ,  $\bar{c} \approx c \rightarrow 0$  (4.2.1.1.j)

For distances far enough downstream, the concentrations in the stagnant and the moving phase are almost the same. Thus for long beds, the non-Fickian model becomes identical to the Fickian model for a point source, steady state and no reaction, at distances far enough downstream.

#### 4.2.2 Mechanism II

For steady state, no chemical reaction, the equations for this mechanism are:

$$v_z \frac{\partial c}{\partial z} + \frac{g}{\epsilon_A} (c - \bar{c}) - \frac{1}{2} \frac{g}{\epsilon_A} \left( \frac{\lambda}{2} \right)^2 \frac{\partial^2 \bar{c}}{\partial y^2} = 0 \quad (4.2.2.a)$$



$$\frac{g}{\epsilon_B} (\bar{c} - c) - \frac{1}{2} \frac{g}{\epsilon_B} \left(\frac{\lambda}{2}\right)^2 \cdot \frac{\partial^2 c}{\partial y^2} = 0 \quad (4.2.2.b)$$

These can be rewritten as

$$\left( \frac{\epsilon_A^V z}{\epsilon_T} \right) \frac{\partial c}{\partial z} - D'_y \frac{\partial^2 c}{\partial y^2} - \frac{\epsilon_T D_y'^2}{4g} \frac{\partial^4 c}{\partial y^4} = 0 \quad (4.2.2.c)$$

and,

$$\bar{c} = c + \frac{\epsilon_T D_y'}{2g} \frac{\partial^2 c}{\partial y^2} \quad (4.2.2.d)$$

If it is assumed that  $\frac{\partial^2 c}{\partial y^2} = \frac{\partial^2 \bar{c}}{\partial y^2}$ , then eqns. 4.2.2.a and 4.2.2.b can be rewritten as

$$\left( \frac{\epsilon_A^V z}{\epsilon_T} \right) \frac{\partial c}{\partial z} - D'_y \cdot \frac{\partial^2 c}{\partial y^2} = 0 \quad (4.2.2.e)$$

and  $\bar{c}$  is given as in eqn. 4.2.2.d. Thus equivalence with the Fickian model (axial diffusion term neglected) is established as in Section 4.2.1.

#### 4.2.2.1 Cylindrical Bed With Axial Symmetry

For a cylindrical bed with axial symmetry equations equivalent to eqns. 4.2.2.a and 4.2.2.b are

$$v_z \frac{\partial c}{\partial z} + \frac{g}{\epsilon_A} (c - \bar{c}) - \frac{1}{2} \frac{g}{\epsilon_A} \left(\frac{\lambda}{2}\right)^2 \cdot \left[ \frac{\partial^2 \bar{c}}{\partial r^2} + \frac{1}{r} \frac{\partial \bar{c}}{\partial r} \right] = 0 \quad (4.2.2.1.a)$$

$$\frac{g}{\epsilon_B} (c - \bar{c}) - \frac{1}{2} \frac{g}{\epsilon_A} \left(\frac{\lambda}{2}\right)^2 \cdot \left[ \frac{\partial^2 c}{\partial r^2} + \frac{1}{r} \frac{\partial c}{\partial r} \right] = 0 \quad (4.2.2.1.b)$$

These equations can be rewritten as

$$\left[ \frac{\epsilon_A^V}{\epsilon_T} \right] \frac{\partial c}{\partial z} - D_y' \left( \frac{\partial^2 c}{\partial r^2} + \frac{1}{r} \frac{\partial c}{\partial r} \right) - \frac{\epsilon_T D_y'}{4g} \left[ \frac{1}{r^2} \left( \frac{\partial}{\partial r} \left( \frac{\partial}{\partial r} \left( r^2 \frac{\partial^3 c}{\partial r^3} \right) \right) - \frac{1}{r^2} \left( \frac{\partial}{\partial r} \left( \frac{1}{r} \frac{\partial c}{\partial r} \right) \right) \right) \right] = 0 \quad (4.2.2.1.c)$$

$$\bar{c} = c + \frac{\epsilon_T D_y'}{2g} \left( \frac{\partial^2 c}{\partial r^2} + \frac{1}{r} \frac{\partial c}{\partial r} \right) \quad (4.2.2.1.d)$$

The conditions for equivalence with the Fickian model are

$$\frac{\partial c}{\partial r} = \frac{\partial \bar{c}}{\partial r} \quad (4.2.2.1.e)$$

$$\frac{\partial^2 c}{\partial r^2} = \frac{\partial^2 \bar{c}}{\partial r^2} \quad (4.2.2.1.f)$$

and these when substituted in eqns. 4.2.2.1.a and 4.2.2.1.b, give the following equation:

$$\left[ \frac{\epsilon_A^V}{\epsilon_T} \right] - D_y' \left( \frac{\partial^2 c}{\partial r^2} + \frac{1}{r} \frac{\partial c}{\partial r} \right) = 0 \quad (4.2.2.1.g)$$

and  $\bar{c}$  is given as in eqn. 4.2.2.1.d.

As far as the tracer is concerned, it is going through bands of stirred tanks in series alternately, with the moving phase in between (see Fig. 2.1.2.a). The exit concentration in a stirred tank is the concentration in the tank itself; thus any change in the concentration of a stirred tank band should be reflected equally in the adjoining moving phase. The balance equations are made continuous (see Section 2.1) in the radial direction by using the Taylor series. Eqns. 4.2.2.1.e and 4.2.2.1.f show that the first and second deriva-

tives have to be equal in a cylindrical bed with axial symmetry to establish similar dispersion effects in the two mixing mechanisms that have been studied. Hence similar results are obtained for Mechanism II as in Section 4.2.1.1 for Mechanism I by substituting  $D'_y$  for  $D_y$  and using the conditions of equivalence (eqns. 4.2.2.1.e and 4.2.2.1.f).

### 4.3 Evaluation of Parameters Through Experimental Values of Peclet Number

#### 4.3.1 Mechanism I

The asymptotic axial and radial Peclet numbers are defined as

$$(Pe)_z = \frac{d_p v}{D_z} = \frac{d_p \cdot g \cdot \epsilon_T}{\left( \frac{\epsilon_A v_z}{\epsilon_T} \right) \epsilon_B^2} \quad (4.3.1.a)$$

$$(Pe)_y = \frac{d_p \cdot v}{D_y} = d_p \cdot \left( \frac{\epsilon_A v_z}{\epsilon_T} \right) \frac{2\epsilon_T}{g\lambda^2} \quad (4.3.1.b)$$

$$\text{Therefore, } \lambda = \sqrt{\frac{2}{(Pe)_y (Pe)_z}} \cdot \frac{\epsilon_T d_p}{\epsilon_B} \quad (4.3.1.c)$$

McHenry and Wilhelm 1957, have reported the following values of Peclet numbers for a void fraction  $\epsilon_T = 0.388$  :

$$(Pe)_z = 1.88 \quad \text{and} \quad (Pe)_y = 12$$

The parameter  $\epsilon_B$  is given by eqn. 1.1.b. Therefore,

$$\lambda = 0.628 d_p$$

From the structural point of view, if "random dense packed" bed

is considered as described by Oman and Watson 1944, then ideally it would have a closed packed structure for spheres:

$$\lambda = \sqrt{\frac{2}{3}} d_p = 0.817 d_p$$

For a random packing, it would be expected that

$$\lambda = d_p / \sqrt{2} = 0.707 d_p$$

#### 4.3.2 Mechanism II

The asymptotic Peclet numbers are defined as

$$(Pe)'_z = \frac{d_p v}{D'_z} = \frac{d_p g \epsilon_T}{\left( \frac{\epsilon_{A'z}}{\epsilon_T} \right)^2 \epsilon_B^2} \quad (4.3.2.a)$$

$$(Pe)'_y = \frac{d_p v}{D'_y} = d_p \left( \frac{\epsilon_{A'z}}{\epsilon_T} \right) \frac{4\epsilon_T}{g\lambda^2} \quad (4.3.2.b)$$

$$\text{Therefore, } \lambda' = 2 \sqrt{\frac{1}{(Pe)'_z (Pe)'_y} \frac{\epsilon_T d_p}{\epsilon_B}} \quad (4.3.2.c)$$

For the values of Peclet numbers reported by McHenry and Wilhelm,  $\lambda' = 0.888 d_p = \sqrt{2} \lambda$ . Hence for random packing,

$$\lambda' = \sqrt{2} \lambda = d_p \quad (4.3.2.d)$$

From the manner in which the physical structure is set up in Chapter 2 based on which balance equations are written, it is reasonable to expect that a typical eddy has to traverse a radial distance equal to a particle diameter in mixing Mechanism II before

it becomes entrained by another wake. In mixing Mechanism I, the radial distance traveled is less than for Mechanism II by a factor of  $\sqrt{2}$ .

#### 4.4 Momentum Transfer in Turbulent Flow in Packed Beds

When fluid leaves a flowing channel and enters a stagnant region, its forward momentum is lost without corresponding pressure recovery. An equal volume of stagnant fluid is then returned to the flowing stream and must be accelerated up to the stream velocity. It is this acceleration, or momentum generation, that gives rise to the contribution to the total pressure gradient usually recognized as "form drag". The "viscous drag" arises from flow of the moving fluid over the surface of the particle (see Fig. 4.4.a).

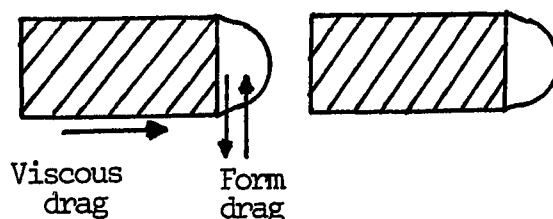


FIGURE 4.4.a

In a lateral slice of the bed of thickness  $\delta z$  and unit cross-section, the mass flux into the flow region from the stagnant region is  $\alpha \cdot g \cdot \delta z$  and it must be accelerated from rest up to a velocity  $v_z$ . Thus the rate of generation of momentum is  $\delta z \cdot \alpha \cdot g \cdot v_z$ . This is equal to the force acting on the moving fluid at the faces of the slab:

$$\epsilon_A [p(z) - p(z+\delta z)] = - \epsilon_A \frac{dp}{dz} \cdot \delta z$$

where,  $p(z)$  is pressure at axial distance  $z$ .

$$\text{Therefore,} \quad - \epsilon_A \left( \frac{dp}{dz} \right)_f = \alpha \cdot g \cdot v_z \quad (4.4.a)$$

The notation  $\left( \frac{dp}{dz} \right)_f$  indicates the contribution due to form drag to the total pressure gradient.

The friction pressure drop  $\Delta P$  in a stream of fluid flowing through length  $L$  of a packed bed of uniform spheres is conventionally represented by the equation

$$- \frac{\Delta P}{L} = \frac{2 \cdot f \cdot \alpha \cdot u^2}{d_p} \quad (4.4.b)$$

where,  $f$  = friction factor

$u = (\epsilon_A v_z)$  = superficial velocity (fluid velocity through the bed calculated as if no particles were present).

For turbulent flows the contribution due to "viscous drag" is negligible and the total pressure drop is mainly due to "form drag". Hence for turbulent flows, if the two correlations are equivalent, then

$$\frac{2 \cdot f \cdot \alpha \cdot (\epsilon_A v_z)^2}{d_p} = \frac{\alpha \cdot g \cdot v_z}{\epsilon_A} \quad (4.4.c)$$

or

$$f = \frac{g \cdot d_p}{2 \cdot \epsilon_A^3 \cdot v_z} \quad (4.4.d)$$

Relating  $g$  with the axial Peclet number (eqn. 4.3.1.a)

$$f = \frac{(Pe)_z}{2} \cdot \left( \frac{\epsilon_B}{\epsilon_A \epsilon_T} \right)^2 \quad (4.4.e)$$

With  $\lambda = \frac{d_p}{\sqrt{2}}$  and  $Pe_z = 2$ , values of  $f$  and  $(Pe)_y$  are written for

various values of  $\epsilon_T$  as shown in Table 4.4.a. Also given in Table 4.4.a are the values of the friction factor,  $f^* = f^*(\epsilon_T)$ , extrapolated from the composite correlation curves provided by Zenz and Othmer 1960, in Fig. 5.1 of their book.

TABLE 4.4.a

$\epsilon_T$	$\epsilon_B$	$\epsilon_A$	$f$	$f^*$	$(Pe)_y$
0.30	0.112	0.188	3.943	14.0	14.167
0.35	0.156	0.194	5.278	10.0	10.070
0.40	0.192	0.208	5.325	6.5	8.680
0.45	0.220	0.230	4.518	5.0	8.368
0.50	0.240	0.260	3.408	3.8	8.680
0.55	0.252	0.298	2.364	3.0	9.527
0.60	0.256	0.344	1.538	2.1	10.987

There is reasonable agreement between values of  $f$  and  $f^*$ ; also, the values of transverse Peclet numbers are within range of experimentally observed values. However, there is a discrepancy for the rarely observed low voidage of 0.35 and 0.3. For beds of randomly placed spheres,  $\epsilon_T$  ranges from 0.38 to 0.47. Of the many investiga-

tions carried out on the structural properties of packing, one of the significant ones was performed by Debbas and Rumpf 1966, on the degree of randomness of packed beds. An interesting result of their study was that the minimum possible porosity for a random packing of spheres is 0.35. The unduly low friction factor predicted for low  $\epsilon_T$  may arise because the mechanism for "form drag" does not hold at such low voidages as the particles are not far enough apart for vortices to form. The flow is more like a series of "jets" and "wakes" as explained earlier in Section 1.1.



## 5. ISOTHERMAL CHEMICAL REACTION IN PACKED BEDS

### 5.1 First Order, Homogeneous Reaction in a One-Dimensional Bed at Steady State

The reaction is taking place in the fluid and the non-catalytic solid particles affect only the fluid dynamics in the bed. The flowing substance is converted by an irreversible first-order reaction so that the rate of removal of the substance is  $k_1 c$ , where  $k_1$  is the reaction rate constant. The chemical reaction involves no volume change and is, say,  $A \rightarrow B$ .

#### 5.1.1 Non-Fickian Model

For a first order chemical reaction taking place in the moving and stagnant phase at steady state, the non-Fickian model becomes:

$$v_z \frac{dc}{dz} + \frac{g}{\epsilon_A} (c - \bar{c}) = -k_1 c \quad (5.1.1.a)$$

$$\frac{g}{\epsilon_B} (\bar{c} - c) = -k_1 \bar{c} \quad (5.1.1.b)$$

Relating  $g$  to the axial asymptotic Peclet number (eqn. 4.3.1.a), and rewriting the equations in dimensionless form, with initial condition  $c_o = \frac{c}{c_i} = 1$  at  $z_o = 0$

$$\frac{dc_o}{dz} = - \left[ \frac{Pe \cdot \epsilon_B^2}{\epsilon_T^2 \left( \frac{Pe \epsilon_B}{J \epsilon_T} + 1 \right)} + \frac{\epsilon_A}{\epsilon_T} J \right] c_o \quad (5.1.1.c)$$

$$\bar{c}_O = \frac{\frac{Pe}{J} \cdot \frac{\epsilon_B}{\epsilon_T} \cdot c_O}{\left(1 + \frac{Pe}{J} \frac{\epsilon_B}{\epsilon_T}\right)} \quad (5.1.1.d)$$

where,  $c_O = \frac{c}{c_i}$  ; dimensionless concentration in m-phase.

$\bar{c}_O = \frac{\bar{c}}{c_i}$  ; dimensionless concentration in s-phase.

$c_i$  = concentration at the inlet of the bed.

$J = \frac{k_1 d_p}{\left(\frac{\epsilon_A v}{\epsilon_T z}\right)}$  ; Damkohler number.

$z_O = \frac{z}{d_p}$  ; dimensionless distance.

The solution to these equations is

$$c_O = \exp \left[ - \left\{ \frac{Pe \cdot \epsilon_B^2}{\epsilon_T^2 \left[ \frac{Pe}{J} \frac{\epsilon_B}{\epsilon_T} + 1 \right]} + \frac{\epsilon_A}{\epsilon_T} J \right\} z_O \right] \quad (5.1.1.e)$$

$$\bar{c}_O = \frac{\frac{Pe}{J} \frac{\epsilon_B}{\epsilon_T}}{1 + \frac{Pe}{J} \frac{\epsilon_B}{\epsilon_T}} \cdot \exp \left[ - \left\{ \frac{Pe \cdot \epsilon_B^2}{\epsilon_T^2 \left[ \frac{Pe}{J} \frac{\epsilon_B}{\epsilon_T} + 1 \right]} + \frac{\epsilon_A}{\epsilon_T} J \right\} z_O \right] \quad (5.1.1.f)$$

$$\text{For } J \ll 1, \quad c_O = \bar{c}_O = e^{-J \cdot z_O} \quad (5.1.1.g)$$

The simplicity of the non-Fickian model will be apparent when the corresponding simulation of the first order chemical reaction is done

with the Fickian model in the next section. The non-Fickian model is essentially a first order linear o.d.e, (eqn. 5.1.1.c) as opposed to the second order linear o.d.e, in the case of the Fickian model (eqn. 5.1.2.a). Also there is no need of an exit boundary condition in the non-Fickian model.

### 5.1.2 Fickian Model

In dimensionless form, the Fickian model is represented by

$$\frac{d^2 c_o}{dz_o^2} - Pe \cdot \frac{dc_o}{dz_o} - Pe \cdot J \cdot c_o = 0 \quad (5.1.2.a)$$

The Danckwerts' boundary conditions are:

$$z_o = 0 : \quad (1 - c_o) = - \frac{1}{Pe} \frac{dc_o}{dz_o} \quad (5.1.2.b)$$

$$z_o = L/d_p : \quad \frac{dc_o}{dz_o} = 0 \quad (5.1.2.c)$$

where,  $L$  = length of the bed.

$$Pe = \frac{d_p v}{D_z} ; \text{ Peclet number}$$

$$J = \frac{k_d d_p}{v} ; \text{ Damkohler number.}$$

The solution is, 
$$c_o = c_1 e^{\lambda_1 z_o} + c_2 e^{\lambda_2 z_o} \quad (5.1.2.d)$$

where 
$$\lambda_1 = \frac{Pe + \sqrt{Pe^2 + 4 \cdot Pe \cdot J}}{2}$$

and, 
$$\lambda_2 = \frac{Pe - \sqrt{Pe^2 + 4 \cdot Pe \cdot J}}{2}$$

$$c_1 = \frac{-\frac{\lambda_2}{\lambda_1} \cdot e^{\frac{(\lambda_2 - \lambda_1) L}{d_p}} \cdot Pe}{\lambda_2 \left[ e^{\frac{(\lambda_2 - \lambda_1) L}{d_p}} - 1 \right] - Pe \left[ \frac{\lambda_2}{\lambda_1} e^{\frac{(\lambda_2 - \lambda_1) L}{d_p}} - 1 \right]}$$

$$c_2 = \frac{Pe}{\lambda_2 \left[ e^{\frac{(\lambda_2 - \lambda_1) L}{d_p}} - 1 \right] - Pe \left[ \frac{\lambda_2}{\lambda_1} e^{\frac{(\lambda_2 - \lambda_1) L}{d_p}} - 1 \right]}$$

The exit concentration can be written as

$$c_o(L) = (c_{11} + c_2) \cdot \exp \left[ \lambda_2 L / d_p \right]$$

$$\text{where, } c_{11} = c_1 \frac{-(\lambda_2 - \lambda_1) L}{d_p}$$

For  $Pe = 2$  and low enough Damkohler number (implying a low enough reaction rate constant),  $J \ll 1$ ; and using the binomial expansion up to the first order terms, the expressions for  $\lambda_2$  and  $\lambda_1$  can be simplified as

$$\lambda_2 = 1 - \sqrt{1 + 2J} = 1 - \left[ 1 + \frac{1}{2} (2J) \right] = -J$$

$\lambda_1$  can be written as,

$$\lambda_1 = 1 + \sqrt{1 + 2J} = 2 + J$$

In addition to the above assumptions, if the bed is sufficiently long the exponent

$$e^{\frac{(\lambda_2 - \lambda_1) L}{d_p}} = e^{-2 \frac{(1+J) L}{d_p}} \approx 0$$

Therefore, 
$$c_2 = \frac{P_e}{P_e - \lambda_2} = \frac{2}{2+J}$$

and 
$$c_{11} = \frac{J}{2(1+J)}$$

Then,  $c_{11} + c_2 = \frac{4 + 6J + J^2}{2(2 + 3J + J^2)} = 1$ , up to first order approximation and the expression for the exit concentration becomes

$$c_o(L) = e^{-JL/d_p} \quad (5.1.2.e)$$

### 5.1.3 Plug-Flow Model

$$\frac{dc_o}{dz_o} = -J \cdot c_o \quad (5.1.3.a)$$

$$z_o = 0, \quad c_o = 1 \quad (5.1.3.b)$$

The solution is 
$$c_o = e^{-Jz_o} \quad (5.1.3.c)$$

Thus for low enough Damkohler number, the concentration profile is identical in the plug flow model and the non-Fickian model (moving phase concentration) at all sections of the bed regardless of the length of the bed (eqns. 5.1.1.g and 5.1.3.c)

For sufficiently long beds and low enough Damkohler number, the exit concentration in all the three models is identical (eqns. 5.1.1.g, 5.1.2.e, and 5.1.3.c)

Figs. 5.a, 5.b, 5.c, 5.d, show concentration profiles obtained by the three models for various values of the parameters.

The concentration profile from the Fickian model is bounded by

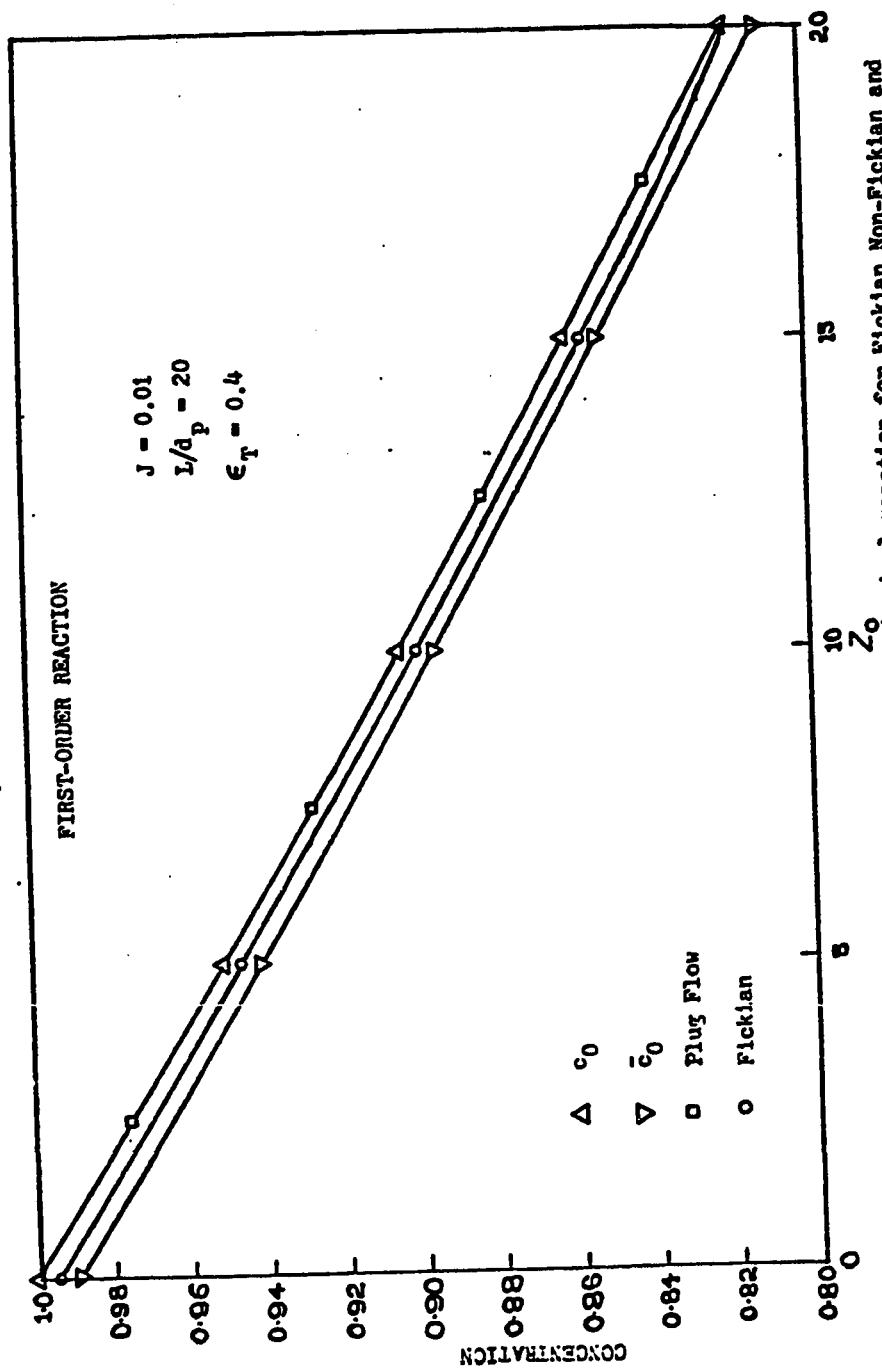


Fig. 5.a. Concentration profiles for first-order chemical reaction for Fickian, Non-Fickian and Plug-Flow models ( $J = 0.01$ ,  $L/d_p = 20$ ).

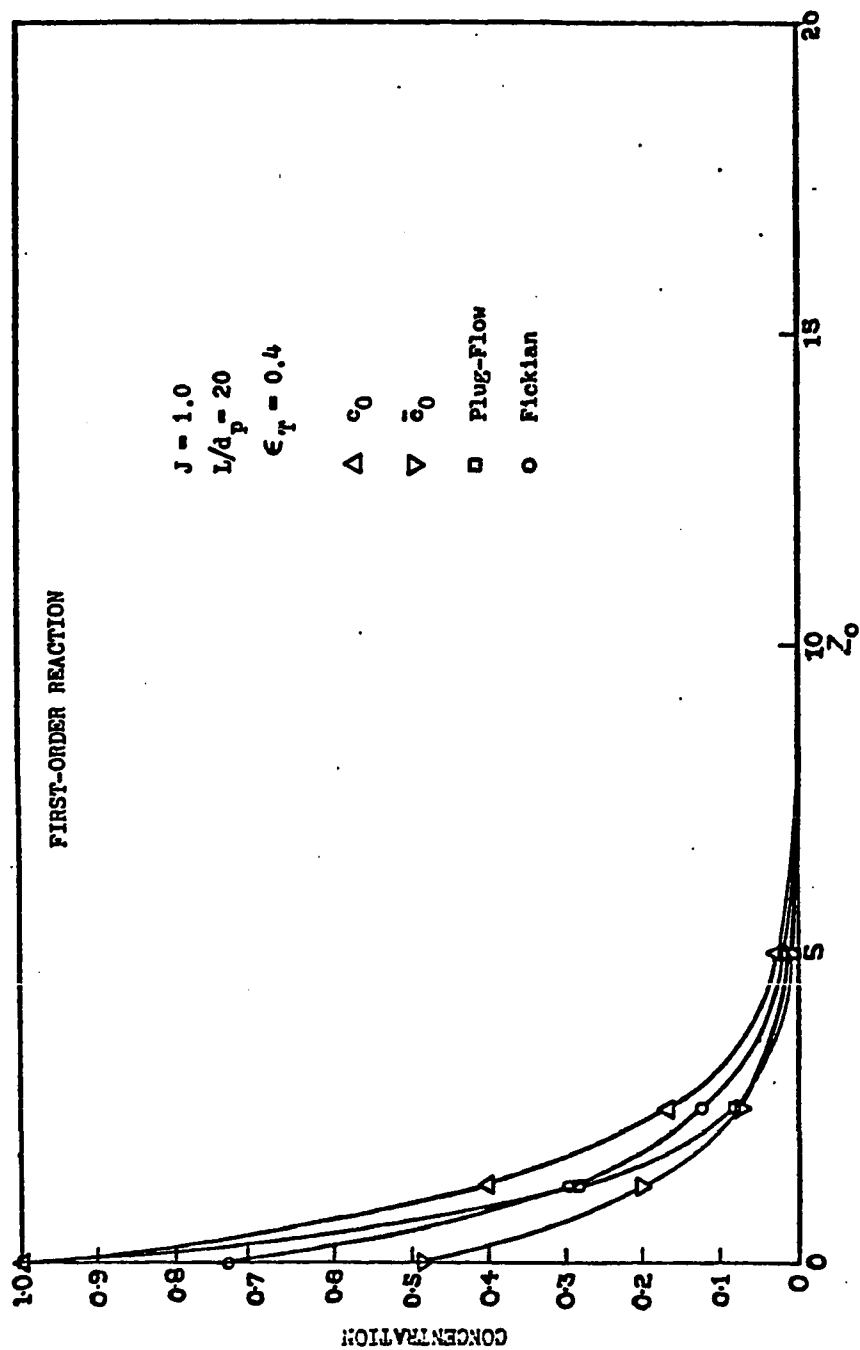


Fig. 5. h. Concentration profiles for first-order chemical reaction for Fickian, Non-Fickian and Plug-Flow models (  $J = 1.0$ ,  $L/d_p = 20$  )

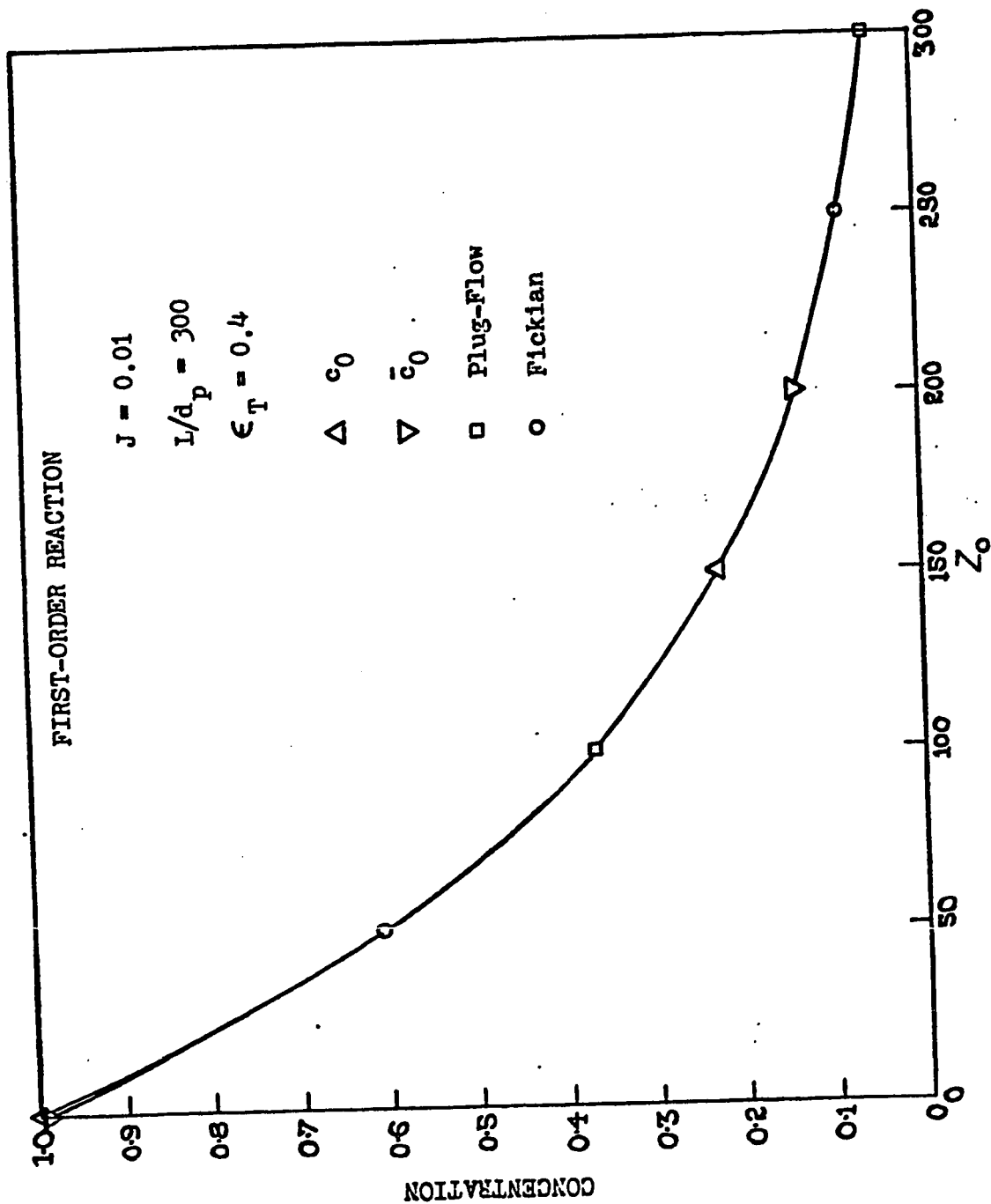


Fig. 5.c. Concentration profiles for first-order chemical reaction for Fickian, Non-Fickian and Plug-Flow models (  $J = 0.01$ ,  $L/a_p = 300$  )



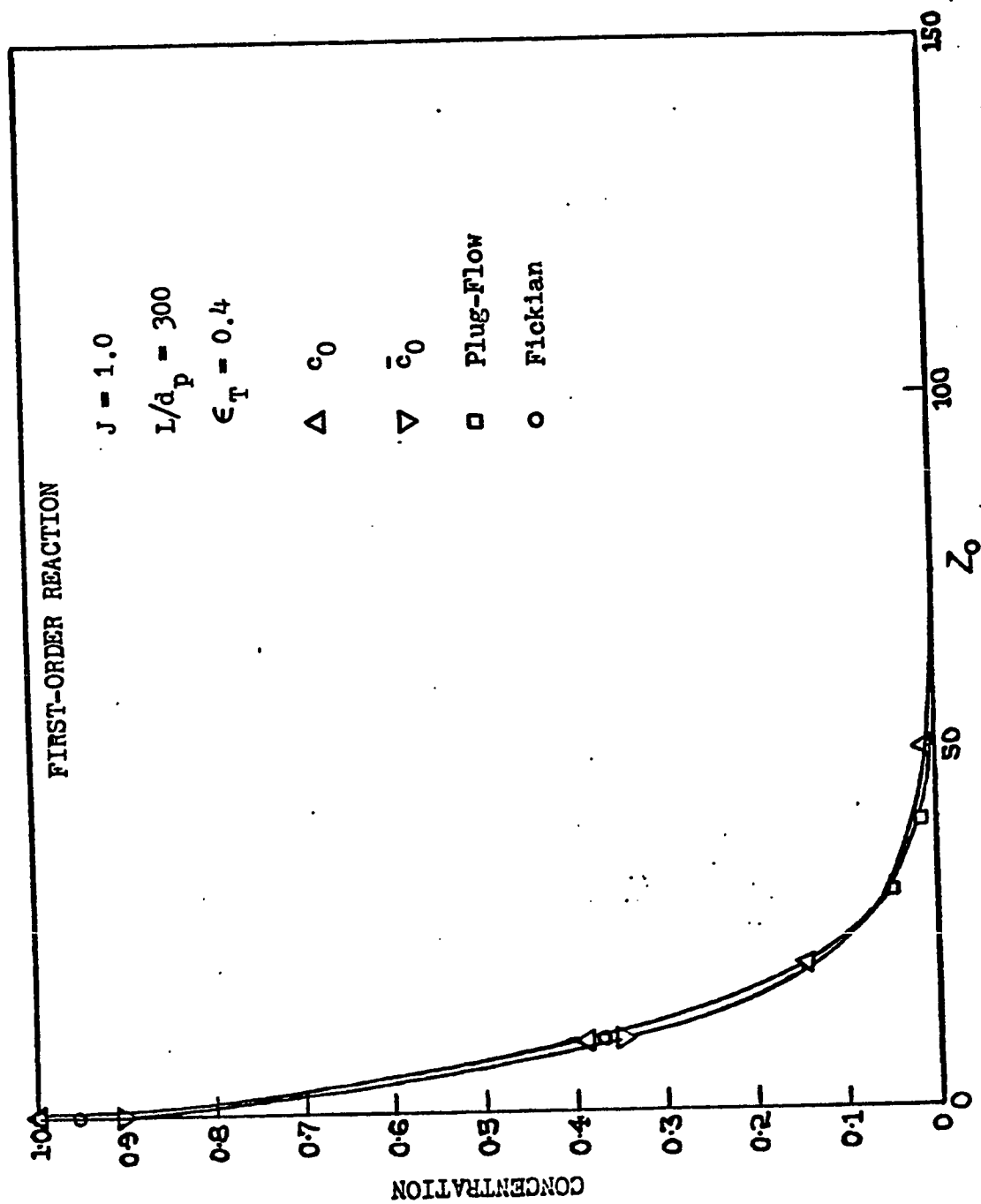


Fig. 5.d. Concentration profiles for first-order chemical reaction for Fickian, Non-Fickian and Plug-Flow models (  $J = 1.0$ ,  $L/d_p = 300$  )

the moving phase and stagnant phase concentration profiles, so that an interstitial average concentration defined as  $\bar{\rho} = \frac{\epsilon_A}{\epsilon_T} c_O + \frac{\epsilon_B}{\epsilon_T} \bar{c}_O$  would correspond quite closely to the values obtained by the Fickian model. Fig. 5.a, which is drawn on an extended scale clearly shows the exit concentration predicted by all three models is the same for low enough Damkohler number and long beds of 20 particle diameters.

## 5.2 Second Order, Homogeneous Reaction in a One-Dimensional Bed at Steady State.

If the flowing substance is converted by an irreversible second order reaction so that the rate of removal of the substance is  $k_2 c^2$ , where  $k_2$  is the reaction rate constant. The chemical reaction involves no volume change and is, say,  $2A \rightarrow 2B$ .

### 5.2.1 Non-Fickian Model

At steady state and second order homogeneous chemical reaction, the equations are

$$v_z \frac{dc}{dz} + \frac{g}{\epsilon_A} (c - \bar{c}) = -k_2 \cdot c^2 \quad (5.2.1.a)$$

$$\frac{g}{\epsilon_B} (\bar{c} - c) = -k_2 \bar{c}^2 \quad (5.2.1.b)$$

Relating  $g$  to the axial asymptotic Peclet number (eqn. 4.3.1.a), and rewriting the equations in dimensionless form

$$\frac{dc_O}{dz_O} = -\frac{\epsilon_A}{\epsilon_T} \cdot J_2 \cdot c_O^2 - Pe \cdot \frac{\epsilon_B^2}{\epsilon_T^2} \cdot \left\{ c_O - \frac{Pe \cdot \epsilon_B}{2J_2 \cdot \epsilon_T} \left[ 1 + \frac{4J_2 \cdot \epsilon_T c_O}{Pe \cdot \epsilon_B} - 1 \right] \right\} \quad (5.2.1.c)$$

where  $J_2 = \frac{k_2 d c_i}{\left( \frac{\epsilon_A v_z}{\epsilon_T} \right)}$ ; Damkohler number .

The initial condition is simply:

$$\text{At } z_0 = 0, \quad c_0 = 1 \quad (5.2.1.d)$$

The stagnant phase concentration can be found explicitly in terms of the moving phase concentration:

$$\bar{c}_0 = \frac{\bar{c}}{c_i} = \frac{\sqrt{1 + \frac{4 J_2 \epsilon_T c_0}{Pe \cdot \epsilon_B}} - 1}{\left( \frac{2 J_2 \epsilon_T}{Pe \epsilon_B} \right)} \quad (5.2.1.e)$$

For low enough Damkohler number,  $J_2 \ll 1$ ,

$$\sqrt{1 + \frac{4 J_2 \epsilon_T c_0}{Pe \cdot \epsilon_B}} \approx 1 + \frac{2 J_2 \epsilon_T c_0}{Pe \cdot \epsilon_B}$$

by Taylor series expansion, neglecting second order terms.

Then equation 5.2.c simplifies to

$$\frac{d c_0}{d z_0} = - \frac{\epsilon_A}{\epsilon_T} \cdot J_2 \cdot c_0^2 \quad (5.2.1.d)$$

and with the initial condition 5.2.d, the solution is

$$c_0 = \frac{1}{1 + \frac{\epsilon_A}{\epsilon_T} J_2 \cdot z_0} \quad (5.2.1.g)$$

and

$$\bar{c}_0 \approx \frac{1 + \frac{2 J_2 \epsilon_T c_0}{Pe \cdot \epsilon_B} - 1}{\frac{2 J_2 \epsilon_T}{Pe \cdot \epsilon_B}} = c_0 \quad (5.2.1.h)$$

### 5.2.2 Fickian Model

For second order homogeneous chemical reaction at steady state,

the dimensionless equation is

$$\frac{d^2 c_o}{dz_o^2} - Pe \cdot \frac{dc_o}{dz_o} - Pe \cdot J_2 \cdot c_o^2 = 0$$

$$z_o = 0 : 1 - c_o = -\frac{1}{Pe} \cdot \frac{dc_o}{dz_o}$$

$$z_o = L/d_p : \frac{dc_o}{dz_o} = 0$$

where,  $J_2 = \frac{k_2 d_p c_i}{v}$  ; Damkohler number.

This is a non-linear second order two point boundary value problem and hence its numerical solution is considerably more complex than that for the solution of the non-Fickian model (eqn. 5.2.1.c) which is an initial value first order problem. Finite difference methods have been used to obtain the numerical solutions. Hamming's predictor-corrector method was used to solve the non-Fickian equation and the solution was, in fact, used as an initial guess for the Newton-Raphson iterative process required to solve the Fickian equation by the quasi-linearization technique. The system is quite stable and converges in less than two iterations. Figs. 5.e, 5.f, 5.g, 5.h, show the concentration profiles for the two models and also for the plug-flow model for various values of the parameters.

### 5.2.3 Plug Flow Model

The dimensionless equation is

$$\frac{dc_o}{dz_o} = -J_2 \cdot c_o^2 \quad (5.2.3.a)$$

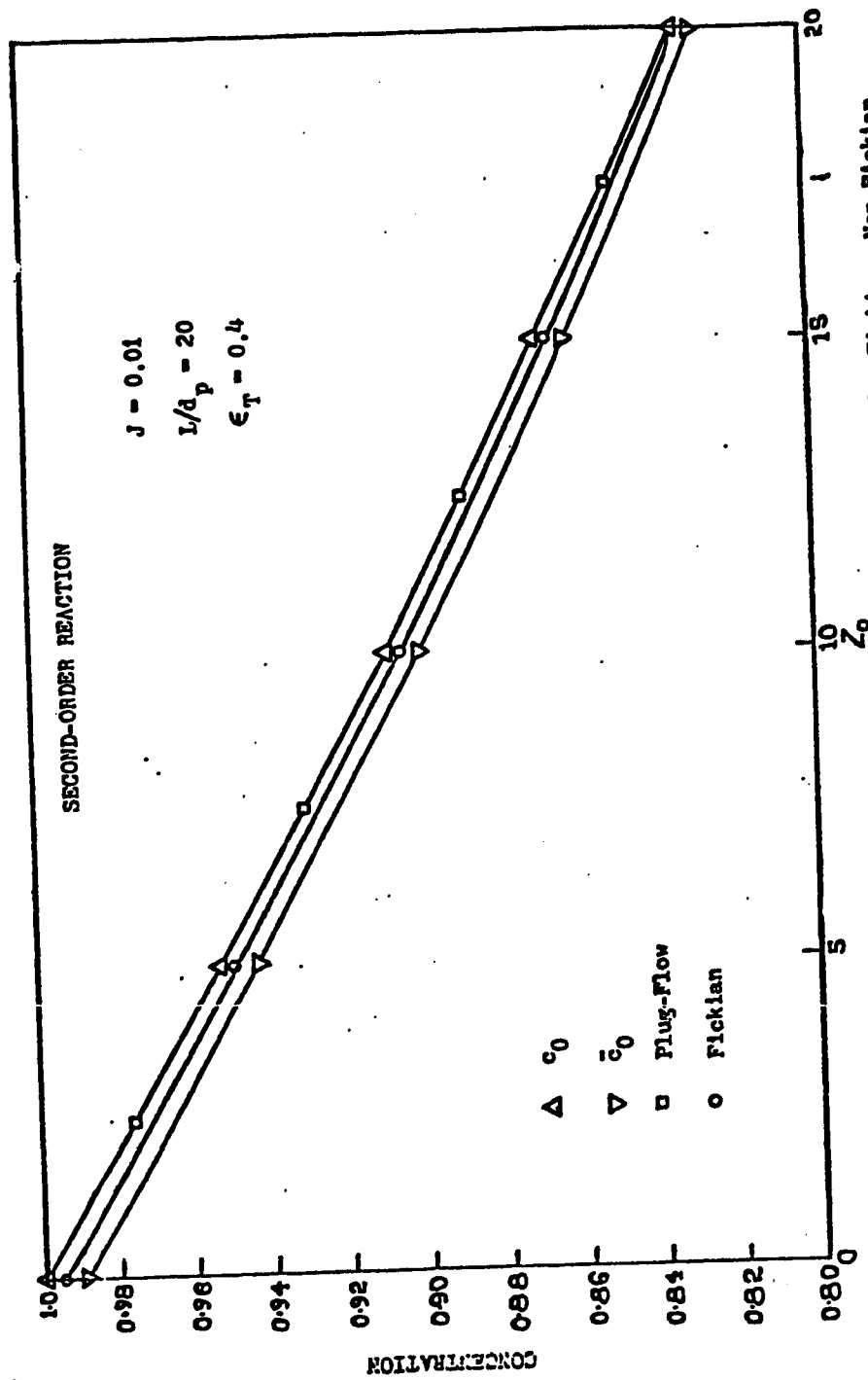


Fig. 5.e. Concentration profiles for second-order chemical reaction for Fickian, Non-Fickian and Plug-Flow models ( $J = 0.01$ ,  $L/d_p = 20$ ).

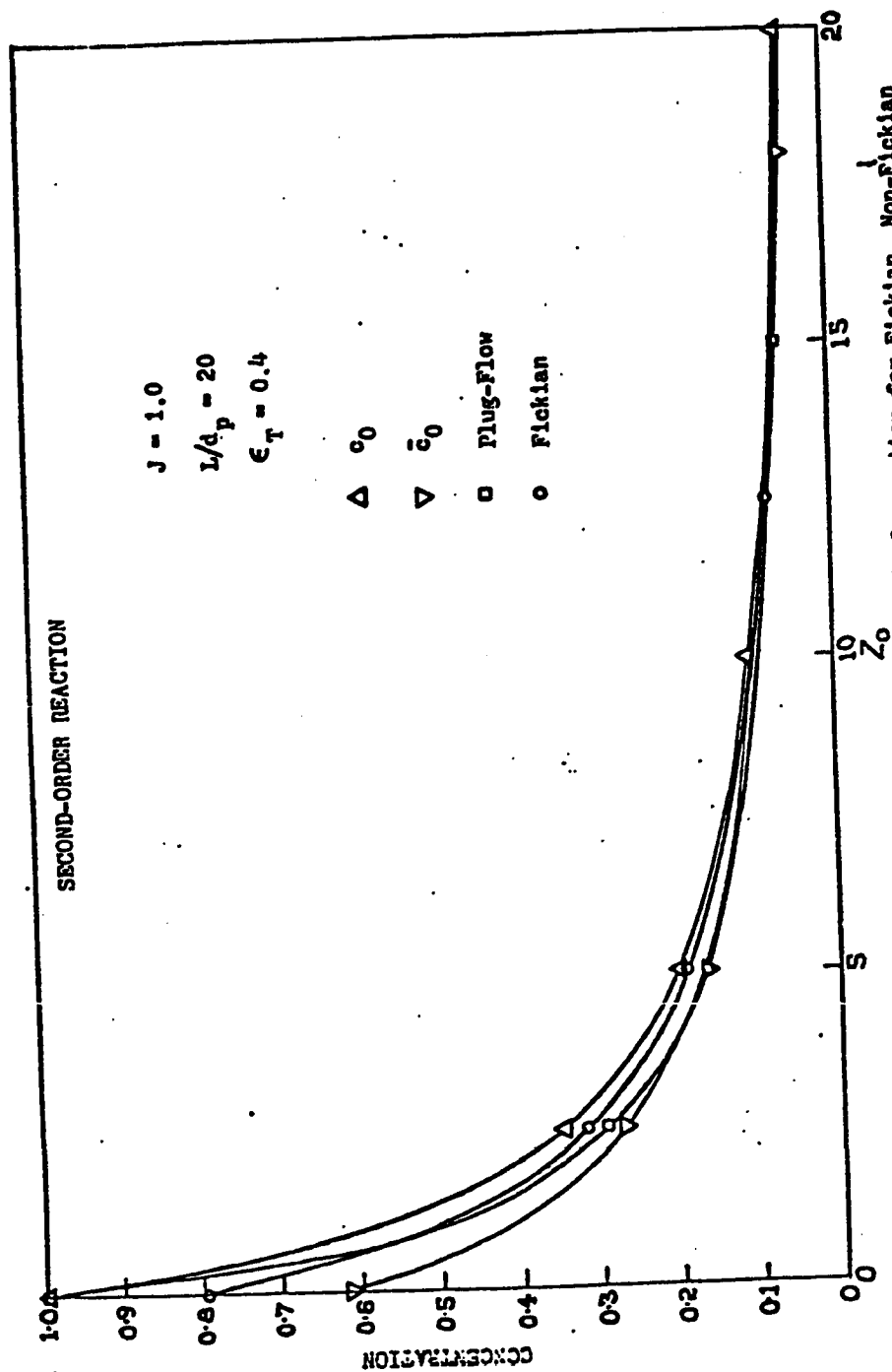


Fig. 5.f. Concentration profiles for second-order chemical reaction for Fickian, Non-Fickian and Plug-Flow models (  $J = 1.0$ ,  $L/d_p = 20$  ).

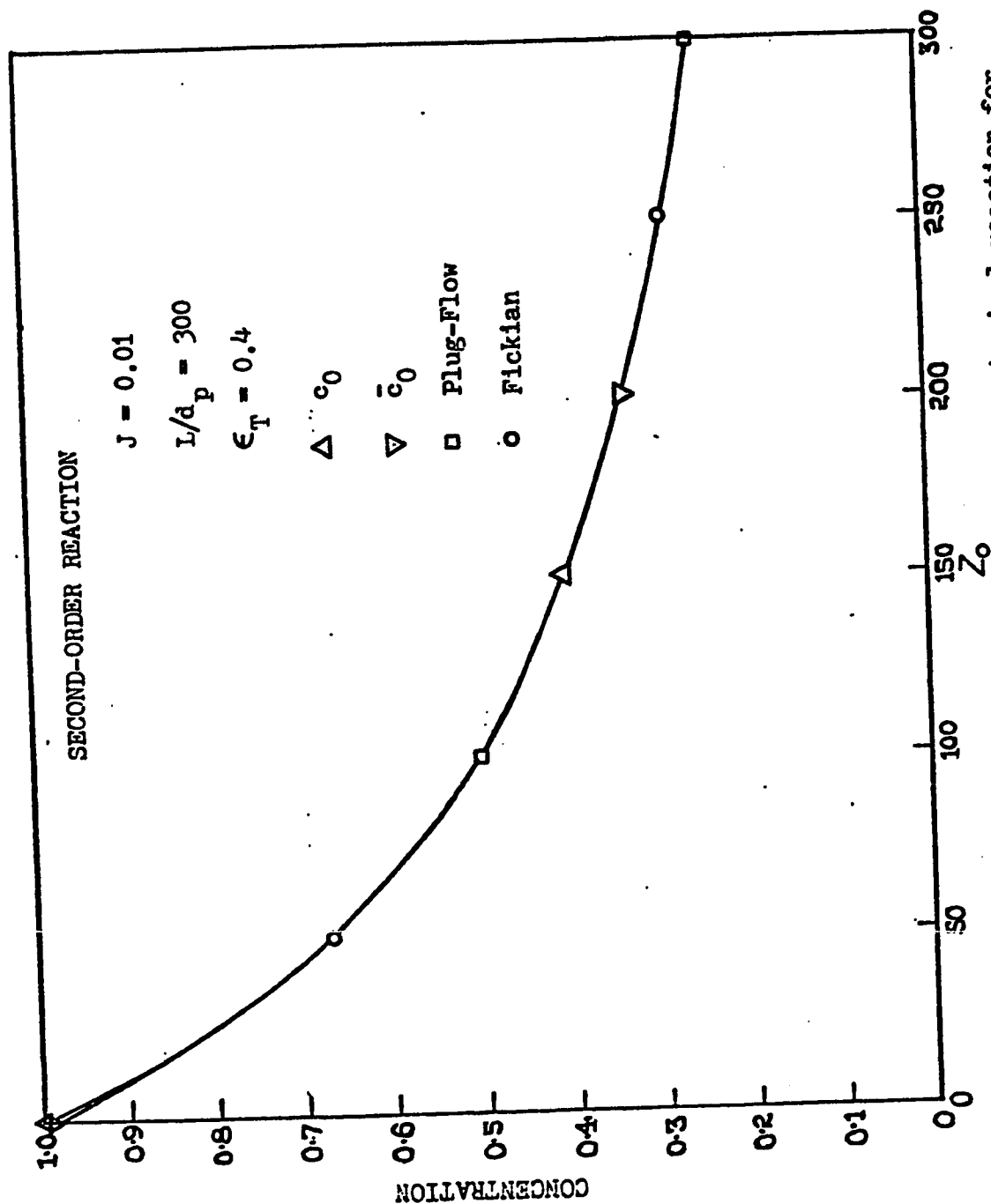


Fig. 5.8. Concentration profiles for second-order chemical reaction for Fickian, Non-Fickian and Plug-Flow models (  $J = 0.01$ ,  $L/d_p = 300$  ).

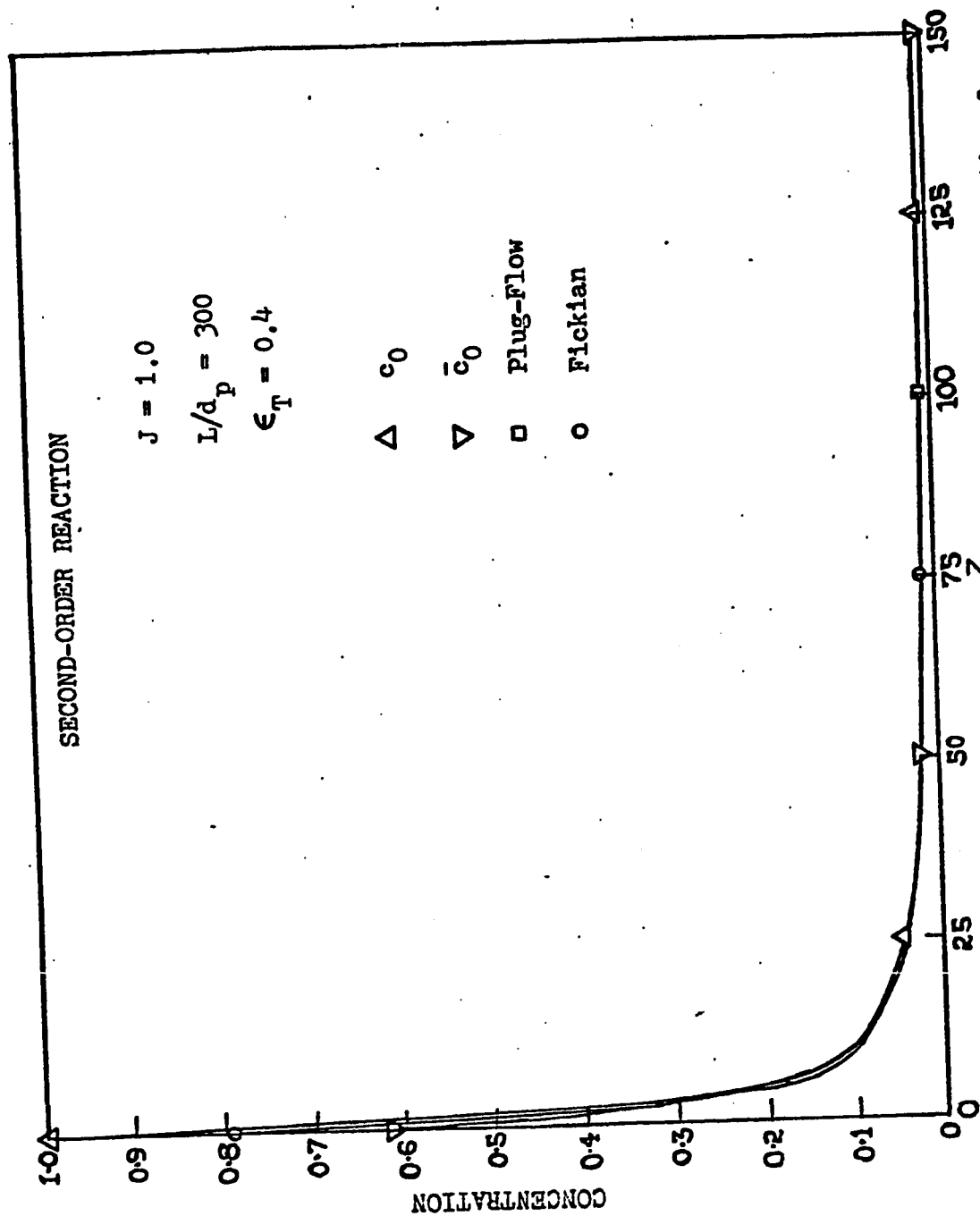


Fig. 5.h. Concentration profiles for second-order chemical reaction for Fickian, Non-Fickian and Plug-Flow models (  $J = 1.0$ ,  $L/d_p = 300$  ).



with the boundary condition

$$z_o = 0 \quad : \quad c_o = 1 \quad (5.2.3.b)$$

The solution is 
$$c_o = \frac{1}{(1 + J_2 z_o)} \quad (5.2.3.c)$$

For low enough Damkohler number, the moving phase concentration profile obtained by the non-Fickian model is very nearly the same as that obtained by the plug-flow model (Fig. 5.e).

Also from the numerical solutions it is observed that the exit concentration in all three models is the same for sufficiently long beds and low enough Damkohler number (Figs. 5.e and 5.g).

The overall behaviour of the plots is similar to that discussed in Section 5.1 for the case of a first order homogeneous chemical reaction.

## 6. HEAT DISPERSION IN PACKED BEDS

The heat transfer equations have been formulated and the assumptions required to formulate them have been discussed in Chapter 2. Analysis of dispersion of heat in packed beds is done in this chapter and is analogous to the isothermal mass dispersion analysis in Chapters 3 and 4.

### 6.1 Moment Analysis

In order to evaluate the axial heat dispersivity in a non-reactive packed bed, a moment analysis of the heat transfer equations is done. Consider an infinite temperature pulse at time  $t = 0$  on the plane  $z = 0$ . The solution is independent of  $y$ ; so the equations become

$$\frac{\partial T}{\partial t} + v_z \frac{\partial T}{\partial z} + \frac{g}{\epsilon_A} (T - \bar{T}) + \frac{2h \cdot \delta S}{\alpha_{c_p} \epsilon_A} (T - \hat{T}) = 0 \quad (6.1.a)$$

$$\frac{\partial \bar{T}}{\partial t} + \frac{g}{\epsilon_B} (T - \bar{T}) = 0 \quad (6.1.b)$$

$$\frac{\partial \hat{T}}{\partial t} + \frac{2h \cdot \delta S}{\rho_B \hat{c}_p} (\hat{T} - T) - \frac{k_s \cdot \delta S \cdot \lambda}{\rho_B \hat{c}_p} \cdot \frac{\partial^2 \hat{T}}{\partial z^2} = 0 \quad (6.1.c)$$

with the initial conditions

$$T(z, 0) = \delta(z) \quad ; \quad \bar{T}(z, 0) = \delta(z) \quad ; \quad \hat{T}(z, 0) = \delta(z) \quad (6.1.d)$$

The  $n$ th moments for  $T(z, t)$ ,  $\bar{T}(z, t)$  and  $\hat{T}(z, t)$  are defined as in Section 3.1,

$$\mu_n(t) = \int_{-\infty}^{\infty} z^n \cdot T(z,t) \cdot dz \quad .$$

$$\bar{\mu}_n(t) = \int_{-\infty}^{\infty} z^n \cdot \bar{T}(z,t) \cdot dz \quad .$$

$$\hat{\mu}_n(t) = \int_{-\infty}^{\infty} z^{\hat{n}} \cdot \hat{T}(z,t) \cdot dz \quad .$$

The moment equations are

$$\frac{d\mu_n}{dt} - n \cdot v_z \cdot \mu_{n-1} + \frac{g}{\epsilon_A} \cdot (\mu_n - \bar{\mu}_n) + \frac{2h \cdot \delta S}{\alpha c_p \epsilon_A} \cdot (\mu_n - \hat{\mu}_n) = 0 \quad (6.1.e)$$

$$\frac{d\bar{\mu}_n}{dt} + \frac{g}{\epsilon_B} \cdot (\bar{\mu}_n - \mu_n) = 0 \quad (6.1.f)$$

$$\frac{d\hat{\mu}_n}{dt} + \frac{2h \cdot \delta S}{\rho_B \hat{c}_p} (\hat{\mu}_n - \mu_n) - \frac{k_s \cdot \delta S \cdot \lambda}{\rho_B \hat{c}_p} \cdot n(n-1) \cdot \hat{\mu}_{n-2} = 0 \quad (6.1.g)$$

$$\left. \begin{aligned} \mu_0(o) &= 1 ; \mu_1(o) = \mu_2(o) = \dots = 0 \\ \bar{\mu}_0(o) &= 1 ; \bar{\mu}_1(o) = \bar{\mu}_2(o) = \dots = 0 \\ \hat{\mu}_0(o) &= 1 ; \hat{\mu}_1(o) = \hat{\mu}_2(o) = \dots = 0 \end{aligned} \right\} \quad (6.1.h)$$

The zeroth, first and second moments are solved for with the help of laplace transforms

$$\mu_0 = 1$$

$$\bar{\mu}_0 = 1$$

$$\hat{\mu}_0 = 1$$

$$\begin{aligned} \mu_1 = v_z \left( \frac{g}{\epsilon_B} + \hat{h} \right) \cdot \frac{1}{B} - \frac{A}{B^2} \cdot v_z \cdot \frac{g}{\epsilon_B} \cdot \hat{h} + v_z \cdot \frac{g}{\epsilon_B} \cdot \hat{h} \cdot \frac{1}{B} \cdot t \\ + e^{\frac{-A}{2} t} \left\{ CN_1 \cdot \cos Ct + (N_2 - \frac{A}{2} N_1) \cdot \sin Ct \right\} \frac{1}{C} \end{aligned}$$

where,

$$\hat{h} = \frac{2h \cdot \delta S}{\rho_B \hat{c}_p}$$

$$\tilde{h} = \frac{2h \cdot \delta S}{\alpha c_p \epsilon_A}$$

$$A = \left( \frac{g}{\epsilon_A} + \frac{g}{\epsilon_B} + \hat{h} + \tilde{h} \right)$$

$$B = \left( \frac{g}{\epsilon_A} \hat{h} + \frac{g}{\epsilon_B} \hat{h} + \frac{g}{\epsilon_B} \tilde{h} \right)$$

$$C = \sqrt{B - \frac{A^2}{4}}$$

$$N_1 = v_z \cdot \left( \frac{g}{\epsilon_B} + \hat{h} \right) \cdot \frac{1}{B} + \frac{A}{B^2} \cdot \frac{v_z g \hat{h}}{\epsilon_B}$$

$$N_2 = v_z + v_z \cdot \left( \frac{g}{\epsilon_B} + \hat{h} \right) \cdot \frac{A}{B} + \frac{v_z g \hat{h}}{\epsilon_B} \cdot \left( \frac{A^2}{B^2} - \frac{1}{B} \right)$$

$$\bar{\mu}_1 = -v_z \hat{h} \cdot \frac{g}{\epsilon_B} \cdot \frac{A}{B^2} + \frac{v_z g \hat{h}}{\epsilon_B B} \cdot t$$

$$+ e^{-\frac{A}{2} t} \left\{ C N_3 \cdot \cos Ct + (N_4 - \frac{A}{2} N_3) \cdot \sin Ct \right\} \frac{1}{C}$$

where,

$$N_3 = \frac{v_z g}{\epsilon_B B} + \frac{v_z g \hat{h} A}{\epsilon_B B^2}$$

$$N_4 = \frac{v_z g A}{\epsilon_B B} + \frac{v_z g \hat{h}}{\epsilon_B} \cdot \left( \frac{A^2}{B^2} - \frac{1}{B} \right)$$

$$\hat{\mu}_1 = -v_z \cdot \frac{g}{\epsilon_B} \cdot \hat{h} \cdot \frac{A}{B^2} + \frac{v_z g \hat{h}}{\epsilon_B B} t$$

$$+ e^{-\frac{A}{2}t} \left\{ CN_5 \cdot \cos Ct + (N_6 - \frac{A}{2} N_5) \cdot \sin Ct \right\} \frac{1}{C}$$

where,  $N_5 = \frac{v_z \hat{h}}{B} + \frac{v_z \hat{gh} A}{\epsilon_B B^2}$

$$N_6 = \frac{v_z \hat{h} A}{B} + \frac{v_z \hat{gh}}{\epsilon_B} \cdot \left( \frac{A^2}{B^2} - \frac{1}{B} \right)$$

The expressions for the first moments,  $\mu_1$ , given above are exact whereas those given below for  $\mu_2$ 's are asymptotic. For large  $t$ , the exponential terms become negligible and,

$$\mu_2 = \frac{4 v_z^2 \hat{gh}}{\epsilon_B B^2} \cdot \left[ \frac{g}{\epsilon_B} + \hat{h} - \frac{A \hat{gh}}{\epsilon_B B} \right] \cdot t + \frac{\tilde{h} \hat{k}_s g}{\epsilon_B B} \cdot t + \left( \frac{v_z \hat{gh}}{\epsilon_B B} \right)^2 \cdot t^2$$

where,  $\hat{k}_s = \frac{2 k_s \cdot \delta S \cdot \lambda}{\rho_B \hat{c}_p}$

$$\bar{\mu}_2 = \frac{2 v_z^2 \hat{gh}}{\epsilon_B B^2} \cdot \left[ \hat{h} + \frac{2g}{\epsilon_B} - \frac{2 A \hat{gh}}{\epsilon_B B} \right] \cdot t + \frac{\tilde{h} \hat{k}_s g}{\epsilon_B B} \cdot t + \left( \frac{v_z \hat{gh}}{\epsilon_B B} \right)^2 \cdot t^2$$

$$\hat{\mu}_2 = \frac{2 v_z^2 \hat{gh}}{\epsilon_B B} \cdot \left[ \frac{g}{\epsilon_B} + 2\hat{h} - \frac{2 A \hat{gh}}{\epsilon_B B} \right] \cdot t + \frac{\tilde{h} \hat{k}_s g}{\epsilon_B B} \cdot t + \left( \frac{v_z \hat{gh}}{\epsilon_B B} \right)^2 \cdot t^2$$

The average temperature pulse velocity in the moving phase is given by

$$\bar{v}_T = \frac{d\bar{z}}{dt} = \frac{d}{dt} \left( \frac{\mu_1}{\mu_0} \right)$$

$$= \frac{v_z \hat{gh}}{\epsilon_B B} + e^{-\frac{A}{2}t} \left\{ (N_2 - AN_1) \cdot \cos Ct - \left( \frac{AN_2}{2C} - \frac{A^2 N_1}{4C} + CN_1 \right) \cdot \sin Ct \right\} \quad (6.1.i)$$

and the limiting vlaues of the velocity are

$$\begin{aligned} t \rightarrow 0 : \bar{v}_T &= v_z \\ t \rightarrow \infty : \bar{v}_T &= \frac{v_z \hat{gh}}{\epsilon_B B} = \frac{\left( \frac{\epsilon_A v_z}{\epsilon_T} \right)}{\left( 1 + \frac{\rho_B \hat{c}_p}{\alpha c_p \epsilon_T} \right)} \end{aligned}$$

Similarly, in the stagnant phase,

$$\begin{aligned} \bar{v}_T &= \frac{d\bar{z}}{dt} = \frac{d \left( \frac{\bar{\mu}_1}{\bar{\mu}_0} \right)}{dt} \\ &= \frac{v_z \hat{gh}}{\epsilon_B B} + e^{-\frac{A}{2}t} \left\{ (N_4 - AN_3) \cdot \cos Ct + \left( \frac{AN_4}{2C} - \frac{A^2 N_3}{4C} + CN_3 \right) \cdot \sin Ct \right\} \quad (6.1.j) \end{aligned}$$

and the limiting values are:

$$\begin{aligned} t \rightarrow 0 : \bar{v}_T &= 0 \\ t \rightarrow \infty : \bar{v}_T &= \frac{\left( \frac{\epsilon_A v_z}{\epsilon_T} \right)}{\left( 1 + \frac{\rho_B \hat{c}_p}{\alpha c_p \epsilon_T} \right)} \end{aligned}$$

In the solid phase, the average temperature pulse velocity is,

$$\begin{aligned}\bar{v}_T &= \frac{d\bar{z}}{dt} = \frac{d\left[\frac{\hat{\mu}_1}{\hat{\mu}_0}\right]}{dt} \\ &= \frac{v_z}{\epsilon_B B} \frac{gh}{\epsilon_B} + e^{-\frac{A}{2}t} \left\{ (N_6 - AN_5) \cdot \cos Ct - \left[ \frac{AN_6}{2C} - \frac{A^2 N_5}{4C} + CN_5 \right] \cdot \sin Ct \right\}\end{aligned}\quad (6.1.k)$$

and the limiting values are:

$$\begin{aligned}t \rightarrow 0 : \bar{v}_T &= 0 \\ t \rightarrow \infty : \bar{v}_T &= \frac{\left[ \frac{\epsilon_A v_z}{\epsilon_T} \right]}{\left[ 1 + \frac{\rho_B \hat{c}_p}{\alpha c_p \epsilon_T} \right]}\end{aligned}$$

The asymptotic temperature pulse velocity for large  $t$  is the same in all three phases,

$$v_T = \bar{v}_T = \overline{\bar{v}}_T = \hat{\bar{v}}_T = \frac{\left[ \frac{\epsilon_A v_z}{\epsilon_T} \right]}{\left[ 1 + \frac{\rho_B \hat{c}_p}{\alpha c_p \epsilon_T} \right]} = \frac{v}{\left[ 1 + \frac{\rho_B \hat{c}_p}{\alpha c_p \epsilon_T} \right]}\quad (6.1.1)$$

The rate of spreading of the temperature pulse or the axial effective heat dispersion coefficient is given in terms of the standard deviation,  $\omega$ , as follows:

For the moving phase,

$$(D_e)_{H,z} = \frac{1}{2} \frac{d}{dt} (\omega^2) = \frac{1}{2} \frac{d}{dt} \left[ \left[ \frac{\mu_2}{\mu_0} \right] - (\bar{z})^2 \right]$$

For the stagnant phase,

$$(\bar{D}_e)_{H,z} = \frac{1}{2} \frac{d}{dt} (\bar{\omega}^2) = \frac{1}{2} \frac{d}{dt} \left[ \left[ \frac{\bar{\mu}_2}{\bar{\mu}_0} \right] - (\bar{z})^2 \right]$$

For the solid phase,

$$(\hat{D}_e)_{H,z} = \frac{1}{2} \frac{d}{dt} (\hat{\omega}^2) = \frac{1}{2} \frac{d}{dt} \left[ \left[ \frac{\hat{\mu}_2}{\hat{\mu}_0} \right] - (\hat{z})^2 \right]$$

For large  $t$ , the asymptotic value of the axial effective heat dispersion coefficient is the same for all three phases,

$$\begin{aligned} D_{H,z} &= (D_e)_{H,z} = (\bar{D}_e)_{H,z} = (\hat{D}_e)_{H,z} \\ &= \frac{\left( \frac{\epsilon_A^V}{\epsilon_T} z \right)^2 \cdot \frac{\epsilon_B^2}{g \epsilon_T}}{\left[ 1 + \frac{\rho_B \hat{c}_p}{\alpha c_p \epsilon_T} \right]^3} + \frac{\left( \frac{\epsilon_A^V}{\epsilon_T} z \right)^2 (\rho_B \hat{c}_p)^2}{(2h\delta S)(\alpha c_p \epsilon_T) \left[ 1 + \frac{\rho_B \hat{c}_p}{\alpha c_p \epsilon_T} \right]^3} + \frac{k_s \cdot \hat{\delta S} \cdot \lambda}{\alpha c_p \epsilon_T \cdot \left[ 1 + \frac{\rho_B \hat{c}_p}{\alpha c_p \epsilon_T} \right]} \end{aligned} \quad (6.1.m)$$

The first term in eqn. 6.1.m represents dispersion due to mixing in the external fluid; the second term is generated due to the heat transfer between the moving fluid and the solid phase; the last term represents the dispersion due to conductive heat transfer in the solid.



## 6.2 Evaluation of Heat Transfer Parameters

Eqn. 6.1.m can be rewritten in terms of the asymptotic mass dispersivity

$$D_{H,z} = \frac{D_z \left[ 1 + \left( \frac{\epsilon_{A,z}^v}{\epsilon_T} \right)^2 \cdot \frac{(\rho_B \hat{c}_p)^2}{D_z \cdot (2h\delta S) \cdot \alpha c_p \epsilon_T} \right]}{\left[ 1 + \frac{\rho_B \hat{c}_p}{\alpha c_p \epsilon_T} \right]^3} + \frac{k_s \cdot \hat{\delta S} \cdot \lambda}{\alpha c_p \epsilon_T \cdot \left[ 1 + \frac{\rho_B \hat{c}_p}{\alpha c_p \epsilon_T} \right]}$$

The asymptotic axial heat Peclet number is defined as,

$$Pe_{H,z} = \frac{v_T d_p}{D_{H,z}} = \frac{\left( \frac{\epsilon_{A,z}^v}{\epsilon_T} \right) \cdot d_p}{D_z \frac{\left[ 1 + \left( \frac{\epsilon_{A,z}^v}{\epsilon_T} \right)^2 \cdot \frac{(\rho_B \hat{c}_p)^2}{D_z \cdot (2h\delta S) \cdot (\alpha c_p \epsilon_T)} \right]}{\left[ 1 + \frac{\rho_B \hat{c}_p}{\alpha c_p \epsilon_T} \right]^2} + \frac{k_s \cdot \hat{\delta S} \cdot \lambda}{\alpha c_p \epsilon_T}} \quad (6.2.a)$$

In most of the experimental work that has been done (Gunn and DeSouza 1974, using the one phase dispersion model or Fickian model; Littman and Sliva 1970, using the two phase model (eqns. 1.2.c, 1.2.d)), it is safe to assume for gaseous flow that the heat capacity ratio,

$$\frac{\rho_B \hat{c}_p}{\alpha c_p \epsilon_T} \gg 1 \quad (6.2.b)$$

With this assumption, eqn. 6.2.a reduces to

$$\begin{aligned}
 Pe_{H,z} &= \frac{\left( \frac{\epsilon_{AVZ}}{\epsilon_T} \right) \cdot d_p}{D_z \left( \frac{\alpha c_p \epsilon_T}{\rho_B \hat{c}_p} \right)^2 + \left( \frac{\epsilon_{AVZ}}{\epsilon_T} \right)^2 \cdot \frac{\alpha c_p \epsilon_T}{2h \delta S} + \frac{k_s \cdot \hat{\delta S} \cdot \lambda}{\alpha c_p \epsilon_T}} \\
 &= \frac{1}{\frac{1}{Pe_z} \cdot \left( \frac{\alpha c_p \epsilon_T}{\rho_B \hat{c}_p} \right)^2 + \left( \frac{\epsilon_{AVZ}}{\epsilon_T} \right) \cdot \frac{1}{d_p} \cdot \frac{\alpha c_p \epsilon_T}{2h \delta S} + \left( \frac{\epsilon_T}{\epsilon_{AVZ}} \right) \cdot \frac{1}{d_p} \cdot \frac{k_s \hat{\delta S} \lambda}{\alpha c_p \epsilon_T}}
 \end{aligned}$$

Now, with  $Pe_z = 2$  and inequality 6.2.b, it is observed that the first term in the denominator is much smaller than the other two terms and hence can be neglected. Thus,

$$Pe_{H,z} = \frac{1}{\left( \frac{\epsilon_{AVZ}}{\epsilon_T} \right) \cdot \frac{1}{d_p} \cdot \frac{\alpha c_p \epsilon_T}{2h \delta S} + \left( \frac{\epsilon_T}{\epsilon_{AVZ}} \right) \cdot \frac{1}{d_p} \cdot \frac{k_s \hat{\delta S} \lambda}{\alpha c_p \epsilon_T}}$$

and with  $\lambda = d_p / \sqrt{2}$

$$Pe_{H,z} = \frac{(\epsilon_{AVZ}) \alpha c_p \cdot d_p}{\frac{[(\epsilon_{AVZ}) \alpha c_p]^2}{2h \cdot \delta S} + \frac{k_s \cdot \hat{\delta S} \cdot d_p}{\sqrt{2}}} \quad (6.2.c)$$

D. Vortmeyer 1975, has an identical expression for the Peclet number (eqn. 6.2.e) neatly correlated with the most recent and extensive experimental work done on axial heat Peclet numbers (Hansen and Jorgensen 1974, Gunn and DeSouza 1974, Littman and Sliva 1970, Yagii, Kunni and Wakao 1960).

Vortmeyer considered the two phase model (eqn. 1.2.c and 1.2.d),

and assumed that the gas phase heat capacity is negligible and also that the gas phase dispersion processes are negligible effects. Only the solid phase contains a feed-back term (eqns. 1.2.c and 1.2.d) with a coefficient  $\lambda_o$  which is approximately equal to the effective conductivity of the quiescent bed. An equivalent one phase model was derived (Vortmeyer and Shaefer 1974) by using an arbitrary assumption called by Vortmeyer the equivalence condition, namely,

$$\frac{\partial^2 T}{\partial z^2} = \frac{\partial^2 \hat{T}}{\partial z^2} \quad (6.2.d)$$

The Peclet number obtained is

$$Pe = \frac{u \alpha_c d_p}{\lambda_o + \frac{m_f^2 c_p^2}{h a}} = \frac{Re \cdot Pr}{\frac{\lambda_o}{\lambda_f} + \frac{Re^2 \cdot Pr^2}{6(1-\epsilon_T) \cdot Nu}} \quad (6.2.e)$$

where,

$$m_f = \text{mass flow rate of fluid (ML}^{-2} \text{ t}^{-1}\text{)}$$

$$\lambda_f = \text{thermal conductivity of fluid (M L t}^{-3} \text{ T}^{-1}\text{)}$$

$$Re = \text{Reynolds number, } m_f d_p / \mu_f$$

$$\mu_f = \text{dynamic viscosity of fluid (M L}^{-1} \text{ t}^{-1}\text{)}$$

$$Pr = \text{Prandtl number, } \frac{c_p \mu_f}{\lambda_f}$$

$$Nu = \text{Nusselt number, } \frac{h d_p}{\lambda_f}$$

Comparing eqn. 6.2.c with eqn. 6.2.e, the parameters in the non-Fickian model are easily correlated as

$$k_s \cdot \hat{\delta S} = \frac{\lambda_o \sqrt{2}}{d_p} \quad (6.2.f)$$

$$2h \cdot \delta S = ha \quad (6.2.g)$$

Hence axial Peclet numbers can be calculated as a function of  $Re$  from known  $\lambda_o/\lambda_f$  ratios of the quiescent bed and from known correlations for particle/fluid heat transfer data.

Eqn. 6.2.a can be rewritten as:

$$Pe_{H,z} = \frac{1}{\frac{1}{Pe_z \left(1 + \frac{\rho_B \hat{c}_p}{\alpha_{c_p} \epsilon_T}\right)^2} + \frac{Re \cdot Pr \cdot \left(\frac{\rho_B \hat{c}_p}{c_p T}\right)^2}{6(1-\epsilon_T) \cdot Nu \cdot \left(1 + \frac{\rho_B \hat{c}_p}{\alpha_{c_p} \epsilon_T}\right)^2} + \frac{\lambda_o}{\lambda_f \cdot Re \cdot Pr}} \quad (6.2.h)$$

Eqn. 6.2.h gives the relationship between asymptotic axial heat Peclet number and Reynolds number.

### 6.3 Transverse Heat Dispersion in Non-Reactive Packed Beds

In this section, radial dispersion of heat is studied with no wall effects.

#### 6.3.1 Moment Analysis

The equations of heat transfer have been written based on Mechanism I (see Chapter 2). Consider an infinite pulse at  $t = 0$  on the plane  $y = 0$ . The solution is independent of  $z$ , so the equations become:

$$\frac{\partial T}{\partial t} + \frac{g}{\epsilon_A} (T - \bar{T}) + \frac{2h \cdot \delta S}{\alpha_{c_p} \epsilon_A} \cdot (T - \hat{T}) - \frac{h \cdot \delta S \cdot \lambda^2}{\alpha_{c_p} \epsilon_A} \cdot \frac{\partial^2 T}{\partial y^2} = 0 \quad (6.3.1.a)$$

$$\frac{\partial \bar{T}}{\partial t} + \frac{g}{\epsilon_B} (\bar{T} - T) - \frac{g \lambda^2}{2 \epsilon_B} \cdot \frac{\partial^2 \bar{T}}{\partial y^2} = 0 \quad (6.3.1.b)$$

$$\frac{\partial \hat{T}}{\partial t} + \frac{2h\delta S}{\rho_B \hat{c}_p} \cdot (\hat{T} - T) - \frac{h \cdot \delta S \cdot \lambda^2}{\rho_B \hat{c}_p} \cdot \frac{\partial^2 T}{\partial y^2} - \frac{k_s \cdot \delta S \cdot \lambda}{\rho_B \hat{c}_p} \cdot \frac{\partial^2 \hat{T}}{\partial y^2} = 0 \quad (6.3.1.c)$$

$$T(y,0) = \delta(y) ; \quad \bar{T}(y,0) = \delta(y) ; \quad \hat{T}(y,0) = \delta(y) \quad (6.3.1.d)$$

The nth moments of  $T(y,t)$ ,  $\bar{T}(y,t)$ , and  $\hat{T}(y,t)$  are defined as in Section 4.1,

Eqs. 6.3.1.a, 6.3.1.b, 6.3.1.c, are multiplied by  $y^n$  and integrated, to obtain the following equations satisfied by moments.

$$\frac{\partial \mu_n}{\partial t} + \frac{g}{\epsilon_A} (\mu_n - \bar{\mu}_n) + \frac{2h \delta S}{\alpha c_p \epsilon_A} \cdot (\mu_n - \hat{\mu}_n) - \frac{h \cdot \delta S \cdot \lambda^2}{\alpha c_p \epsilon_A} \cdot n(n-1) \hat{\mu}_{n-2} = 0 \quad (6.3.1.e)$$

$$\frac{\partial \bar{\mu}_n}{\partial t} + \frac{g}{\epsilon_B} (\bar{\mu}_n - \mu_n) - \frac{g \lambda^2}{2 \epsilon_B} \cdot n(n-1) \mu_{n-2} = 0 \quad (6.3.1.f)$$

$$\frac{\partial \hat{\mu}_n}{\partial t} + \frac{2h\delta S}{\rho_B \hat{c}_p} \cdot (\hat{\mu}_n - \mu_n) - \frac{h \cdot \delta S \cdot \lambda^2}{\rho_B \hat{c}_p} \cdot n(n-1) \mu_{n-2} - \frac{k_s \cdot \delta S \cdot \lambda}{\rho_B \hat{c}_p} \cdot n(n-1) \hat{\mu}_{n-2} = 0 \quad (6.3.1.g)$$

$$\left. \begin{aligned} \mu_0(0) &= 1 ; \mu_1(0) = \mu_2(0) = \dots = 0 \\ \bar{\mu}_0(0) &= 1 ; \bar{\mu}_1(0) = \bar{\mu}_2(0) = \dots = 0 \\ \hat{\mu}_0(0) &= 1 ; \hat{\mu}_1(0) = \hat{\mu}_2(0) = \dots = 0 \end{aligned} \right\} \quad (6.3.1.h)$$

The zeroth, first and second moments are solved for with the help of laplace transforms

$$\mu_0 = \bar{\mu}_0 = \hat{\mu}_0 = 1$$

$$\mu_1 = \bar{\mu}_1 = \hat{\mu}_1 = 0$$

For large  $t$ ,

$$\mu_2 = \bar{\mu}_2 = \hat{\mu}_2 = \frac{2 \left[ \frac{g\lambda^2}{2\epsilon_T} + \frac{2h \cdot \delta S}{\alpha c_p \epsilon_T} \cdot \lambda^2 + \frac{k_s \cdot \delta S \cdot \lambda}{\alpha c_p \epsilon_T} \right] \cdot t}{\left( 1 + \frac{\rho_B \hat{c}_p}{\alpha c_p \epsilon_T} \right)} \quad (6.3.1.i)$$

The rate of spreading of the temperature pulse determines the radial effective heat dispersion coefficient which is defined by:

$$(D_e)_{H,y} = \frac{1}{2} \frac{d}{dt} (\omega^2) = \frac{1}{2} \frac{d}{dt} \left[ \left( \frac{\mu_2}{\mu_0} \right)^2 - \left( \frac{\mu_1}{\mu_0} \right)^2 \right], \text{ for the moving phase.}$$

$$(\bar{D}_e)_{H,y} = \frac{1}{2} \frac{d}{dt} (\bar{\omega}^2) = \frac{1}{2} \frac{d}{dt} \left[ \left( \frac{\bar{\mu}_2}{\bar{\mu}_0} \right)^2 - \left( \frac{\bar{\mu}_1}{\bar{\mu}_0} \right)^2 \right], \text{ for the stagnant phase.}$$

$$(\hat{D}_e)_{H,y} = \frac{1}{2} \frac{d}{dt} (\hat{\omega}^2) = \frac{1}{2} \frac{d}{dt} \left[ \left( \frac{\hat{\mu}_2}{\hat{\mu}_0} \right)^2 - \left( \frac{\hat{\mu}_1}{\hat{\mu}_0} \right)^2 \right], \text{ for the solid phase.}$$

For large  $t$ , the asymptotic value of the radial effective heat dispersion coefficient is the same for all three phases,

$$\begin{aligned} D_{H,y} &= (D_e)_{H,y} = (\bar{D}_e)_{H,y} = (\hat{D}_e)_{H,y} \\ &= \frac{\left[ \frac{g\lambda^2}{2\epsilon_T} + \frac{2h \cdot \delta S \cdot \lambda^2}{\alpha c_p \epsilon_T} + \frac{k_s \cdot \delta S \cdot \lambda}{\alpha c_p \epsilon_T} \right]}{\left( 1 + \frac{\rho_B \hat{c}_p}{\alpha c_p \epsilon_T} \right)} \end{aligned} \quad (6.3.1.j)$$

The first term in the numerator in eqn. 6.3.1.j represents the heat dispersion due to mixing in the external fluid; the second term is generated due to the heat transfer between the moving fluid and

the solid phase; the last term represents the dispersion due to conductive heat transfer in the solid.

The asymptotic radial heat Peclet number is defined as

$$Pe_{H,y} = \frac{v_T d_p}{D_{H,y}} = \frac{\left[ \frac{\epsilon_{AVZ}}{\epsilon_T} \right] d_p}{\left[ \frac{g\lambda^2}{2\epsilon_T} + \frac{2h \cdot \delta S \cdot \lambda^2}{\alpha c_p \epsilon_T} + \frac{k_s \cdot \hat{\delta S} \cdot \lambda}{\alpha c_p \epsilon_T} \right]} \quad (6.3.1.k)$$

With  $\lambda = d_p/\sqrt{2}$  and, relating  $g$  with axial mass Peclet number (eqn. 4.3.1.a), the radial heat Peclet number can be written in terms of axial and radial mass Peclet numbers and the heat transfer parameters already correlated in Section 6.2.

$$Pe_{H,y} = \frac{Pe_{m,y}}{\left[ 1 + \frac{2(2h \cdot \delta S) d_p}{(\alpha c_p \epsilon_T) \left( \frac{\epsilon_{AVZ}}{\epsilon_T} \right) Pe_z} \cdot \left( \frac{\epsilon_T}{\epsilon_B} \right)^2 + \frac{2k_s \cdot \hat{\delta S} \cdot \sqrt{2}}{(\alpha c_p \epsilon_T) \left( \frac{\epsilon_{AVZ}}{\epsilon_T} \right) Pe_z} \cdot \left( \frac{\epsilon_T}{\epsilon_B} \right)^2 \right]} \quad (6.3.1.1)$$

or, in terms of dimensionless parameters like Reynolds number, Nusselt number and Prandtl number,

$$Pe_{H,y} = \frac{Pe_{m,y}}{\left[ 1 + \frac{12(1-\epsilon_T) \cdot Nu}{Re \cdot Pr \cdot Pe_z} \cdot \left( \frac{\epsilon_T}{\epsilon_B} \right)^2 + \frac{4 (\lambda_o/\lambda_f)}{Re \cdot Pr \cdot Pe_z} \cdot \left( \frac{\epsilon_T}{\epsilon_B} \right)^2 \right]} \quad (6.3.1.m)$$

#### 6.4 Steady State Heat Transfer Equations

At steady state the heat transfer equations reduce to

$$v_z \frac{\partial T}{\partial z} + \frac{g}{\epsilon_A} (T - \bar{T}) + \frac{2h \cdot \delta S}{\alpha c_p \epsilon_A} (T - \hat{T}) - \frac{h \cdot \delta S \cdot \lambda^2}{\alpha c_p \epsilon_A} \cdot \frac{\partial^2 \hat{T}}{\partial y^2} = \frac{R(-\Delta H)}{\alpha c_p} \quad (6.4.a)$$

$$\frac{g}{\epsilon_B} (\bar{T} - T) - \frac{g \lambda^2}{2 \epsilon_B} \frac{\partial^2 T}{\partial y^2} = \frac{\bar{R}(-\Delta H)}{\alpha c_p} \quad (6.4.b)$$

$$\frac{2h \cdot \delta S}{\rho_B \hat{c}_p} (\hat{T} - T) - \frac{k_s \cdot \delta S \cdot \lambda}{\rho_B \hat{c}_p} \cdot \frac{\partial^2 \hat{T}}{\partial z^2} - \frac{k_s \cdot \delta S \cdot \lambda}{\rho_B \hat{c}_p} \cdot \frac{\partial^2 \hat{T}}{\partial y^2} - \frac{h \cdot \delta S \cdot \lambda^2}{\rho_B \hat{c}_p} \cdot \frac{\partial^2 T}{\partial y^2} = \frac{\hat{R} \rho_B (-\Delta H)}{\rho_B \hat{c}_p} \quad (6.4.c)$$

Substituting for  $\frac{g}{\epsilon_A} (T - \bar{T})$  from eqn. 6.4.b and  $\frac{2h \cdot \delta S}{c_p \epsilon_A} (T - \hat{T})$  from eqn. 6.4.c into eqn. 6.4.a, the following equation is obtained.

$$\left( \frac{\epsilon_A v_z}{\epsilon_T} \right) \frac{\partial T}{\partial z} - \frac{k_s \cdot \delta S \cdot \lambda}{\alpha c_p \epsilon_T} \frac{\partial^2 \hat{T}}{\partial z^2} - \left( \frac{g \lambda^2}{2 \epsilon_T} + \frac{h \cdot \delta S \cdot \lambda^2}{\alpha c_p \epsilon_T} \right) \cdot \frac{\partial^2 T}{\partial y^2} - \left( \frac{h \cdot \delta S \cdot \lambda^2}{\alpha c_p \epsilon_T} + \frac{k_s \cdot \delta S \cdot \lambda}{\alpha c_p \epsilon_T} \right) \frac{\partial^2 \hat{T}}{\partial y^2} = \frac{(\epsilon_A R + \epsilon_B \bar{R} + \hat{R} \rho_B) (-\Delta H)}{\alpha c_p \epsilon_T} \quad (6.4.d)$$

If the Vortmeyer equivalence condition (eqn. 6.2.d) is extended to the radial direction also,

$$\frac{\partial^2 T}{\partial y^2} = \frac{\partial^2 \hat{T}}{\partial y^2} \quad (6.4.e)$$

then eqn. 6.4.d becomes identical to the Fickian model and can be written as,



$$\begin{aligned}
\left( \frac{\epsilon_A^V z}{\epsilon_T} \right) \frac{\partial T}{\partial z} - \left( \frac{k_S \cdot \hat{\delta S} \cdot \lambda}{\alpha c_p \epsilon_T} \right) \frac{\partial^2 T}{\partial z^2} - \left( \frac{g\lambda^2}{2\epsilon_T} + \frac{2h \cdot \delta S \cdot \lambda^2}{\alpha c_p \epsilon_T} + \frac{k_S \cdot \hat{\delta S} \cdot \lambda}{\alpha c_p \epsilon_T} \right) \frac{\partial^2 T}{\partial y^2} \\
= \frac{(\epsilon_A R + \epsilon_B \bar{R} + R \rho_B)(-\Delta H)}{\alpha c_p \epsilon_T} \quad (6.4.f)
\end{aligned}$$

Eqn. 6.4.f assumes that the Vortmeyer condition is satisfied both axially and transversely. Hence, the detailed, general, two-dimensional non-Fickian model for heat transfer can always be reduced to the Fickian model with the help of Vortmeyer-type conditions. However, these conditions should be used with caution as there is no physical basis for these assumptions. Also, as will be shown in Chapter 7, the Vortmeyer assumption introduces a significant change in the gain profile in the frequency response analysis of a non-isothermal, first-order chemical reaction case.

From eqn. 6.4.f, the steady state axial and radial Peclet numbers are

$$(Pe_{H,z})_{s.s.} = \frac{\left( \frac{\epsilon_A^V z}{\epsilon_T} \right) dp}{\left( \frac{k_S \cdot \hat{\delta S} \cdot \lambda}{\alpha c_p \epsilon_T} \right)} = \frac{Re \cdot Pr}{\frac{\lambda_o}{\lambda_f}} \neq Pe_{H,z} \quad (6.4.g)$$

$$(Pe_{H,y})_{s.s.} = \frac{\left( \frac{\epsilon_A^V z}{\epsilon_T} \right) d_p}{\left( \frac{g\lambda^2}{2\epsilon_T} + \frac{2h \cdot \delta S \cdot \lambda^2}{\alpha c_p \epsilon_T} + \frac{k_S \cdot \hat{\delta S} \cdot \lambda}{\alpha c_p \epsilon_T} \right)} = Pe_{H,y} \quad (6.4.h)$$

Eqn. 6.4.g clearly indicates that the axial heat Peclet number,

which is a parameter associated with the Fickian model, is inadequate to represent behaviour in general. If one must use the Fickian model, then the value of the axial heat Peclet number in the dynamic case is smaller than the value in a steady state case, in order to incorporate the dynamic heat transfer effects of convective heat transfer.

#### 6.5 Numerical Simulation to Validate Use of Asymptotic Values

It is important to determine how soon the pulse velocity reaches its asymptotic value in order to ascertain the range of validity of asymptotic values of dispersion coefficients and hence Peclet numbers as parameters to describe heat and mass transfer in packed beds.

Hansen and Jorgensen 1974, have experimentally investigated the dynamics of a catalytic packed bed reactor. A pilot plant packed bed was designed to eliminate secondary heat dispersion effects (like heat transfer to the wall) and the dynamics were primarily due to the packed bed itself. The reactor bed was used as a heat regenerator whereby the heat transfer parameters were evaluated by studying the response on step and pulse disturbances in inlet temperature at otherwise constant operating conditions.

A typical set of experimental data (Exp. No. F22) will be considered in this section from the results published by Hansen and Jorgensen 1974 (shown on page 108). In the experiment, with  $H_2$  gas flowing, a temperature pulse was injected in the adiabatic bed. A one-dimensional homogeneous model (Fickian model) was used and two parameters were estimated, namely, the Peclet number for heat transport,  $Pe_H$ , and the thermal residence time,  $\tau$ . Results are given on

Table I. Properties of Reactor and Catalyst

Parameter	Value
Reactor length ( $L$ )	50 cm
Reactor diameter ( $D$ )	0.6 cm
Reactor porosity ( $\epsilon$ )	0.41
Thickness of reactor wall	0.01 cm
Catalyst density ( $\rho_s$ )	1.24 gram/cm <sup>3</sup>
Pore volume ( $V$ )	0.54 cm <sup>3</sup> /gram
Catalyst porosity ( $\rho_v V$ )	0.67
Surface area ( $S$ ), BET	$24 \times 10^4$ cm <sup>2</sup> /gram
Av. pore radius ( $2V/S$ )	450 Å
Catalyst diameter ( $d$ )	0.37 cm
Specific heat capacity of catalyst (calorimetric measurement)	0.23 cal/gram

Table II. Experimental Conditions

Exp. No.	$g$ , gram/ cm <sup>2</sup> sec	$Y$ , mole %	$T$ , °K	$P_{\text{tot}}$ , atm	$\Delta P$ , atm	Reynolds No. (Inlet)
F22	0.00437	0.70	371.3	1.072	0.066	15.5
F31	0.00298	0.80	371.8	1.000	0.033	10.6

Table III. Estimation of Heat Transfer Parameters; Data Series of 64 Points Prolonged to 512 Points

Exp. No.	$T$ , min	$z$	$Pe_h$	$\tau$ , min	Av. Values
F22	168	0.393	121.5 ( $\pm 10\%$ )	10.17 ( $\pm 0.8\%$ )	$\tau = 10.4$ min
F22	168	0.496	121 ( $\pm 8\%$ )	10.00 ( $\pm 0.5\%$ )	$Pe_h = 118$
F22	168	0.790	117 ( $\pm 7\%$ )	10.75 ( $\pm 0.4\%$ )	$Pe_h \times d/L = 0.87$
F22	168	0.890	111.5 ( $\pm 4\%$ )	10.59 ( $\pm 0.2\%$ )	
F31	196	0.393	112 ( $\pm 4\%$ )	16.17 ( $\pm 0.3\%$ )	$\tau = 16.1$ min
F31	196	0.496	110.5 ( $\pm 5\%$ )	15.74 ( $\pm 0.4\%$ )	$Pe_h = 103.5$
F31	196	0.790	98 ( $\pm 8\%$ )	16.33 ( $\pm 0.4\%$ )	$Pe_h \times d/L = 0.77$
F31	196	0.890	93.5 ( $\pm 11\%$ )	16.00 ( $\pm 0.6\%$ )	

page 108, Table III.

Under the experimental conditions of F22, if a pulse of tracer is injected into the bed, the velocity in the moving phase would be given by eqn. 3.1.h. The density of the flowing gas,  $\alpha = \frac{P_O M}{R_g T_O}$

where,  $P_O$  = average pressure in the bed = 1.072 atm  
 $M$  = molecular weight = 2  
 $R_g$  = gas law constant =  $82.05 \text{ cm}^3\text{-atm-g mole}^{-1}\text{ }^\circ\text{K}^{-1}$   
 $T_O$  = temperature =  $371.3 \text{ }^\circ\text{K}$

For the experimental conditions of F22,

$$\alpha = 7.038 \times 10^{-5} \text{ g/c}\cdot\text{c}\cdot$$

The superficial velocity,

$$u = (\epsilon_A v_z) = \frac{G}{\alpha} = 62.095 \text{ cm/sec}$$

where,  $G$  = superficial mass flow rate =  $.00437 \text{ g/cm}^2 \text{ sec}$

The two basic parameters in the non-Fickian model to describe fluid flow in packed beds are  $\epsilon_B$  and  $g$ .

From eqn. 1.1.b,  $\epsilon_B = 0.198$

The parameter  $g$  can be calculated in two ways.

The first way is from dispersion data in packed beds. Assuming

$Pe_z = 2$ , eqn. 4.3.1.a gives

$$g = 78.28 \text{ sec}^{-1}$$

The second way to evaluate the parameter  $g$  is from friction factor

data in packed beds. Fig. 5.1 in Zenz and Othmer 1960, shows that the friction factor,  $f$ , for  $\epsilon_T = 0.41$  and large Reynolds number is 6. For highly turbulent flows (large Reynolds number) eqn. 4.4.d is valid and hence can be used to evaluate  $g$ .

$$g = 90.51 \text{ sec}^{-1}.$$

The discrepancy is due to the approximate method of estimating the friction factor from the data presented in Zenz and Othmer.

The average value is taken for further calculations:  $g = 84.40 \text{ sec}^{-1}$ .

The pulse velocity in the moving phase given by eqn. 3.1.h is, then,

$$\bar{v} = 151.45 + 141.45 e^{-824.3 t}$$

The negative exponent of the exponential is so large that the pulse velocity reaches its asymptotic value almost instantaneously

$$v = \bar{v} = \bar{\bar{v}} = \left( \frac{\epsilon_{AZ}}{\epsilon_T} \right) = 151.45 \text{ cm/sec}$$

The thermal residence time and the Peclet number can be predicted from the analysis of the heat transfer equations of the non-Fickian model in Sections 6.1 and 6.2. The thermal conductivity of  $H_2$  is obtained from graph B-36a of the publication by McCarty 1975. The heat capacity is obtained from p. 318 of the publication by American Petroleum Institute Research Project 44, 1947. The Prandtl number is obtained from Section 8.3 of the book by Bird, Stewart and Lightfoot 1960.

$$\begin{aligned}
 c_p &= 3.453 \text{ cal/g} - o_c \\
 \lambda_f &= 4.609 \times 10^{-4} \text{ cal/cm-sec } o_K \\
 Pr &= 0.73
 \end{aligned}$$

For  $13 < Re < 180$ , the correlation for Nusselt number is

$$Nu = 1.75 Re^{0.49} Pr^{1/3} \quad (\text{Vortmeyer 1975})$$

$$\text{with } Re = 15.5 \quad (\text{Table II})$$

$$Nu = \frac{hd_p}{\lambda_f} = 6.036$$

$$\text{Therefore, } h = 7.519 \times 10^{-3} \text{ cal/cm-sec } o_K$$

$$a = \frac{6(1-\epsilon_T)}{d_p} = 9.568 \text{ cm}^2/\text{cm}^3 .$$

$$\text{Therefore, } 2h \cdot \delta S = ha = 7.194 \times 10^{-2} \text{ cal/cm}^3\text{-sec } o_K .$$

Eqn. 6.1.i gives the average temperature pulse velocity in the moving phase. The parameters in the equation are defined in Section 6.1 in terms of three of the four basic parameters in the one-dimensional non-Fickian model, namely,  $\epsilon_p$ ,  $g$ , and  $2h\delta S$  which have been evaluated above.

$$\begin{aligned}
 \text{Hence, } \hat{h} &= 0.4282 \text{ sec}^{-1} \\
 \tilde{h} &= 1.396 \times 10^3 \text{ sec}^{-1} \\
 A &= 2.22 \times 10^3 \text{ sec}^{-1} \\
 B &= 5.95 \times 10^5 \text{ sec}^{-2} \\
 C &= 7.979 \times 10^2 \text{ i sec}^{-1} \\
 N_1 &= 0.2103 \\
 N_2 &= 7.59 \times 10^2
 \end{aligned}$$

and

$$\bar{v}_T = 0.0896 e^{-1110 t} \{292.13 \cosh (797.9 t) - 898.4 \sinh (797.9 t)\}$$

The exponent is so small that the pulse velocity reaches its asymptotic value almost instantaneously.

Therefore,

$$v_T = \bar{v}_T = \overline{\bar{v}}_T = \hat{\bar{v}}_T = \frac{\left( \frac{\epsilon_A v_z}{\epsilon_T} \right)}{\left( 1 + \frac{\rho_B \hat{c}_p}{\alpha c_p \epsilon_T} \right)} = 0.0896 \text{ cm/sec}$$

The thermal residence time in the bed is

$$\tau = \frac{L}{v_T} = \frac{50}{(60)(0.0896)} = 9.3 \text{ min}$$

In order to calculate the Peclet number for heat transport both parameters of the non-Fickian heat transfer model,  $2h\delta S$  and  $k_s \hat{\delta S}$ , are needed. Vortmeyer 1975, uses

$$\frac{\lambda_o}{\lambda_f} = \frac{k_s \hat{\delta S} d_p}{\sqrt{2} \lambda_f} = 7$$

Hence, from eqn. 6.2.h,  $Pe_{H,z}$  can be calculated

$$Pe_{H,z} = 0.8714$$

Eqn. 6.2.e is the reduced form of eqn. 6.2.h with the assumption that  $\frac{\rho_B \hat{c}_p}{\alpha c_p \epsilon_T} \gg 1$ . Eqn. 6.2.e gives

$$Pe_{H,z} = 0.8709$$

Hence assuming the heat capacity ratio,  $\frac{\rho_B \hat{c}_p}{\alpha c_p \epsilon_T} \gg 1$ , is a fairly good assumption and affects the value of the Peclet number only in the third decimal place and agrees closely with the experimentally observed value of Peclet number, 0.87 (Table III), by Hansen and Jorgensen.

It is concluded from this section that it is appropriate to use asymptotic values of mass and thermal parameters for analysis of packed beds.



## 7. DYNAMIC MODELING OF A GAS PHASE CATALYTIC PACKED BED REACTOR

### 7.1 Introduction

Hansen 1973, has briefly summarised the state of the art in the simulation of the transient behaviour of a packed bed reactor. Research in the dynamics of a packed bed reactor with exothermic chemical reactions has been split into two main areas: (a) Multiple steady state behaviour and (b) dynamic modeling in a single steady state. The theoretical work done in these two areas has been considerable (Liu and Amundson 1963, McGuire and Lapidus 1965, Feick and Quon 1970, Hansen 1971, Hansen et al. 1971, Stewart and Sorensen 1972, Hansen 1973); whereas the reported experiments have been few (Lyche 1967, Hoiberg and Lyche 1971, Padberg and Wicke 1967, Fieguth and Wicke 1971, Hoiberg 1969, Doesburg and De Jong 1974, Hansen and Jorgensen 1974, Hlavacek and Votruba 1974, Hansen and Jorgensen 1976).

In spite of all the research work done, it is still not possible to discriminate unambiguously between the various types of models; for example, the multiple steady state experiments of Wicke and co-workers can be described by both homogeneous and heterogeneous models. As a matter of fact, although these two kinds of models are based on different physical assumptions, both describe such important aspects of reactor behaviour as multiplicity of steady states, ignition and extinction, hysteresis, and migrating reaction zones. Vortmeyer and Shaefer 1974, have demonstrated that both models are equivalent in these respects if the second derivatives of gas and solid temperature

profiles are the same. Also in Section 6.4 it has been demonstrated that this equivalence can even be extended to the radial direction.

It should be noted that the performance of a packed bed reactor is highly non-linear due to the Arrhenius type temperature dependence of the reaction rate. Hence analyses based on linearised models have to be approached with caution. However, with fast computers and efficient numerical procedures it has become possible to solve very complicated models within reasonable computing time. Various researchers in the field have identified dominant dynamic characteristics in the packed bed and have also indicated the simplifications that could be introduced in the complicated models. Hansen 1971, and Hansen et al. 1971, have justified the following:

(1) Internal catalyst mass diffusion restriction is more important than the external diffusion restriction. Internal catalyst heat transport resistance is usually smaller than the external heat transport resistance, but they may be of the same order of magnitude.

(2) For many reaction systems the temperature change across the catalyst film and the internal pellet is very much smaller than the temperature change between reactor inlet and outlet. It is very important, however, to include the catalyst heat transport restrictions in the heterogeneous models in order to simulate dynamic behaviour.

(3) The gas residence time in the reactor is very much smaller than the thermal response time of the reactor, which is dominated by

the heat capacity of the solid catalyst particles (and the wall). The concentration profile can be considered to be quasi-stationary. This means that the model equations neglect the finite rate with which the very fast change in concentration profile takes place, almost without any change in the temperature profile. Thus the accumulation terms in the heat and mass balances for the gas can be considered to be negligible.

## 7.2 Dynamic Modeling Studies of Hansen and Jorgensen

In the present work, studies have been made comparing the Fickian model used by Hansen and Jorgensen 1976, to simulate dynamic modeling of a gas phase catalytic packed bed reactor, with the non-Fickian model which has been developed in the previous chapters.

Hansen and Jorgensen constructed a large scale fixed bed pilot plant reactor for the dynamic experiments. The reactor system was especially designed to suppress secondary dispersion effects not characteristic of the packed bed itself, particularly heat exchange with the wall and surroundings. The chemical reaction taking place is between hydrogen (99%) and oxygen (below 1%) on a platinum catalyst supported by alumina. The inlet temperature was 100°C and the pressure in the reactor was constant at a value slightly above atmospheric in their experiments. Under these conditions the gas behaves nearly ideally. The relatively high inlet temperature of 100°C prevents adsorption of water from being a dominating factor. Thus it is not necessary to include balances for the catalyst surface in the dynamic model (Kabel et al. 1968, Denis and Kabel 1970).

Hansen and Jorgensen describe the experimental apparatus and the modeling of the reaction kinetics in Part I of their three-part report. In parts II and III, the results of the dynamic experiments are compared with the simulation by the one dimensional Fickian model where no radial variations are considered.

The reaction between oxygen and hydrogen is normally considered close to first order in oxygen partial pressure with Arrhenius-type temperature dependence. The reaction rate expression is

$$R_g = k_f \cdot P \cdot \exp(-E/R_g \cdot T) \quad (7.2.a)$$

where,  $R$  = reaction rate; mole/(cm<sup>3</sup> sec)  
 $k_f$  = frequency factor, mole/(cm<sup>3</sup> sec atm)  
 $P$  = partial pressure of oxygen, atm.  
 $E$  = activation energy, cal/mole  
 $R_g$  = gas constant, cal (mole °K)  
 $T$  = temperature, °K

However, the chemical reaction rate is not clear-cut first order. Nevertheless, a first order kinetic model was used with axially variable parameters. The reactor was divided into three or four axial segments. In order to fit the experimental data, combinations of  $k_f$  and  $E$  have been estimated simultaneously in these axial segments and given in Table 5 of Part I of their paper for the various experiments that they performed.

It is assumed that the temperature difference between catalyst and gas is small and that the heat dispersion phenomena can be com-

bined into one overall dispersion mechanism. Also, it is assumed that the concentration profile behaves quasi-stationarily and that the total pressure is constant in the reactor. Then the model used by Hansen and Jorgensen takes the following form:

$$\frac{\partial y}{\partial t} + \frac{\partial y}{\partial z} = \frac{1}{Pe_h} \cdot \frac{\partial^2 y}{\partial z^2} + D_h \cdot x \cdot e^{\gamma(1-\frac{1}{y})} \quad (7.2.b)$$

$$\frac{\partial x}{\partial z} = \frac{1}{Pe_m} \cdot \frac{\partial^2 x}{\partial z^2} - D_m \cdot x \cdot e^{\gamma(1-\frac{1}{y})} \quad (7.2.c)$$

with boundary conditions:

$$y(0) = y_0 \quad (7.2.d)$$

$$x(0) = x_0 \quad (7.2.e)$$

$$\frac{\partial y}{\partial z}(1) = \frac{\partial x}{\partial z}(1) = 0 \quad (7.2.f)$$

where,

$$y = \frac{T}{T_{os}} ; \quad x = \frac{P}{P_{os}} ; \quad z = l/L ; \quad \gamma = \frac{E}{R_g T_{os}}$$

$$D_h = \frac{(-\Delta H) \cdot L \cdot k_f \cdot e^{-\gamma} \cdot P_{os} (1 - \epsilon_T)}{G_s \cdot c_p \cdot T_{os}}$$

$$D_m = \frac{L \cdot k_f \cdot e^{-\gamma} \cdot P_{tot} \cdot M \cdot (1 - \epsilon_T)}{G_s}$$

and,

$T_{os}$  = inlet temperature at steady state, °K

$L$  = reactor length, cm

$l$  = axial coordinate, cm

$P_{os}$  = inlet partial pressure of oxygen at steady state, atm.

- $P_{\text{tot}}$  = average pressure in reactor, atm.  
 $t$  = dimensionless time,  $t'/\tau$   
 $t'$  = time, sec or min  
 $\tau$  = thermal residence time, sec or min  
 $Pe_h$  = axial Peclet number for heat transport  
 $Pe_m$  = axial Peclet number for mass transport.  
 $-\Delta H$  = heat of reaction = 116,300 cal/mole  
 $G_s$  = mass flow rate (empty tube), g/(cm<sup>2</sup> sec)  
 $M$  = molecular weight of gas, g/mole

The thermal parameters  $Pe_h$  and  $\tau$  are determined by fitting the model response to the experimental response following disturbances in the inlet temperature. For the mass transport Peclet number  $Pe_m$  a value of 271 has been used corresponding to the relation  $Pe_m \times \frac{d}{L} = 2$  which is the asymptotic value for the Peclet number at high Reynolds number.

### 7.3 Corresponding Non-Fickian Model

The non-Fickian model corresponding to the Fickian model described in Section 7.2, is derived in this section for the same assumptions. Assuming the concentration profile behaves quasi-stationarily, the mass-transfer equations reduce to the steady state case. Neglecting gas heat dynamics (Vortmeyer), and taking the heat source term due to chemical reaction to be in the solid phase, the model equations (see eqns. 2.1.1.e, 2.1.1.f, 2.2.c, 2.2.f, 2.2.j) become:

$$v_z \frac{dc}{dz} + \frac{g}{\epsilon_A} (c - \bar{c}) = -R \quad (7.3.a)$$

$$\frac{g}{\epsilon_B} (\bar{c} - c) = - \bar{R} \quad (7.3.b)$$

$$v_z \frac{dT}{dz} + \frac{g}{\epsilon_A} (T - \bar{T}) + \frac{2h \cdot \delta S}{\alpha_c \epsilon_A} \cdot (T - \hat{T}) = 0 \quad (7.3.c)$$

$$\frac{g}{\epsilon_B} (\bar{T} - T) = 0 \quad (7.3.d)$$

$$\frac{\partial \hat{T}}{\partial t} + \frac{2h \delta S}{\rho_B \hat{c}_p} \cdot (\hat{T} - T) - \frac{k_s \cdot \delta S \cdot \lambda}{\rho_B \hat{c}_p} \frac{\partial^2 \hat{T}}{\partial z^2} = \frac{\hat{R} \cdot \rho_B \cdot (-\Delta H)}{\rho_B \hat{c}_p} \quad (7.3.e)$$

### 7.3.1 Mass Transfer Equations

Substituting for the rate expressions in eqns. 7.3.a and 7.3.b, the mass transfer equations become

$$v_z \frac{dc}{dz} + \frac{g}{\epsilon_A} (c - \bar{c}) = - k_f \cdot P \cdot e^{-\gamma} \cdot e^{\gamma(1 - \frac{1}{y})} \quad (7.3.1.a)$$

$$\frac{g}{\epsilon_B} (\bar{c} - c) = - k_f \cdot \bar{P} \cdot e^{-\gamma} \cdot e^{\gamma(1 - \frac{1}{y})} \quad (7.3.1.b)$$

Since,  $T = \bar{T}$  (eqn. 7.3.d)

$$c = \frac{P}{RT} \quad ; \quad \bar{c} = \frac{\bar{P}}{RT} \quad (7.3.1.c)$$

The term involving the temperature gradient is much smaller than the pressure gradient and hence is neglected. The equations become

$$\frac{dP}{dz} + \frac{g}{\epsilon_A v_z} \cdot (P - \bar{P}) = - k_f (RT) \cdot P \cdot e^{-\gamma} \cdot e^{\gamma(1 - \frac{1}{y})} \quad (7.3.1.d)$$

$$\frac{g}{\epsilon_B} (\bar{P} - P) = -k_f (RT) \cdot \bar{P} \cdot e^{-\gamma} \cdot e^{\gamma(1 - \frac{1}{y})} \quad (7.3.1.e)$$

$$\text{Now, } RT = \frac{P_{\text{tot}} \cdot V_{\text{tot}}}{n} = \frac{P_{\text{tot}} \cdot M \cdot (\epsilon_A V_Z)}{(\epsilon_A V_t) \cdot \alpha} = \frac{P_{\text{tot}} \cdot M \cdot (\epsilon_A V_Z)}{G_S} \quad (7.3.1.f)$$

where,  $n$  = number of moles of gas in the reactor

$V_{\text{tot}}$  = volume occupied by gas in the reactor

$\alpha$  = density of gas,  $\left[ \frac{n \cdot M}{V_{\text{tot}}} \right]$ .

Substituting for  $(P - \bar{P})$  and  $RT$  in eqn. 7.3.1.d from eqn. 7.3.1.e and 7.3.1.f, respectively,

$$\frac{dP}{dz_0} + D'_m \cdot e^{\gamma(1 - \frac{1}{y})} \cdot \left[ \frac{\epsilon_B}{\epsilon_T} \bar{P} + \frac{\epsilon_A}{\epsilon_T} P \right] = 0 \quad (7.3.1.g)$$

$$\text{where } D'_m = \frac{k_f \cdot L \cdot e^{-\gamma} \cdot P_{\text{tot}} \cdot M \cdot \epsilon_T}{G_S} \quad (7.3.1.h)$$

$$\bar{P} = \frac{P}{\left[ 1 + \frac{D'_m \cdot d_p \cdot \epsilon_T}{L \cdot P \cdot \epsilon_B} \cdot e^{\gamma(1 - \frac{1}{y})} \right]} \quad (7.3.1.i)$$

Writing the equations in terms of  $x$

$$\frac{dx}{dz_0} + D'_m \cdot e^{\gamma(1 - \frac{1}{y})} \cdot \left[ \frac{\epsilon_B / \epsilon_T}{\left[ 1 + \frac{D'_m \cdot d_p \cdot \epsilon_T}{P \cdot L \cdot \epsilon_B} \cdot e^{\gamma(1 - \frac{1}{y})} \right]} + \frac{\epsilon_A}{\epsilon_T} \right] x = 0 \quad (7.3.1.j)$$



$$\bar{x} = \frac{x}{\left[ 1 + \frac{D'_m \cdot d_p \cdot \epsilon_T}{L \cdot Pe \cdot \epsilon_B} \cdot e^{\gamma(1 - \frac{1}{y})} \right]} \quad (7.3.1.k)$$

or

$$\frac{dx}{dz_0} + R_1(x, y) = 0 \quad (7.3.1.l)$$

where,

$$R_1(x, y) = D'_m \cdot e^{\gamma(1 - \frac{1}{y})} \left[ \frac{\epsilon_B / \epsilon_T}{\left[ 1 + \frac{D'_m \cdot d_p \cdot \epsilon_T}{Pe \cdot L \cdot \epsilon_B} \cdot e^{\gamma(1 - \frac{1}{y})} \right]} + \frac{\epsilon_A}{\epsilon_T} \right] x$$

### 7.3.2 Heat Transfer Equations

$$\text{With } \hat{R}_B = k_f e^{-\gamma \cdot x} e^{\gamma(1 - \frac{1}{y})} \cdot P_{os} ,$$

the heat transfer equations (eqns. 7.3.c, 7.3.d, 7.3.e) are written in dimensionless form as follows:

$$\frac{\partial \hat{y}}{\partial z_0} + (HA) (\hat{y} - \hat{y}) = 0 \quad (7.3.2.a)$$

$$\frac{\partial \hat{y}}{\partial t} + (HA) (\hat{y} - y) - \frac{1}{P} \cdot \frac{\partial^2 \hat{y}}{\partial z_0^2} = R_2(x, y) \quad (7.3.2.b)$$

where,

$$R_2(x, y) = D'_h \cdot x \cdot e^{\gamma(1 - \frac{1}{y})} .$$

$$HA = \frac{L \cdot 2h \cdot \delta S}{G_s \cdot c_p}$$

$$t = t' / \tau$$

$$\tau = \frac{L \cdot \rho_B \cdot \hat{c}_p}{G_s \cdot c_p}$$

$$P = \frac{L \cdot G_s \cdot c_p}{k_s \cdot \hat{\delta S} \cdot \lambda} = \frac{L \cdot G_s \cdot c_p}{\lambda_o}$$

$$D'_h = \frac{(-\Delta H) \cdot L \cdot k_f \cdot e^{-\gamma_{P_{os}}}}{G_s \cdot c_p \cdot T_{os}}$$

$$\hat{y} = \hat{T}/T_{os}$$

Hence the complete (non-Fickian two-phase) model which can be used to simulate dynamic experiments is represented by the set of eqns.

7.3.1.k, 7.3.1.l, 7.3.2.a, 7.3.2.b.

However, an equivalent one-phase heat transfer model can be derived using the Vortmeyer condition. Given below is the derivation of the one-phase non-Fickian model by introducing the Vortmeyer assumption. In this chapter both the non-Fickian one-phase model and the non-Fickian two-phase model have been compared with the Fickian model used by Hansen and Jorgensen.

Adding eqns. 7.3.2.a and 7.3.2.b, the following equation is obtained

$$\frac{\partial \hat{y}}{\partial t} + \frac{\partial (y - \hat{y})}{\partial z_o} + \frac{\partial \hat{y}}{\partial z_o} - \frac{1}{P} \frac{\partial^2 \hat{y}}{\partial z_o^2} = R_2(x, y) \quad (7.3.2.c)$$

Taking the derivative w.r.t.  $z$  in eqn. 7.3.2.a and substituting for  $\frac{\partial (y - \hat{y})}{\partial z_o}$  in eqn. 7.3.2.c, and with the Vortmeyer assumption (eqn. 6.2.d), the following equivalent one phase model is obtained:

$$\frac{\partial \hat{y}}{\partial t} + \frac{\partial \hat{y}}{\partial z_o} - \frac{1}{Pe_h} \frac{\partial^2 \hat{y}}{\partial z_o^2} = R_2(x, y) \quad (7.3.2.d)$$

where, 
$$\frac{1}{Pe_h} = \frac{1}{HA} + \frac{1}{P} \quad (7.3.2.e)$$

Eqn. 7.3.2.d is not the energy conservation equation as is apparent from the way it was derived. However, since most of the energy in a gas flow packed bed reactor is stored in the solid phase, it can be regarded as a pseudo-energy balance equation equivalent with the Fickian model. Note that the reaction rate terms have been written in terms of  $y$ , the dimensionless temperature of the moving fluid. However, they could well have been written in terms of  $\hat{y}$ , the dimensionless temperature of the solid phase. This is because of the intrinsic difficulty of comparing one-phase and two-phase heat transfer models and also due to the uncertainty of experimental temperature measurements being of the solid or fluid phase. Since in the present simulation it has been experimentally determined that there is negligible difference between the gas and solid temperature, not much importance is given to this aspect.

Eqns. 7.3.1.1 and 7.3.2.d represent the non-Fickian model in its simplest form (non-Fickian one phase) and when one compares the corresponding Fickian model (eqns. 7.2.b and 7.2.c), the mathematical advantage of the non-Fickian model is clearly seen. The heat transfer equations are identical (eqns. 7.3.2.d and 7.2.b). However, the mass transfer equation is second order non-linear in the Fickian model (eqn. 7.2.c), whereas it is a first order non-linear equation in the non-Fickian model which should be simpler to handle computationally. At any rate, it cannot be more difficult. In later sections in this chapter, it is shown that this mathematically simpler model simulates

the experiments of Hansen and Jorgensen adequately.

#### 7.4 Steady State Profiles

For steady state operations, the equivalent one phase model can be derived as follows (see Section 6.4).

$$\left( \frac{\epsilon_A^V z}{\epsilon_T} \right) \frac{dT}{dz} - \frac{k_s \cdot \delta \hat{S} \cdot \lambda}{\alpha c_p \epsilon_T} \cdot \frac{d^2 T}{dz^2} = \frac{\hat{R} \rho_B \cdot (-\Delta H)}{\alpha c_p \epsilon_T} \quad (7.4.a)$$

or, in dimensionless form

$$\frac{dy}{dz_0} - \frac{1}{P} \cdot \frac{d^2 y}{dz_0^2} = R_2(x, y) \quad (7.4.b)$$

Thus in terms of the Fickian model, the Peclet number is  $Pe_h$  in the dynamic case and its value is  $P$  in the steady state case.

However, the steady state complete non-Fickian model (i.e., the non-Fickian, two-phase model) without the Vortmeyer assumption would have its heat transfer equations as in eqn. 7.3.2.a and 7.3.2.b without the time dependent term.

Steady state profiles have been obtained by solving the steady state Fickian model (see eqns. 7.2.b and 7.2.c), the steady state non-Fickian one phase model (eqns. 7.3.1 and 7.4.b), and the steady state non-Fickian two-phase model (see eqns. 7.3.1.1, 7.3.2.a, 7.3.2.b) for various sets of parameters  $\gamma$ ,  $D_h$ ,  $D_h'$ ,  $D_m$ ,  $D_m'$ , and the plots are shown in Fig. 7.4.a. The parameters chosen correspond to the "high flow" experiments of Hansen and Jorgensen at Reynolds number equal to 14.

The numerical solution of all the models was done by using the orthogonal collocation technique (Villadsen 1970, Finlayson 1972,

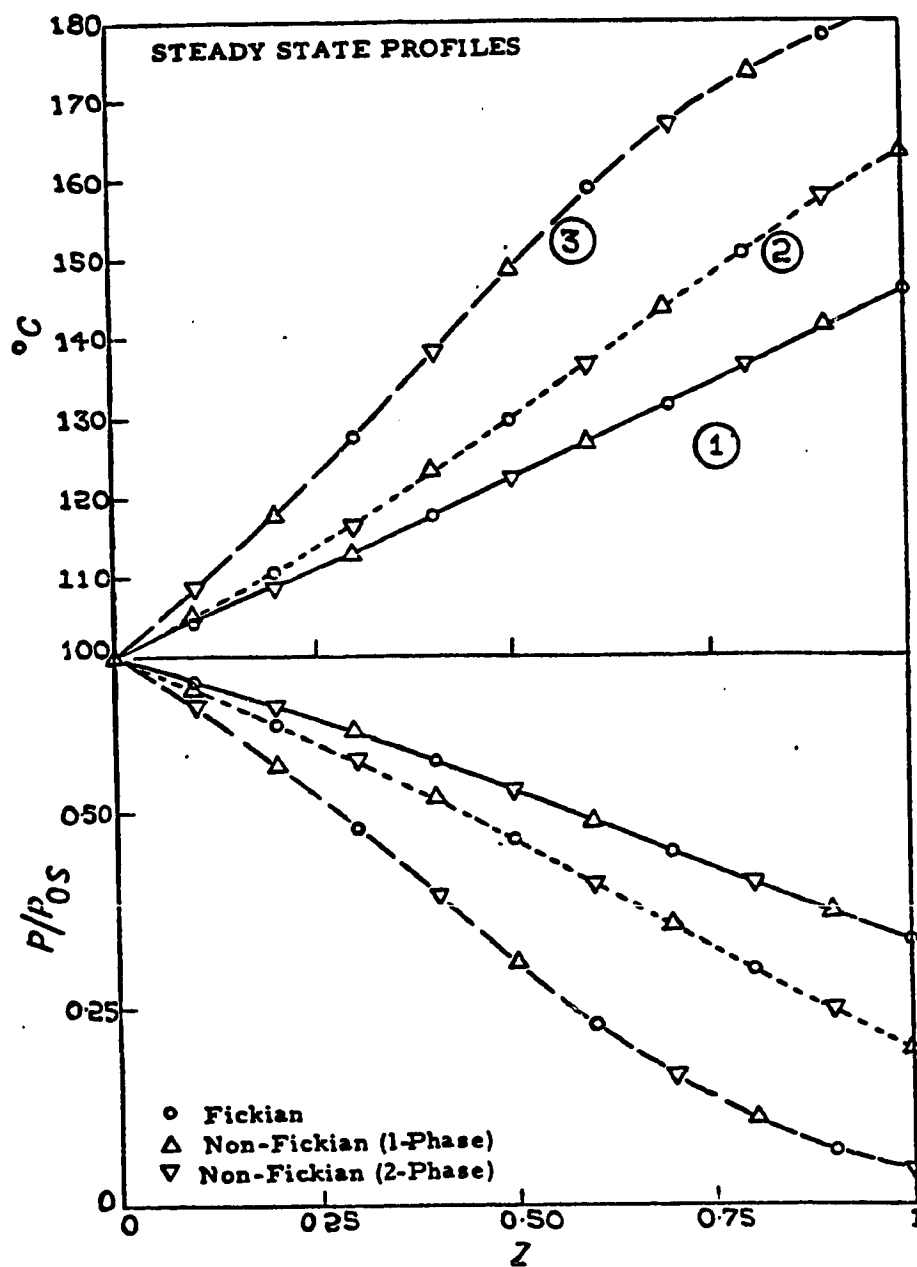


Fig. 7.4.a Steady State Profiles. Curve 1 has parameters  $= 8.23$ ,  $D_h = D_h' = 0.153$ ,  $D_m = D_m' = 0.455$ . Curve 2 has parameters  $= 9.95$ ,  $D_h = D_h' = 0.189$ ,  $D_m = D_m' = 0.561$ . Curve 3 has parameters  $= 9.50$ ,  $D_h = D_h' = 0.301$ ,  $D_m = D_m' = 0.896$ .

Finlayson 1974, Villadsen and Michelsen 1977) which was first developed by Villadsen and Stewart 1967. It is a special case of the collocation method and the method of weighted residuals and is particularly suitable for chemical reaction engineering problems. Details of the method are explained in the references given above.

In the method of weighted residuals, the unknown exact solution is expanded in a series of known functions,  $\{y_i(x)\}$ , called the trial functions

$$y^*(x) = \sum_{i=1}^N a_i \cdot y_i(x) \quad (7.4.c)$$

This trial function is substituted into the differential equation to form the residual. If the trial function were the exact solution the residual would be zero. In the method of weighted residuals, the constants  $a_i$  are chosen in such a way that the residual is forced to be zero in an average sense.

In the collocation method the residual is required to be zero at  $N$  specified collocation points  $x_j$ , and this determines the unknown coefficients in the trial function. As  $N$  increases, the residual is zero at more and more points. Hence as  $N$  approaches infinity, and the residual is zero everywhere, the approximate solution that has been generated approaches the exact solution.

There are two basic improvements made by Villadsen in the orthogonal collocation method. One is that the trial functions are orthogonal polynomials (this improves the rate of convergence as  $N$  increases). Secondly, the computer programs are written in terms of

the solution at the collocation points,  $\{y^*(x_j)\}$ , rather than the coefficients  $\{a_i\}$ . Also, the collocation points are the roots of the particular orthogonal polynomials chosen in the approximation.

Since the models are coupled non-linear ordinary differential equations, discretisation in space by orthogonal collocation results in a set of non-linear algebraic equations. These equations are linearised by the Newton-Raphson procedure. The linearised equations are solved by refined Gaussian elimination method. Successive application of the Newton-Raphson method gives the solution in 4 to 6 iterations.

Solutions of all the three models seem to fall on the same curve as is apparent in the plots of the steady state profiles. Hence the non-Fickian model would also adequately simulate the experiments of Hansen and Jorgensen at steady state.

## 7.5 Frequency Response Analysis

Hansen and Jorgensen have done frequency response measurements and simulated them with the non-steady state Fickian model. In this section frequency response simulations are done using the non-Fickian model and the results are compared. The theoretical analysis is based on a method similar to the one explained in Section 3.4 for the isothermal case.

### 7.5.1 Fickian Model

The analysis will be shown below for the Fickian model (eqns. 7.2.b and 7.2.c). At the steady state the equations become:

$$\frac{dy_s}{dz} = \frac{1}{Pe_h} \cdot \frac{d^2 y_s}{dz^2} + R_2(x_s, y_s) \quad (7.5.1.a)$$

$$\frac{dx_s}{dz} = \frac{1}{Pe_m} \cdot \frac{d^2 x_s}{dz^2} - R_1(x_s, y_s) \quad (7.5.1.b)$$

where the subscript s represents steady state values and

$$R_2(x, y) = D_h \cdot x \cdot e^{\gamma(1 - \frac{1}{y})}$$

$$R_1(x, y) = D_m \cdot x \cdot e^{\gamma(1 - \frac{1}{y})}$$

Perturbation variables are defined as

$$Y = y - y_s \quad ; \quad X = x - x_s \quad (7.5.1.c)$$

Linearising the rate terms about the steady state

$$R_2(x, y) = R_2(x_s, y_s) + \left( \frac{\partial R_2}{\partial x_s} \right)_{y_s} \cdot X + \left( \frac{\partial R_2}{\partial y_s} \right)_{x_s} \cdot Y \quad (7.5.1.d)$$

$$R_1(x, y) = R_1(x_s, y_s) + \left( \frac{\partial R_1}{\partial x_s} \right)_{y_s} \cdot X + \left( \frac{\partial R_1}{\partial y_s} \right)_{x_s} \cdot Y \quad (7.5.1.e)$$

Subtracting equations 7.5.1.a and 7.5.1.b from equations 7.2.b and 7.2.c, respectively, with the rate terms linearised, the following equations are obtained in terms of the perturbation variables

$$\frac{\partial Y}{\partial t} + \frac{\partial Y}{\partial z} = \frac{1}{Pe_h} \cdot \frac{\partial^2 Y}{\partial z^2} + \left( \frac{\partial R_2}{\partial x_s} \right)_{y_s} \cdot X + \left( \frac{\partial R_2}{\partial y_s} \right)_{x_s} \cdot Y \quad (7.5.1.f)$$

$$\frac{\partial X}{\partial z} = \frac{1}{Pe_m} \frac{\partial^2 X}{\partial z^2} - \left( \frac{\partial R_1}{\partial x_s} \right)_{y_s} \cdot X - \left( \frac{\partial R_1}{\partial y_s} \right)_{x_s} \cdot Y \quad (7.5.1.g)$$



where, 
$$\left( \frac{\partial R_2}{\partial x_s} \right)_{y_s} = D_h \cdot e^{\gamma(1 - \frac{1}{y_s})} ; \quad \left( \frac{\partial R_2}{\partial y_s} \right)_{x_s} = D_h \cdot x_s \cdot \frac{\gamma}{y_s^2} e^{\gamma(1 - \frac{1}{y_s})}$$

$$\left( \frac{\partial R_1}{\partial x_s} \right)_{y_s} = D_m \cdot e^{\gamma(1 - \frac{1}{y_s})} ; \quad \left( \frac{\partial R_1}{\partial y_s} \right)_{x_s} = D_m \cdot x_s \cdot \frac{\gamma}{y_s^2} \cdot e^{\gamma(1 - \frac{1}{y_s})} .$$

It is convenient to write the variables as complex harmonic functions with a circular frequency  $\omega$ . Let  $Y = T e^{i\omega t}$  ;  $X = C e^{i\omega t}$  where,  $T = (TR) + i (TI)$  and  $C = (CR) + i (CI)$ .

Substituting in eqns. 7.5.1.f and 7.5.1.g,

$$i\omega T + \frac{\partial T}{\partial z} = \frac{1}{Pe_h} \frac{\partial^2 T}{\partial z^2} + \left( \frac{\partial R_2}{\partial x_s} \right)_{y_s} \cdot C + \left( \frac{\partial R_2}{\partial y_s} \right)_{x_s} \cdot T \quad (7.5.1.h)$$

$$\frac{\partial C}{\partial z} = \frac{1}{Pe_m} \cdot \frac{\partial^2 C}{\partial z^2} - \left( \frac{\partial R_1}{\partial x_s} \right)_{y_s} \cdot C - \left( \frac{\partial R_1}{\partial y_s} \right)_{x_s} \cdot T \quad (7.5.1.i)$$

Writing these equations in terms of real and imaginary parts it is observed that four coupled linear second order o.d.e's have to be solved for the frequency response analysis of the Fickian model.

$$\frac{d^2(TR)}{dz^2} - Pe_h \cdot \frac{d(TR)}{dz} + Pe_h \left( \frac{\partial R_2}{\partial y_s} \right)_{x_s} \cdot (TR) + Pe_h \left( \frac{\partial R_2}{\partial x_s} \right)_{y_s} (CR) + \omega \cdot Pe_h (TI) = 0$$

$$\frac{d^2(CR)}{dz^2} - Pe_m \cdot \frac{d(CR)}{dz} - Pe_m \left( \frac{\partial R_1}{\partial x_s} \right)_{y_s} (CR) - Pe_m \left( \frac{\partial R_1}{\partial y_s} \right)_{x_s} (TR) = 0$$

$$\frac{d^2(TI)}{dz^2} - Pe_h \frac{d(TI)}{dz} + Pe_h \left( \frac{\partial R_2}{\partial y_s} \right)_{x_s} (TI) + Pe_h \left( \frac{\partial R_2}{\partial x_s} \right)_{y_s} (CI) - \omega Pe_h (TR) = 0$$

$$\frac{d^2(CI)}{dz^2} - Pe_m \frac{d(CI)}{dz} - Pe_m \left( \frac{\partial R_1}{\partial x_s} \right)_{y_s} (CI) - Pe_m \left( \frac{\partial R_1}{\partial y_s} \right)_{x_s} (TI) = 0 \quad (7.5.1.j)$$

For the T/T frequency response (temperature response to perturbation of inlet temperature), the boundary conditions are

$$\underline{z = 0} : \quad TR = 0.035, \quad CR = TI = CI = 0 \quad (7.5.1.k)$$

$$\underline{z = 1} : \quad \frac{d(TR)}{dz} = \frac{d(TI)}{dz} = \frac{d(CR)}{dz} = \frac{d(CI)}{dz} = 0 \quad (7.5.1.l)$$

For unsteady state processes, the exit boundary condition (eqn. 7.5.1.l) is not physically justifiable. Even so, it is widely used in simulation studies. In frequency response experiments with sinusoidal inlet perturbations, the exit boundary condition would be strictly valid only when the feedback is such that a standing wave is generated with the exit at the "loop" point where the axial gradient is zero. However, such a condition is unlikely to occur at the exit point.

The method of orthogonal collocation has been used to numerically solve the model equations. The frequency response equations have also been solved with the differential equations (eqn. 7.5.1.j) being satisfied at the last collocation point (exit point) rather than the exit boundary condition (eqn. 7.5.1.l). The results are discussed in Section 7.5.3.

For the C/C frequency response (concentration response to perturbation of inlet concentration), the following initial condition is written instead of eqn. 7.5.1.k.

$$\underline{z = 0} : \quad TR = 0, \quad CR = 0.035, \quad TI = CI = 0 \quad (7.5.1.m)$$

The equations are discretised in space by orthogonal collocation. Eighteen internal collocation points have been used to ensure sufficient accuracy.

### 7.5.2 Non-Fickian Model

The equations are locally linearised around the steady state and equations corresponding eqns. 7.5.1.j of the Fickian model are obtained. For the non-Fickian one-phase model (eqns. 7.3.1.1 and 7.3.2.d) the equations are four linear coupled o.d.e.'s; however, two of them are first order and two second order:

$$\frac{d^2(TR)}{dz_0^2} - Pe_h \cdot \frac{d(TR)}{dz_0} + Pe_h \cdot \left( \frac{\partial R_2}{\partial y_s} \right)_{x_s} \cdot (TR) + Pe_h \cdot \left( \frac{\partial R_2}{\partial x_s} \right)_{y_s} \cdot (CR) + \omega \cdot Pe_h \cdot (TI) = 0$$

$$\frac{d(CR)}{dz_0} + \left( \frac{\partial R_1}{\partial x_s} \right)_{y_s} \cdot (CR) + \left( \frac{\partial R_1}{\partial y_s} \right)_{x_s} \cdot (TR) = 0$$

$$\frac{d^2(TI)}{dz_0^2} - Pe_h \cdot \frac{d(TI)}{dz_0} + Pe_h \cdot \left( \frac{\partial R_2}{\partial y_s} \right)_{x_s} \cdot (TI) + Pe_h \cdot \left( \frac{\partial R_2}{\partial x_s} \right)_{y_s} \cdot (CI) - \omega \cdot Pe_h \cdot (TR) = 0$$

$$\frac{d(CI)}{dz_0} + \left( \frac{\partial R_1}{\partial x_s} \right)_{y_s} \cdot (CI) + \left( \frac{\partial R_1}{\partial y_s} \right)_{x_s} \cdot (TI) = 0$$

(7.5.2.a)

For the T/T frequency response the boundary conditions are:

$$\underline{z_0 = 0} : \quad TR = 0.035, CR = TI = CI = 0 \quad (7.5.2.b)$$

$$\underline{z_0 = 1} : \quad \frac{d(TR)}{dz_0} = \frac{d(TI)}{dz_0} = 0 \quad (7.5.2.c)$$

For the C/C frequency response instead of eqn. 7.5.2.b, the initial condition is

$$\underline{z_0 = 0} : \quad TR = 0, CR = 0.035, TI = CI = 0$$

For the non-Fickian two-phase model (eqns. 7.3.1.1, 7.3.2.a, 7.3.2.b), the equations are as follows:

$$\frac{d(TR)}{dz_0} + (HA) \cdot (TR - THR) = 0$$

$$\frac{d^2(THR)}{dz_0^2} + (HA) \cdot P \cdot (TR - THR) + \omega \cdot P \cdot (THI) + P \cdot \left( \frac{\partial R_2}{\partial x_s} \right)_{y_s} \cdot (CR) + P \cdot \left( \frac{\partial R_2}{\partial y_s} \right)_{x_s} \cdot (TR) = 0$$

$$\frac{d(CR)}{dz_0} + \left( \frac{\partial R_1}{\partial x_s} \right)_{y_s} \cdot (CR) + \left( \frac{\partial R_1}{\partial y_s} \right)_{x_s} \cdot (TR) = 0$$

$$\frac{d(TI)}{dz_0} + (HA) \cdot (TI - THI) = 0$$

$$\frac{d^2(THI)}{dz_0^2} + (HA) \cdot P \cdot (TI - THI) - \omega \cdot P \cdot (THR) + P \cdot \left( \frac{\partial R_2}{\partial x_s} \right)_{y_s} \cdot (CI) + P \cdot \left( \frac{\partial R_2}{\partial y_s} \right)_{x_s} \cdot (TI) = 0$$

$$\frac{d(CI)}{dz_0} + \left( \frac{\partial R_1}{\partial x_s} \right)_{y_s} \cdot (CI) + \left( \frac{\partial R_1}{\partial y_s} \right)_{x_s} \cdot (TI) = 0 \quad (7.5.2.d)$$

where the solid phase perturbation variable is

$$\hat{Y} = \hat{y} - \hat{y}_s \quad \text{with} \quad \hat{Y} = \hat{T} e^{i\omega t}$$

where

$$\hat{T} = (THR) + i (THI)$$

For the T/T frequency response, if the periodic signal is introduced in the gas phase (which is generally the case in the experimental studies) then the initial conditions are

$$\underline{z_0 = 0} : \quad TR = 0.035, \quad THR = CR = TI = THI = CI = 0 \quad (7.5.2.e)$$

If the periodic signal is introduced in the solid phase, then the corresponding initial conditions are:

$$\underline{z_0 = 0} : \quad TR = 0, \quad THR = 0.035, \quad CR = TI = THI = CI = 0 \quad (7.5.2.f)$$

However, for the signal introduced in the gas as well as solid phase:

$$\underline{z_0 = 0} : \quad TR = THR = 0.035, \quad CR = TI = THI = CI = 0 \quad (7.5.2.g)$$

For the C/C frequency response:

$$\underline{z_0 = 0} : \quad TR = THR = 0, \quad CR = 0.035, \quad TI = THI = CI = 0 \quad (7.5.2.h)$$

The exit boundary conditions are:

$$\underline{z_o = 1} : \quad \frac{d(\text{THR})}{dz_o} = \frac{d(\text{THI})}{dz_o} = 0 \quad (7.5.2:i)$$

### 7.5.3 Discussion of Results

The values of the parameters chosen to get the steady state around which periodic perturbations are simulated correspond to the "high flow" experiments of Hansen and Jorgensen.

$$\gamma = 9.58$$

$$D_h = D'_h = 0.151$$

$$D_m = D'_m = 0.446$$

Fig. 7.5.a and 7.5.b show the T/T frequency response profiles for various values of the disturbance period for both the Fickian model and the non-Fickian model. The ordinate dB represents the T/T amplitude ratio in decibels (gain curve) and  $\phi$  is the phase angle. The range of frequencies in this plot goes through rather critical conditions. The disturbance frequencies are close to the break frequency below which the attenuation is severe. Any defect in the parameters or in the model would be easily seen, particularly in the gain curve. However, the results of both the Fickian as well as the non-Fickian model fall on the same curve. Hence the frequency response experiments of Hansen and Jorgensen could be simulated by the non-Fickian model to the same degree of accuracy as the Fickian model, with similar assumptions.

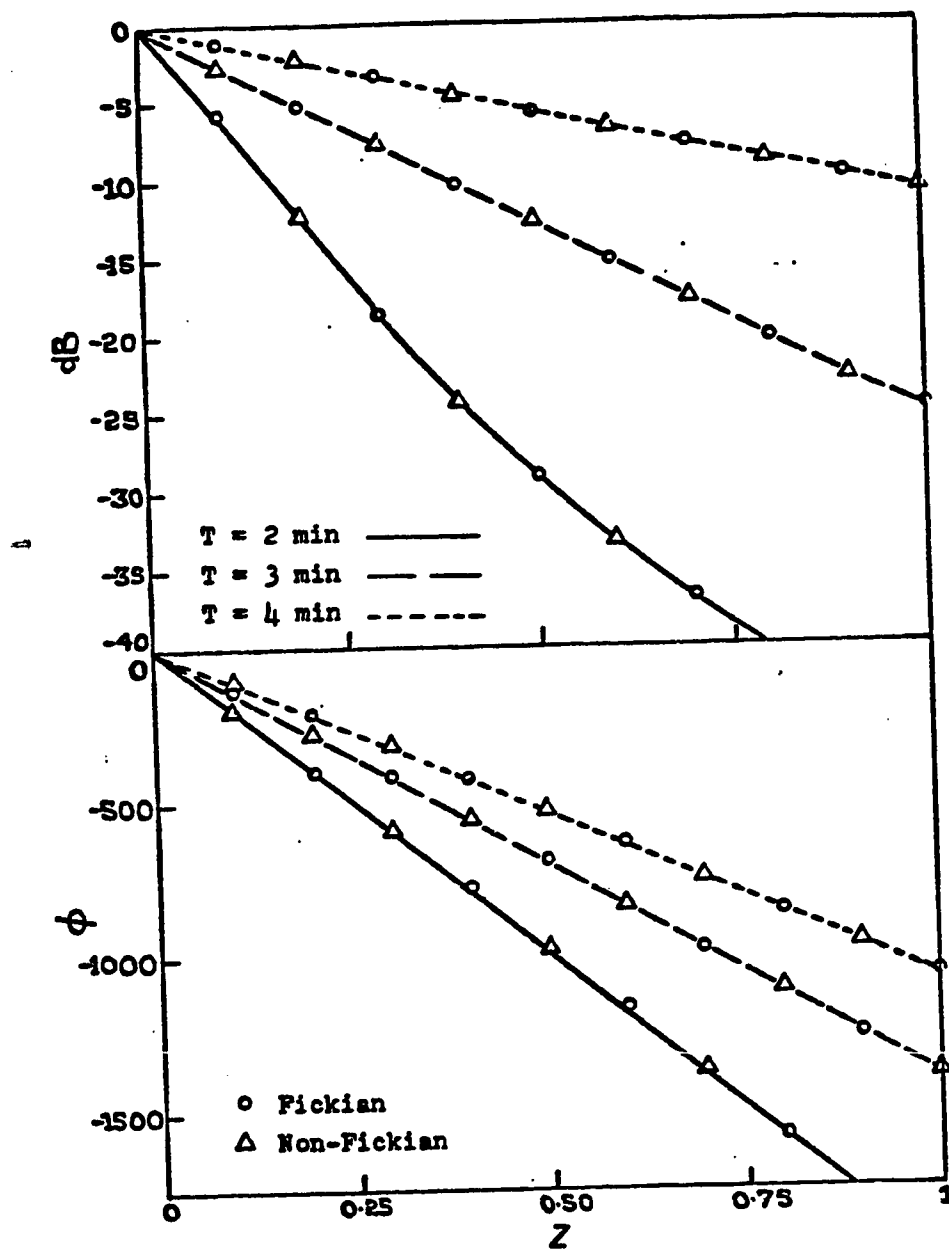


Fig. 7.5.a.  $T/\tau$  axial gain and phase lag profiles for  $T = 2, 3, 4 \text{ min}$  ( $\tau = 12.1 \text{ min}$ ,  $Pe_h = 145$ .)

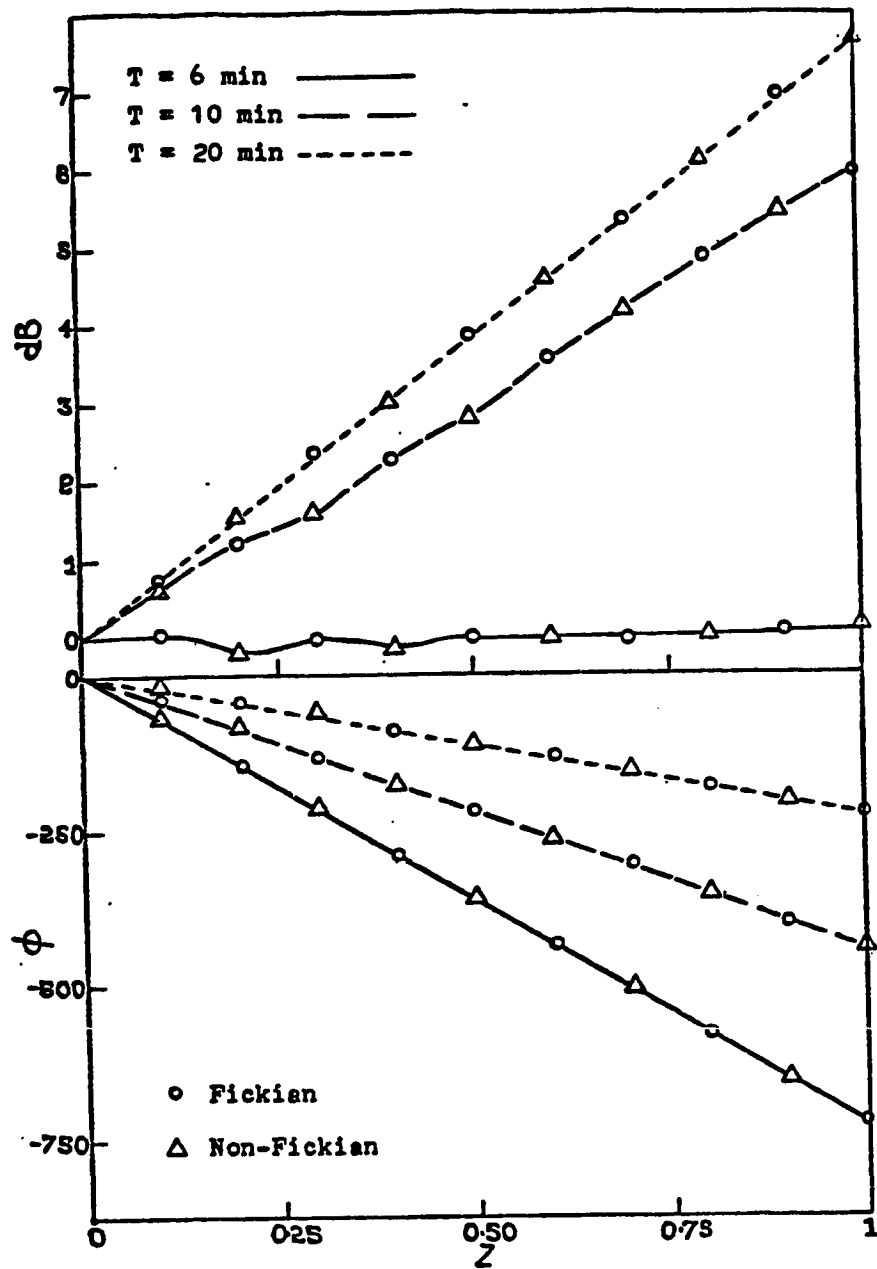


Fig. 7.5.b.  $T/T$  axial gain and phase lag profiles for  $T=6, 10, 20$  min ( $\tau=12.1$  min,  $Pe_h=145$ )



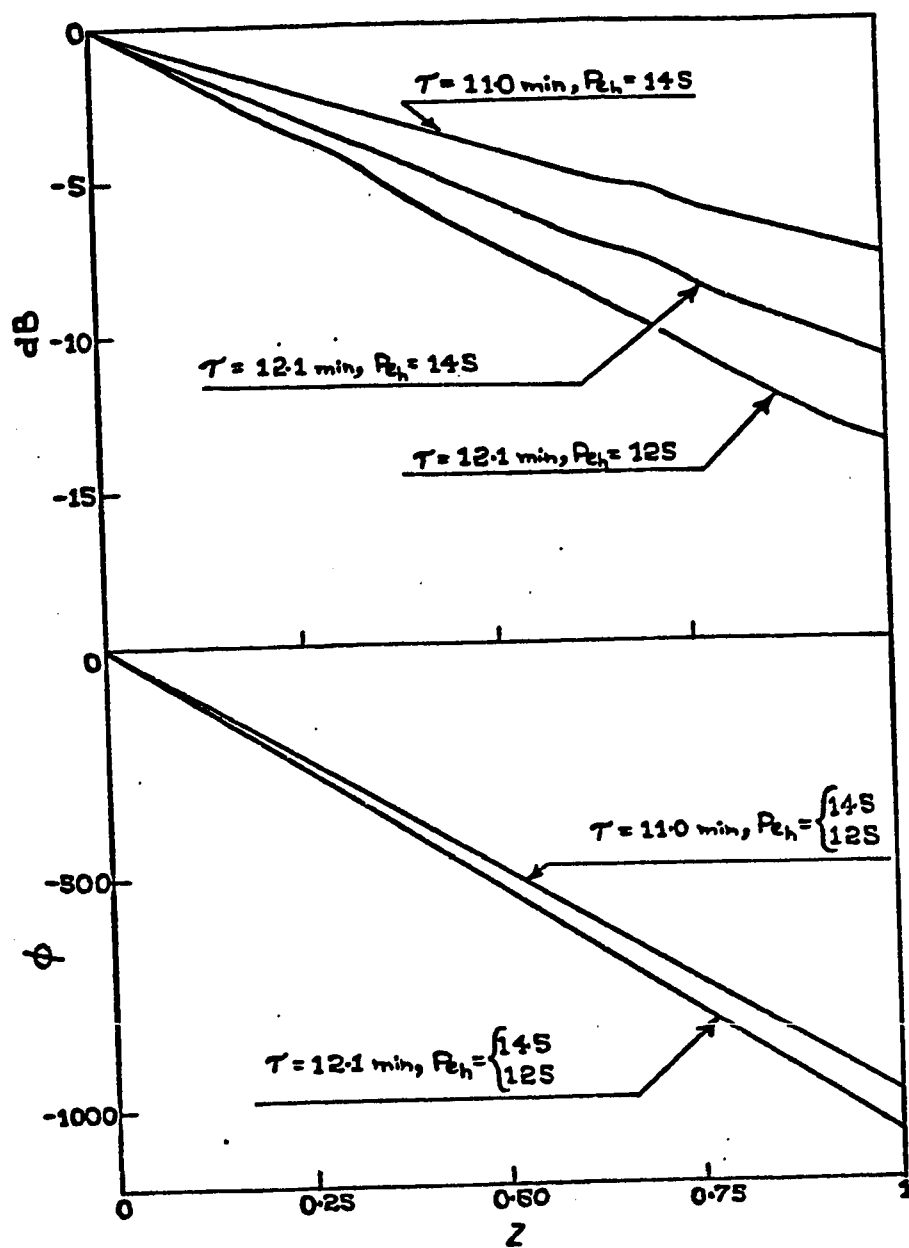


Fig. 7.5.c. T/T axial gain and phase lag profiles for  $T = 4 \text{ min}$ . Both Fickian and Non-Fickian model values fall on the same curve.

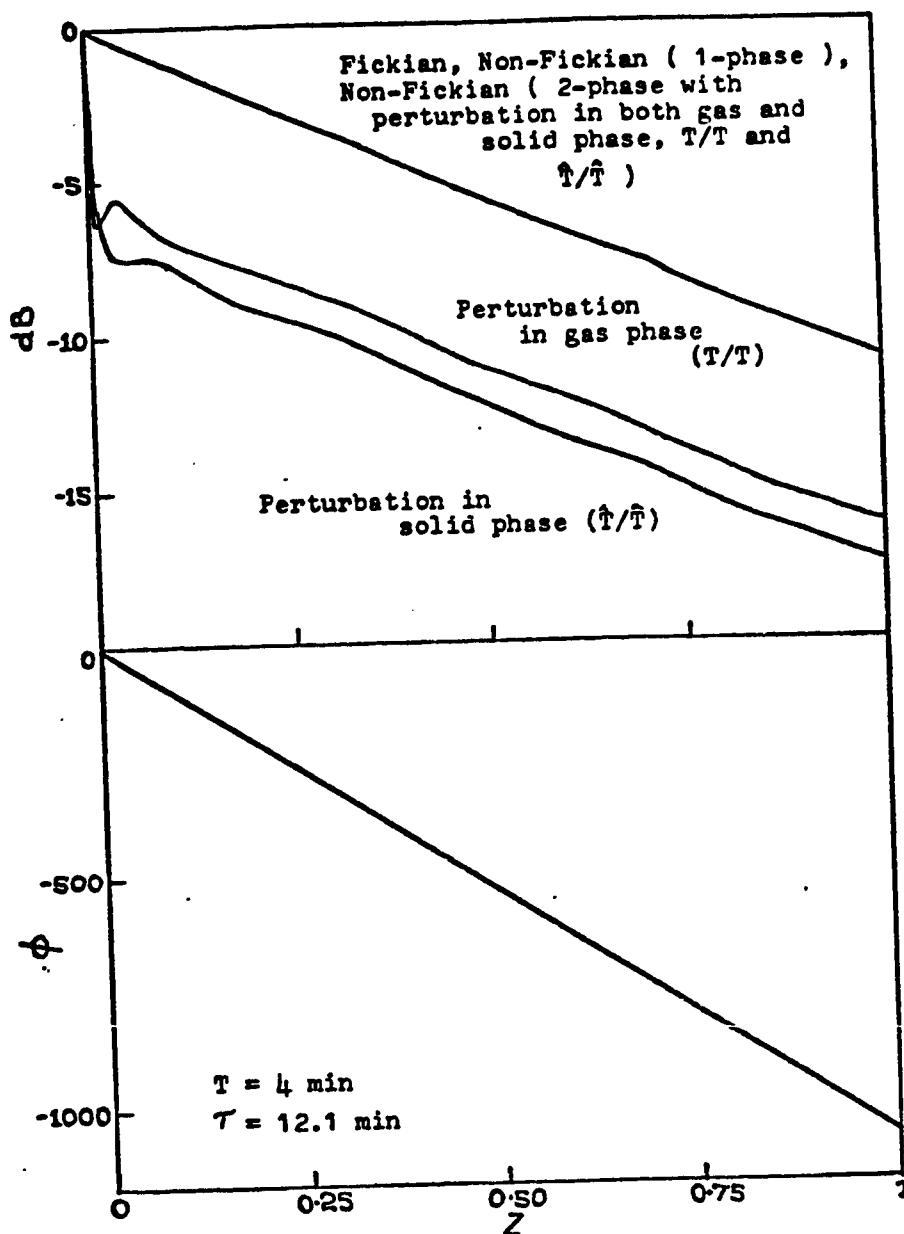


Fig. 7.5.d.  $T/T$  and  $\hat{T}/\hat{T}$  axial gain and phase lag profiles for  $T = 4 \text{ min}$  ( $\tau = 12.1 \text{ min}$ ,  $Pe_h = 145$ ,  $P = 188.36$  )

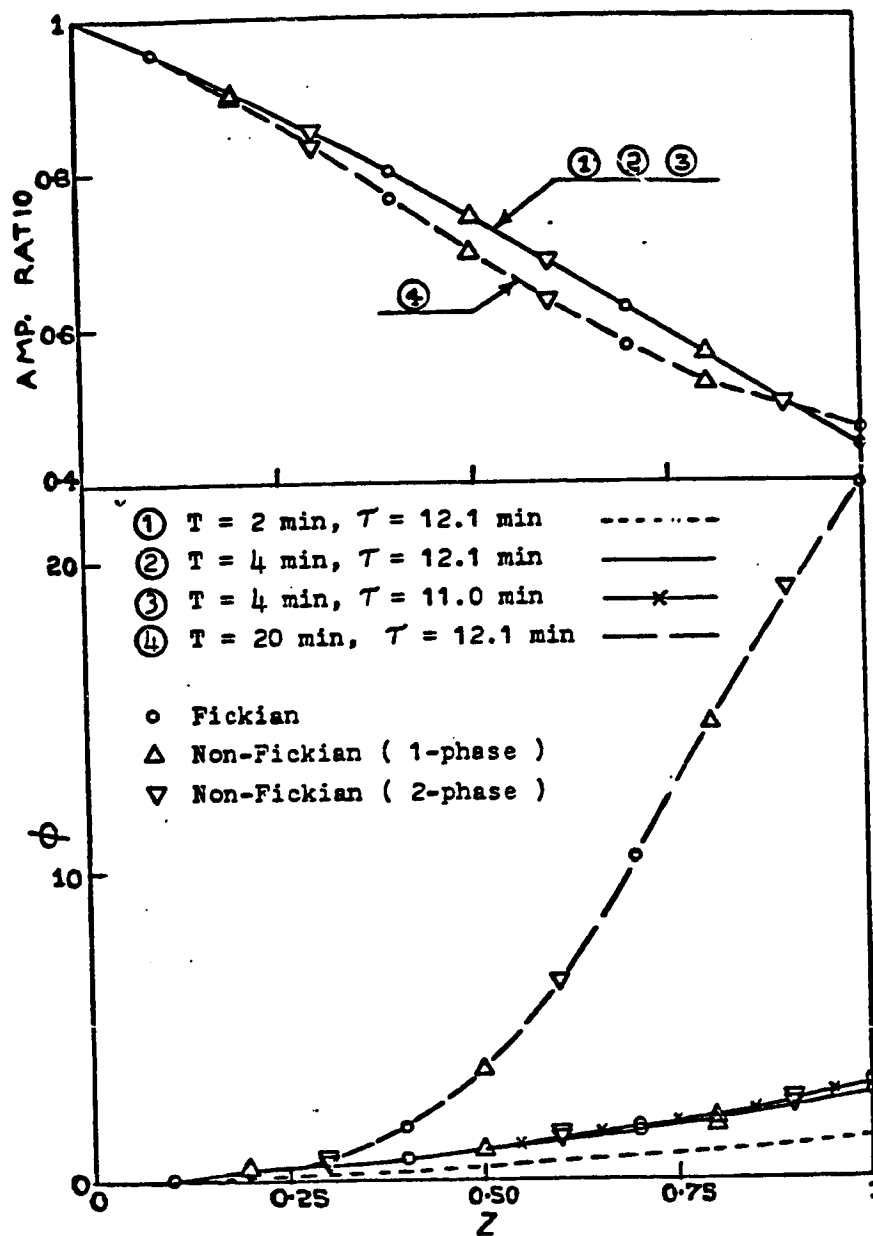


Fig. 7.5.e. C/C axial amplitude ratio and phase lag profiles for Fickian, Non-Fickian (1-phase), Non-Fickian (2-phase) models. ( $Pe_h=145$ ,  $P=188.36$ )

Hansen and Jorgensen have shown sensitivity of the gain and phase curves to the parameters  $\tau$  and  $Pe_h$  characterising heat dynamics. Fig. 7.5.c shows a sensitivity of the non-Fickian model identical to the Fickian model. Plots for both the models fall on the same curve. A decrease in  $Pe_h$  from 145 to 125 does not affect the phase angle but decreases the gain profile. A decrease in the value of  $\tau$  from 12.1 min to 11.0 min increases the phase angle a little and also the gain curve.

Hansen and Jorgensen have noted that the theoretical amplitude ratio obtained was higher than the experimental. In order to obtain a better fit with the experiments, they added 10% to the estimated residence time as a compensation for the dynamics of the insulation. However, the reason for higher theoretical amplitude ratio could also be due to the inadequacy of the model itself as is evident from Fig. 7.5.d. When the non-Fickian two phase model is used, it becomes important to ascertain whether the inlet periodic temperature signals are introduced in the gas phase or solid phase. If identical inlet periodic signals are provided both in the gas and solid phase, then the non-Fickian two-phase model frequency response corresponds to the Fickian and non-Fickian one-phase model. However, if the inlet perturbation is made only in the gas phase (which is generally the practicable thing to do and also which seems to be the case in the experiments of Hansen and Jorgensen), then the gain is about 5 dB lower for the particular set of parameters in Fig. 7.5.d. If the inlet perturbation is made only in the solid phase (which can be done by microwave tech-

niques as explained by Bhattacharya and Pei 1975), then the gain curve is about 6 dB lower. The phase angle, however, is completely unaffected by the three types of inlet conditions.

Also it was observed by Hansen and Jorgensen that the theoretical phase curve fit the experimental close to the reactor inlet but later the phase angle is about 10-15% too large theoretically. This suggests that the exit boundary condition may play a part in the discrepancy. The frequency response solutions were solved with the differential equations being satisfied at the exit collocation point (no exit boundary conditions case) rather than the exit boundary conditions as written in Sections 7.5.1 and 7.5.2. With no exit boundary conditions, the phase angle as well as the gain curve have lower values near the exit of the bed particularly for high frequency disturbances. For a disturbance of period  $T = 2$  min (high frequency disturbance) and parameter values as in Fig. 7.5.a, the phase angle is 3.7% lower and the gain is 4 dB lower than the case where the exit boundary conditions are used. For low frequency disturbances the differences are much smaller.

Fig. 7.5.e shows the C/C frequency response diagrams. The amplitude ratio is always less than unity and the shape remains the same for most sets of parameters. The shape changes slightly for low frequency disturbances. The phase angle is positive and close to zero, but rises rather steeply for low frequencies as has been observed experimentally by Hansen and Jorgensen. A change in the value of the thermal residence time,  $\tau$ , from 12.1 min to 11.0 min did not affect the gain curve but

increased the phase angle slightly at a distance beyond half the length of the reactor. Note that the values obtained by the three models fall on the same curve. Hence the non-Fickian model is adequate representation for the experiments of Hansen and Jorgensen.

## NOMENCLATURE

- $a$  -- particle surface area per unit bed volume; for spheres,  $6(1-\epsilon_T)/d_p$   
 $a_i$  -- coefficients  
 $A$  --  $\frac{\epsilon_A \epsilon_B}{g\epsilon_T}$   
     --  $\left[ \frac{\bar{g}}{\epsilon_A} + \frac{g}{\epsilon_B} + \hat{h} + \tilde{h} \right]$  in section 6.1  
 $\delta A$  -- elemental cross-sectional area of the bed  
 $B$  --  $\left[ \frac{\bar{g}}{\epsilon_A} \hat{h} + \frac{g}{\epsilon_B} \hat{h} + \frac{g}{\epsilon_B} \tilde{h} \right]$  ; parameter defined in section 6.1  
 $c$  -- concentration in the moving phase  
 $c_f$  -- concentration in the Fickian model  
 $c_n(z)$  -- concentration of  $i$  in the moving phase at section  $n$  and axial distance  $z$   
 $c_p$  -- heat capacity of the fluid  
 $\hat{c}_p$  -- heat capacity of the solid catalyst  
 $c_o$  -- dimensionless concentration  
 $C$  -- deviation of a sinusoidal signal (tracer concentration) from its average value in section 3.4  
     --  $\sqrt{B - \frac{A^2}{4}}$  ; parameter defined in section 6.1  
     -- complex magnitude of concentration perturbation variable in section 7.5  
 $CI$  -- imaginary part of complex magnitude of concentration  
 $CR$  -- real part of complex magnitude of concentration  
 $dB$  -- amplitude ratio in decibels  
 $d_p$  -- particle diameter

- $D$  -- axial effective diffusion coefficient in the Fickian model  
 $D_h$  -- parameter defined in section 7.2  
 $D_h'$  -- parameter defined in section 7.3  
 $D_m$  -- parameter defined in section 7.2  
 $D_m'$  -- parameter defined in section 7.3  
 $D_y, D_y'$  -- asymptotic radial dispersivity for large  $t$   
 $D_z$  -- asymptotic axial dispersivity for large  $t$   
 $D_{H,y}, D_{H,z}$  -- asymptotic value of the effective heat dispersion coefficient in the radial and axial directions, respectively  
 $(De)_y, (De)_z$  -- effective mass dispersion coefficient in the moving phase in the radial and axial direction, respectively  
 $(De)_{H,y}, (De)_{H,z}$  -- effective heat dispersion coefficient in the moving phase in the radial and axial direction, respectively  
 $(exp)$  -- exponential defined in section 3.2  
 $E$  -- activation energy  
 $f, f^*$  -- friction factor  
 $g$  -- interphase volumetric flow rate between the moving phase and the stagnant phase per unit volume of the bed  
 $G, G_s$  -- superficial mass velocity  
 $h$  -- heat transfer coefficient between the moving fluid and the catalyst surface  
 $h'$  -- total heat transfer coefficient from particle surface to fluid or to other particles  
 $\hat{h}$  --  $\frac{2h \cdot \delta S}{\rho_B \hat{c}_p}$



$\tilde{h}$	--	$\frac{2h \cdot \delta S}{\alpha c_p \epsilon_A}$
HA	--	$\frac{L \cdot 2h \cdot \delta S}{G_s \cdot c_p}$
$\Delta H$	--	heat of chemical reaction
$I_0, I_1$	--	modified Bessel functions of zeroth and first order, respectively
$J, J_2$	--	Damkohler number
$k_e, (k_e)_n$	--	effective thermal conductivity in the packed bed in the axial and radial direction, respectively
$k_e^0$	--	axial effective thermal conductivity in the packed bed with no flow
$k_f$	--	frequency factor
$k_s$	--	thermal conductivity of the solid particles
	--	ratio of mean projected area of a particle (sphere, cylinder, ellipsoid) to that of a sphere of the same volume, in section 1.1
$\hat{k}_s$	--	$\frac{2 \cdot k_s \cdot \hat{\delta S} \cdot \lambda}{\rho_B \hat{c}_p}$
$k_1, k_2$	--	first order and second order reaction rate constant, respectively
$l$	--	axial distance
$L$	--	length of the bed
$m$	--	moles of tracer injected as a pulse
$m_f$	--	mass flow rate of fluid
$M$	--	molecular weight
$n$	--	number of moles of gas in the reactor
$N$	--	number of collocation points
$Nu$	--	Nusselt number

$N_1, N_2, N_3, N_4, N_5, N_6$  -- parameters defined in section 6.1

$p(z)$  -- pressure at axial distance  $z$

$\left(\frac{dp}{dz}\right)_f$  -- contribution due to form drag to the total pressure gradient

$P$  -- probability density function in section 3.3

-- partial pressure of oxygen in section 7.3.1

--  $\frac{L G_s c_p}{\lambda_o}$ , in section 7.3.2

$\Delta P$  -- pressure drop

$Pe, Pe_f, Pe_m$  -- Peclet number

$(Pe)_y, (Pe)_{m,y}, (Pe)_{m,r}$  -- asymptotic radial mass Peclet number

$Pe_z$  -- asymptotic axial mass Peclet number

$Pe_h, (Pe)_{H,z}$  -- asymptotic axial heat Peclet number

$(Pe)_{H,y}$  -- asymptotic radial heat Peclet number

$Pr, Pr_f$  -- Prandtl number

$P_{tot}, P_o$  -- average pressure in the bed

$P_{os}$  -- inlet partial pressure of oxygen at steady state

$(q_z)_n$  -- conductive heat flux in the "necks" (solid phase) in the axial direction at section  $n$

$Q$  -- rate of injection of tracer (moles/time)

$r$  -- radial distance

$R$  -- rate of production of  $i$  by chemical reaction, moles of  $i$ /volume-time, in the moving phase

$\hat{R}$  -- rate of production of  $i$  by chemical reaction, moles of  $i$ /mass of catalyst-time, in the solid phase

$Re$  -- Reynolds number

$R_g$	--	gas law constant
$R_1(x,y)$	--	rate expressions defined in sections 7,3, 7.5
$R_2(x,y)$	--	rate expressions defined in sections 7,3, 7.5
$\delta S$	--	surface area of the particle which is effective in convective heat transfer between the moving fluid and solid per unit volume of the bed
$\hat{\delta S}$	--	cross-sectional area of the "necks" which is effective in conductive heat transfer between adjacent particles per unit volume of the bed
$t$	--	time
	--	dimensionless time in chapter 7
$t'$	--	time
$t_m$	--	$\frac{z}{v_z}$ ; average time spent by a tracer molecule in the moving phase
$t_s$	--	average time spent by a tracer molecule in the stagnant phase
$T$	--	temperature of the external fluid
	--	temperature of the moving phase
	--	complex magnitude of temperature perturbation variable, in section 7.5
$THI$	--	imaginary part of the complex magnitude of the solid phase temperature
$THR$	--	real part of the complex magnitude of the solid phase temperature
$TI$	--	imaginary part of the complex magnitude of temperature
$TR$	--	real part of the complex magnitude of temperature
$\hat{T}$	--	temperature of the solid catalyst pellet
	--	complex magnitude of temperature perturbation variable in the solid phase, in section 7.5
$T_n(z)$	--	temperature of the moving phase at section n and axial distance z

- $T_{os}$  -- inlet temperature at steady state  
 $u$  -- superficial velocity  
 $v$  -- interstitial velocity in the Fickian model  
     -- asymptotic velocity for large  $t$ , in section 3.1  
 $v_T$  -- asymptotic temperature pulse velocity for large  $t$   
 $\bar{v}_T, \bar{\bar{v}}_T, \hat{\bar{v}}_T$  -- average temperature pulse velocity in the moving phase, stagnant phase and solid phase, respectively  
 $v_z$  -- actual average velocity of the moving phase (based on cross-sectional area available to the moving phase)  
 $V_{tot}$  -- volume occupied by gas in the reactor  
 $x$  --  $P/P_{os}$  ; dimensionless partial pressure  
 $X$  --  $\frac{2 \epsilon_A \epsilon_B^2 Pe_z}{\epsilon_T^2} \sqrt{\frac{z_o \left( \frac{\epsilon_T}{\epsilon_A} \tau - z_o \right)}{\epsilon_A \epsilon_B}}$  ; dimensionless arguments in section 3.2  
     --  $\left( 4 \frac{g}{\epsilon_A} \frac{g}{\epsilon_B} \frac{z}{v_z} t_s \right)^{1/2}$  ; dimensionless argument, in section 3.3  
     -- concentration perturbation variable in Chapter 7  
 $y$  --  $T/T_{os}$  ; dimensionless temperature  
     -- radial coordinate  
 $y_i(z)$  -- trial functions  
 $Y$  -- complex magnitude of concentration, in section 3.4  
     -- temperature perturbation variable, in Chapter 7  
 $\hat{Y}$  -- temperature perturbation variable in the solid phase  
 $Y_e, Y_i$  -- complex magnitude of harmonic signal at the exit and at the entrance, respectively

$z$	--	axial coordinate
	--	dimensionless axial coordinate in Chapter 7
$\bar{z}$	--	$\frac{\mu_1}{\mu_0}$
$z_0$	--	dimensionless distance
$\delta z$	--	differential axial distance

### Greek symbols

$\alpha$	--	density of the fluid
$\gamma$	--	$\frac{E}{R_g T_{os}}$
$\delta(z)$	--	Dirac delta function
$\epsilon_A$	--	fraction of total bed volume occupied by the moving phase
$\epsilon_B$	--	fraction of total bed volume occupied by the stagnant phase
$\epsilon_r$	--	emissivity of the catalyst particles
$\epsilon_T$	--	fraction of total bed volume not occupied by solids
$\lambda$	--	radial length parameter
$\lambda_f$	--	thermal conductivity of the fluid
$\lambda_o$	--	axial effective thermal conductivity of the quiescent bed, that is, a bed with no fluid flow
$\mu_f$	--	dynamic viscosity of fluid
$\mu_n(t)$	--	nth moment
$\rho$	--	interstitial average concentration
$\rho_B$	--	bulk density of the catalyst

$\rho_s$	--	density of the solid
$\sigma$	--	radiation constant
$\tau$	--	thermal residence time
	--	$\frac{\epsilon_A v_z t}{\epsilon_T d_p}$ ; dimensionless time, in section 3.2
$\bar{\tau}$	--	average residence time, in section 3.4
$\tau_f$	--	$\frac{vt}{d_p}$ ; dimensionless time, in section 3.2
$\phi$	--	phase angle
$\omega$	--	standard deviation
	--	circular frequency

### Superscripts

$\text{---}$	--	refers to stagnant phase
$\wedge$	--	refers to solid phase

REFERENCES

- Adler, K., Henkel, Hertwig, Nagel, *Chemische Tech.*, 25, 10 (1973).
- Amer. Petr. Inst. Res. Project #44, Circular of The National Bureau of Standards C461, November 1974 (Washington, D.C.).
- Amundson, N.R., *Berichte Bunsen-Gesel*, 74, 90 (1970).
- Argo, W.B., J.M. Smith, *Chem. Eng. Progr.*, 49, 443 (1953).
- Aris, R., N.R. Amundson, *A.I. Ch E J.*, 3, No. 2, 280 (1957).
- Bakhurov, V.G., Boreskov, G.K., *J. Appl. Chem. (U.S.S.R.)*, 20, 721, (1947).
- Balakrishnan, A.R., Pei, D.C.T., *IEC (Proc. Des. Dev.)*, 13, 441 (1974).
- Baron, T., *Chem. Eng. Progr.*, 48, 118 (1952).
- Beek, J., Miller, R.S., *Chem. Eng. Progr. Symp. Ser. 55*, No. 25 (Reaction Kinetics and Unit Operations), 23 (1959).
- Beek, J., *Symp. Chem. React. Eng.*, 5th, Amsterdam 1972, review section 4.
- Bernard, R.A., R.H. Wilhelm, *CEP*, 46, 233 (1950).
- Bhattacharya, D., Pei, D.C.T., *CES*, 30, 293 (1975).
- Bird, R.B., W.E. Stewart, E.N. Lightfoot, "Transport Phenomena," John Wiley and Sons, Inc., N.Y., 1960.
- Buffham, B.A., Gibilaro, L.G., *Chem. Eng. J.*, 1, 31 (1970).
- Buffham, B.A., Gibilaro, L.G., and M.N. Rathor, *A.I. Ch E J.*, 16, 218 (1970).
- Chu, Y.C., J.A. Storrow, *CES*, 1, 230 (1952).
- De Wasch, A.P., Froment, G.F., *CES*, 27, 567 (1972).
- Deans, H.A., Lapidus, L., *AIChE J.*, 6, 656; 663 (1960).
- Deans, H.A., *SPE J1.*, 49 (1963).
- Debbas, S., Rumf, H., *CES*, 21, 583 (1966).
- Denis, G.H., Kabel, R.L., *AIChE J.*, 16, 972 (1970).
- ibid., *CES*, 25, 1057 (1970).

- Doesburg, H.V., W.A. De Jong, Adv. Chem. Ser., 133, 489 (1974).
- Eigenberger, G., CES, 27, 1909; 1917 (1972).
- Feick, J., D. Quon, Can. J. Chem. Eng., 48, 205 (1970).
- Fieguth, P., Wicke, E., Chem. Ing. Tech., 43, 604 (1971).
- Finlayson, B.A., "The Method of Weighted Residuals and Variational Principles," Academic, N.Y., 1972.
- Finlayson, B.A., Cat. Revs., 10, 69 (1974).
- Froment, G.F., Symp. Chem. React. Eng., 5th, Amsterdam 1972, review section 5.
- Fulton, J.W., O.K. Crossner, AIChE J., 11, 513 (1965).
- Galloway, T.R., Sage, B.H., CES, 25, 495 (1970).
- Gauvin, W.H., Katta, S., AIChE J., 19, 775 (1973).
- Giddings, J.C., "Dynamics of Chromatography," Part I, Marcel Dekker, N.Y., 1965.
- Gunn, D.J., J.F.C. De Souza, CES, 29, 1363 (1974).
- Hansen, K.W., CES, 26, 1555 (1971).
- Hansen, K.W., CES, 28, 723 (1973).
- Hansen, K.W., Jorgensen, S.B., Adv. Chem. Ser., 133, 505 (1974).
- Hansen, K.W., Jorgensen, S.B., CES, 31, 579 (1976).
- ibid., 587 (1976).
- ibid., 473 (1976).
- Hansen, K.W., Livbjerg, H., Villadsen, J.V., IFAC Symp. DISCOP, Győr, Hungary, 1971, paper W1.
- Hawthorn, R.D., Ackerman, G.H., Nixon, A.C., AIChE J., 14, 69 (1968).
- Hiby, J.W., Interaction Between Fluids and Particles, Institution of Chemical Engineers Symp., Ser. No. 9, 1963.
- Hlavacek, V., J. Votruba, Adv. Chem. Ser., 133, 545 (1974).



- Hoffman, H., Chem. Ing. Techn., 46, 236 (1974).
- Hoiberg, J.A., Ph.D. Thesis, University of California, Berkeley, 1969.
- Hoiberg, J.A., Lyche, B.C., Foss, A.S., AIChE J., 17, 1434 (1971).
- Horak, J., Jiracek, F., Symp. Chem. React. Eng., 5th, Amsterdam, 1972, B8-1.
- Hougen, O.A., JEC, 53, 509 (1961).
- Hughes, R., H.P. Koh, Chem. Eng. J., 1, 186 (1970).
- Hutchings, J., J.J. Carberry, AIChE J., 12, 20 (1966).
- Irving, J.P., Butt, J.B., CES, 22, 1859 (1967).
- Kabel, R.L., Lehr, C.G., Yurchak, S., AIChE J., 14, 627 (1968).
- Karanth, N.G., Hughes, R., Adv. in Chem. Ser., 133, 449 (1974).
- Kehoe, J.P.G., Butt, J.B., Symp. Chem. React. Eng., 5th, Amsterdam 1972, B8-13.
- Kramers, H., Alberda, G., CES, 2, 173 (1953).
- Kusik, C.L., Happel, J., IEC (Fund), 1, 163 (1962).
- Kyle, C.R., Perrine, R.L., Can. Jl. Chem. Eng., 49, 19 (1971).
- Littman, H., Sliva, D.E., 4th Int. Heat Transfer Conference Paris-Versailles 1970, Vol. 7, paper CT 1.4.
- Liu, S.L., Amundson, N.R., IEC (Fund), 2, 183 (1963).
- Lyche, B.C., Ph.D. Thesis, University of California, Berkeley, 1967.
- Maymo, J.A., Smith, J.M., AIChE J., 12, 845 (1966).
- McCarty, R.D., "Hydrogen Technological Survey--Thermophysical Properties," NASA, Washington, D.C. (1975).
- McGuire, M., Lapidus, L., AIChE J., 6, 656 (1965).
- Mickley, H.S., Smith, K.A., Korchak, E.I., CES, 20, 237 (1965).
- Oman, A.O., Watson, K.M., Natl. Petrol. News, 36, R 795 (1944).
- Padberg, G., Wicke, E., CES, 22, 1035 (1967).

- Paris, J.R., Stevens, W.F., Can. J. Chem. Eng., 48, 100 (1970).
- Ranz, W.E., Chem. Eng. Progr., 48, 247 (1952).
- Ray, W.H., Symp. Chem. React. Eng., 5th, Amsterdam 1972, review section 8.
- Richarz, V.W., Lattmann, M.A.S., Symp. Chem. React. Eng., 4th, Brussels, 1968.
- Singer, E., Wilhelm, R.H., CEP, 46, 343 (1950).
- Stewart, W.E., Sorensen, J.P., "Transient Reactor Analysis by Orthogonal Collocation," Present at 2nd International Symp. on Chemical Engineering, 1972.
- Villadsen, J., "Selected Approximation Methods for Chemical Engineering Problems," Institutet for Kemiteknik Numerisk Institut, Danmarks Tekniske Højskole, 1970.
- Villadsen, J., Michelsen, M.L., "Solution of Differential Equations Models by Polynomial Approximation," Prentice-Hall, Englewood Cliffs, 1977.
- Villadsen, J., Stewart, W.E., CES, 22, 1483 (1967).
- Vortmeyer, D., CES, 30, 999 (1975).
- Vortmeyer, D., Shaefer, R.J., CES, 29, 485 (1974).
- Votruba, J., Hlavacek, V., Marek, M., CES, 27, 1845 (1972).
- Watson, G.N., "Theory of Bessel Functions," Cambridge, London (1966).
- Wehner, J.F., Wilhelm, R.H., CES, 6, 89 (1956).
- Wilhelm, R.H., McHenry, K.W., AIChE J., 3, 83 (1957).
- Wilson, H.A., Proc. Cambridge Phil. Soc., 12, 406 (1904).
- Yagii, S., Kunni, D., Wakao, N., AIChE J., 6, 543 (1960).
- Yamazaki, T., Noguchi, Y., Akazuka, T., Iwamuru, T., Otani, S., Kagaku Kogaku, 34, 402 (1970).
- Zenz, F.A., Othmer, D.F., "Fluidization and Fluid Particle Systems," Reinhold Publishing Corporation, N.Y., 1960.